

ANIONIC MICROGELS FABRICATED WITH A NEW MICROEMULSION APPROACH
FOR THE ENCAPSULATION AND RELEASE OF PROTEINS AND HIGHER ORDER
CONSTRUCTS

A Dissertation

Presented to the Faculty of the Graduate School
of Cornell University

In Partial Fulfillment of the Requirements for the Degree of
Doctor of Philosophy

by

Jose L. Rios

August 2016

© 2016 Jose L. Rios

ANIONIC MICROGELS FABRICATED WITH A NEW MICROEMULSION APPROACH FOR THE ENCAPSULATION AND RELEASE OF PROTEINS AND HIGHER ORDER CONSTRUCTS

Jose L. Rios, Ph.D.

Cornell University 2016

Hydrogels and microgels have the potential to enhance the delivery of pharmaceuticals by controlling the release rate, delivering pharmaceutical active agents to the site of action, protecting delicate drugs (e.g. protein therapeutics) from degradation and by enabling targeting of drugs at different physiological length scales (e.g. tissue, organ, cellular). The work discussed in this thesis reports the fabrication of poly(acrylic acid)-oligo(ethylene glycol) (pAA-OEG) and poly(acrylic acid)-polyethylene glycol (pAA-PEG) microgels for the controlled release of proteins and higher order constructs. An extensive background of hydrogels/microgels, protein drugs and phage therapy is discussed to provide a premise for this work (Chapter 1).

Therapeutic proteins have become integral to health care but controlled delivery remains challenging. Protein function depends on its three dimensional structure and formulation methods should not be detrimental to the protein's native structure. In this work, proteins were encapsulated in pAA-OEG microgels fabricated with a new microemulsion approach using the post-loading method to prevent protein damage during fabrication. Microgels of different size and morphology were synthesized and proteins with different physico-chemical characteristics were encapsulated. pAA-OEG microgels showed high loading efficiencies and prolonged release of bioactive proteins (Chapter 2).

In subsequent work, higher order constructs (bacteriophage) were investigated for

encapsulation and controlled release with microgels. There is an alarming emergence of antibiotic resistant pathogens due to over-prescription of antibiotics. It is estimated by the Center for Disease Control and Prevention (CDC) that 1 in 7 surgical site infections obtained in hospitals are caused by antibiotic resistant bacteria. Phage therapy is being considered again for infection treatment and it is still widely used in the Eastern European country of Georgia. Bacteriophages are viruses able to infect bacteria, multiply within the bacterial host and ultimately lyse the bacteria. Driven by the previous success of encapsulation and prolonged release of proteins, we investigated the potential use of the microgels for the controlled release of phage. pAA-PEG microgels successfully encapsulated phage and released over a prolonged period while still retaining activity (Chapter 3).

Chapter 4 highlights future work for further development of the pAA-OEG and pAA-PEG microgels and to increase their potential for translation into clinical application. The suggestions include strategies to increase the biodegradability of microgels, the use of microfluidics to create monodisperse formulations and in-vivo evaluation to determine safety and efficacy.

BIOGRAPHICAL SKETCH

Jose Luis Rios was born in the Mexican coastal city of Mazatlán, Sinaloa. He spent his childhood in Mazatlán and at the age of 13 moved to Phoenix, Arizona. A difficult transition at first, from Mexico to the United States, from Spanish to English, from the tropical coast to the southwest desert. With time he learned to appreciate the wonders of the desert and made Arizona his new home. As an immigrant and first generation student, Jose had to overcome many challenging barriers to pursuit a higher education. He received a Bachelor's of Science in Engineering in Bioengineering from Arizona State University. He is the first in his immediate and extended family to obtain a college degree. He began his PhD in Biomedical Engineering at Cornell University where he had one of the most formative times of his life.

To my parents Jose Luis Rios Espinoza and Maribel Lizarraga Zatarain de Rios.

ACKNOWLEDGMENTS

I would like to first thank my advisor Professor David Putnam whom took me into his lab, supported my scientific work and guided me to bring my project forward.

I would like to acknowledge the Coleman Foundation and the NSF Graduate Research Fellowship for their funding. Without their support the body of work in this thesis would not have been possible.

I would like to thank my committee members Professor Geoffrey Coates and Professor Michael Shuler for providing constructive critique of my work. I would also like to thank Professor Christopher Schaffer for providing advice at different points throughout my PhD.

I would also like to thank all members of the Putnam Lab past and present for being supportive and allowing me to be part of a constructive scientific environment.

Finally, I would like to thank all my friend and family for their support.

TABLE OF CONTENTS

Introduction	1
1.1 Hydrogels and Microgels.....	1
1.1.1 Summary	1
1.1.2 A Brief Historical Perspective of Hydrogels and Microgels.....	1
1.1.3 Microgel Fabrication Methods	6
1.1.4 Microgels for Drug Delivery	8
1.2 Delivery of Protein Therapeutics.....	10
1.2.1 Background of Protein Therapeutics.....	10
1.2.2 Strategies for Protein Therapeutic Delivery	11
1.2.3 Summary of Proposed Research Project.....	13
1.3 Phage Therapy and Phage Delivery	15
1.3.1 Background	15
1.3.2 A Historical Account of Phage Therapy.....	15
1.3.3 Modern Phage Therapy	20
1.3.4 Materials for Phage Delivery.....	21
1.4 References.....	23
2 Prolonged Release of Bioactive Model Proteins from Anionic Microgels Fabricated with a New Microemulsion Approach	38

2.1	Abstract	38
2.2	Introduction	39
2.3	Materials and Methods	42
2.3.1	Materials	42
2.3.2	Synthesis of Poly(acrylic acid)	42
2.3.3	Preparation and Characterization of Microgels	43
2.3.4	Protein Loading	47
2.3.5	Protein Release	48
2.3.6	Lysozyme Activity Assay	48
2.4	Results and Discussion	49
2.4.1	Synthesis and Characterization of Poly(acrylic acid)	49
2.4.2	Characterization of pAA-OEG Microgels	50
2.4.3	Protein Capture by Microgels	57
2.4.4	In-vitro Protein Release and Activity	62
2.5	Conclusion	70
2.6	References	72
3	Encapsulation and Prolonged Release of Bacteriophage from Anionic Microgels	78
3.1	Abstract	78
3.2	Introduction	79

3.3	Materials and Methods	82
3.3.1	Materials	82
3.3.2	Synthesis of Poly(acrylic acid)	82
3.3.3	Preparation and Characterization of Microgels	83
3.3.4	Bacteriophage Propagation, Encapsulation and Release	84
3.3.5	Plaque Assay	85
3.4	Results and Discussion	85
3.4.1	Synthesis and Characterization of Poly(acrylic acid)	85
3.4.2	Characterization of pAA-PEG Microgels	86
3.4.3	In-Vitro Phage Encapsulation, Release and Lytic Activity	91
3.5	Conclusion	100
3.6	References	101
4	Conclusions and Recommendations for Future Work	107
4.1	Conclusions	107
4.2	Future Work	108
4.2.1	Engineer Better Biodegradability into pAA/PEG Microgels	108
4.2.2	Microfluidic Fabrication of Microgels	113
4.2.3	In Vivo-Studies to Assess Toxicity and Therapeutic Efficacy	113
4.3	References	115
A.	Delivery of Bacteriophage Loaded-Microgels for the Treatment of	

Intracellular Pathogens	118
A.1 Abstract	118
A.1 Introduction	119
A.2 Materials and Methods	120
A.2.1 Materials	120
A.2.2 Synthesis of poly(acrylic acid)	120
A.2.3 Preparation of Microgels	121
A.2.4 Bacteriophage Propagation and Encapsulation	121
A.2.5 Macrophage Cell Culture	122
A.2.6 Confocal Microscopy of Microgel Phagocytosis by Macrophages	122
A.2.7 Invasion Assay and Bacteriophage Treatment	123
A.3 Results and Discussion	124
A.4 Conclusion	128
A.5 References	129

LIST OF FIGURES

Figure 1.1. Representation of glucose responsive microgel..	5
Figure 1.2: First electron microscopy images of phages	18
Figure 2.1. Schematic of cross-linking reaction to form microgels.	46
Figure 2.2. ¹ H NMR of pAA synthesized by RAFT polymerization.	52
Figure 2.3. Representative scanning electron microscopy of microgels	53
Figure 2.4. Differential centrifugation of microgels.....	54
Figure 2.5. FT-IR spectroscopy of microgels, OEG and pAA.	55
Figure 2.6. GPC chromatogram of pAA used in microgel synthesis (solid line) and product from forced microgel degradation (dashed line).	56
Figure 2.7. Protein loading efficiency into all microgel formulations.	59
Figure 2.8: Images showing qualitative information on myoglobin and hemoglobin loading..	60
Figure 2.9 Confocal orthogonal images showing the distribution of lysozyme within formulation M1 (densely cross-linked, left figure) and M4 (lightly cross-linked, right figure).	61
Figure 2.10: Lysozyme release kinetics from all formulations..	65
Figure 2.11: Comparison of lysozyme release in 1X and 4X PBS for microgel formulations M5 and M8.....	66
Figure 2.12: Myoglobin release from all formulations.....	68
Figure 2.13: Hemoglobin release kinetics from microgels.....	69
Figure 3.1 ¹ H NMR of pAA synthesized by RAFT polymerization.	87

Figure 3.2. Schematic of cross-linking reaction for microgel fabrication.	88
Figure 3.3. Representative SEM images of microgel.	89
Figure 3.4. FTIR analysis of microgels.	90
Figure 3.5. Loading efficiency of EA and P1 phage..	92
Figure 3.6. Release of phage P1 (a) and EA (b) from different formulations.	93
Figure 3.7. Trend lines of the Korsmeyer-Peppas model overlaid on the fraction release data of phage P1 (a,b) and EA (c,d) from different formulations.	95
Figure 3.8. Lytic activity of released EA phage	98
Figure 3.9. Lytic activity of released P1 phage	99
Figure 4.1 Chemical structure of non-degradable pAA (left) and biodegradable PGAC (right).	110
Figure 4.2. Sample synthetic scheme for the fabrication of microgels with cross-links with enhanced biodegradability.	112
Figure A.1: Phagocytosis of microgels by J774 A.1 macrophage cells after 4-hour exposure.	125
Figure A.2: Confocal z-section images were taken and cross-sections of the y-z plane (right) and x-z plane (bottom) are shown demonstrating that microgels are internalized within the cell membrane and not just adhering to the macrophages.	125
Figure A.3: Phage loaded microgel treatment of 528-2 <i>e. col</i> infected macrophages..	127
Figure A.4: Phage loaded microgel treatment of NC101 <i>e. col</i> infected macrophages..	127

LIST OF TABLES

Table 2.1. Properties of proteins loaded in microgels	41
Table 2.2: Formulation parameters of synthesized microgels used in this study	45
Table 2.3: Percent of lysozyme activity remaining upon release from microgels relative to native lysozyme.	67
Table 4 . Kinetic parameters obtained by fitting the Korsmeyer-Peppas model fraction cumulative release of phage.	96
Table 4.1 Proposed formulation blend of PGAC/pAA for synthesis of biodegradable microgels.	111

Introduction

1.1 Hydrogels and Microgels

1.1.1 Summary

The most basic definition of a hydrogel is a three dimensional network composed of hydrophilic polymers. The hydrogel network is held together by crosslinks that prevent the polymeric constituents from dissolution into the solvent. The hydrophilic nature of the composing polymers leads to high levels of swelling and they can increase several times in weight when fully swollen. Hydrogels fabricated with techniques that lead to micron size colloidal hydrogel particles they are termed microgels. Following is a historical summary of hydrogels and microgels, followed by fabrication techniques and the design rationale for microgels used for drug delivery.

1.1.2 A Brief Historical Perspective of Hydrogels and Microgels

Hydrogels found their first successful use as medical devices in 1960, when Otto Wichterle and Drahoslav Lim from the Institute of Macromolecular Chemistry in Prague wrote a short letter to Nature (1). This was a time when all polymers were mostly referred to as plastics. While predictable in hindsight for hard plastics, the biocompatibility experiments did not show much promise, with the exception of poly(methyl methacrylate) (pMMA), which showed biocompatibility as an orthopedic material as described in report from the Royal Society of Medicine in 1945 (2). What was missing from the plastics that scientists were experimenting with was eloquently described by Wichterle and Lim in their seminal paper of 1960 (1). The demands for a plastic suitable for biological use were defined as the following: “1. a structure

permitting the desired water content, 2. inertness to normal biological processes, 3. permeability to metabolites". Fundamentally, it was with these criteria that Wichterle and Lim developed the first soft contact lenses. Poly(hydroxyethyl methacrylate) (pHEMA) was used to fabricate the first contact lenses (1) but they still had limitations such as inadequate oxygen transport and poor mechanical properties (3). To improve on these properties a highly hydrophilic monomer, N-vinylpyrrolidone, was incorporated into pHEMA via copolymerization during hydrogel preparations (4,5). pHEMA-based contact lenses were the first clinically successful hydrogels and even to date pHEMA remains a primary material for contact lenses (6).

Hydrogels have been used for controlled drug delivery as well. Control over drug pharmacokinetics is essential to achieve a desired therapeutic effect while minimizing side-effects and maximizing patient compliance. Hydrogels have played a role in the controlled release of pharmaceutically active agents (7). pHEMA hydrogels were at first inadequate for controlled release due to a small mesh size which prevented entrapped molecules from diffusing out of the hydrogel matrix (8). Different fabrication methods and incorporation of different monomers helped achieve control over mesh size, producing hydrogels suitable for the release of small molecules and macromolecules (9–11). The early work in modeling the release of solutes from hydrogels was achieved by Peppas and the mathematical models developed are still widely used today (12–14). The release of solutes from hydrogels can be controlled via diffusion, swelling of the hydrogel matrix, and by responding to an external stimulus. The latter mechanism is of great interest to scientists as having control over when release occurs adds to the functionality of the hydrogels. Hydrogels can be designed to respond to physical stimuli or chemical stimuli. Chemically controlled release is defined as solute release in response to cleavage by hydrolytic/enzymatic reactions or by ligand substitution (15,16). Perhaps, one of the

cleverest chemically controlled release systems is that developed by Lee and Park and described in the Journal of Molecular Recognition in 1996 (16). The material consisted of a glucose-grafted polymer cross-linked with tetramer concanavalin A (Con A), a protein lectin able to bind glucose. The binding interaction between Con A and the glucose attached to polymer reversibly cross-links the polymer thus forming a hydrogel. Free glucose present in the environment is able to substitute polymer-attached glucose on Con A's binding site and in turn dissociate the cross-links (Figure 1.1). Park et al. used this novel material to modulate the release of insulin in response to glucose in the environment (17) creating what some have refer to as an "artificial pancreas." Stimuli responsive hydrogels are able to swell/de-swell in response to changes in pH and/or temperature. The change in the swelling behavior impacts the release of solute (18,19). Extensive academic research on the application of hydrogels for controlled release has been conducted, but there are few products on market (7,20). Some examples of market products include Cervidil®, a vaginal insert composed of cross-linked polyethylene oxide/urethane loaded with dinoprostone to induce labor (21) and a subcutaneous hydrogel insert has been developed by Endo Pharmaceuticals Inc. called SUPRELIN LA for the release of histrelin acetate for the treatment of children with central precocious puberty (22).

Microgels, chemically speaking, have very similar properties to hydrogels but due to their colloidal nature they prove to be useful in some distinct applications. The term was coined by Baker from Bell Labs in 1949 to described latex particles of cross-linked polybutadiene (23). The first applications of microgels were for industrial purposes such as rubbers and paint coatings (24). Microgels for controlled release of drug started to be investigated much later than bulk hydrogels. The first patent for the use of microgels, or as called in the patent "hydrogel beads", for drug delivery was file in 1985 by E.R. Squibb & Sons. The patent makes use of co-

polymers of acrylic acid and methyl methacrylate cross-linked with various cross-linkers (25). The first examples of microgel stimuli responsive controlled release was reported in the 1990s by the groups of Snowden and Aizawa. Aizawa et al. synthesized pH-sensitive microgels based on anionic co-polymers of acrylic acid/methyl methacrylate mixed with cationic poly(L-lysine) (PLL). The microgels aggregated at low pH because of the interaction of the positively charged PLL with the anionic microgels. With increased pH, the PLL was no longer ionized therefore leading to dispersion and electrostatic repulsion of the microgels (26). Snowden developed poly(N-isopropylacrylamide) (pNIPAM) microgels for the uptake and temperature controlled release of fluorescein-labelled dextran (27). Microgel protein interactions have been studied for chromatography purposes (24) but their use as controlled release devices for proteins was not investigated until the 2000s. Murthy et al. developed protein-loaded microgels with an acid degradable cross-linker (28), Zhang et al. developed lactic acid-co-Pluronic microgels for the post fabrication loading of proteins and subsequent release (29), and Johansson et al. study in detail the mechanism of lysozyme uptake into poly(acrylic acid) microgels (30).

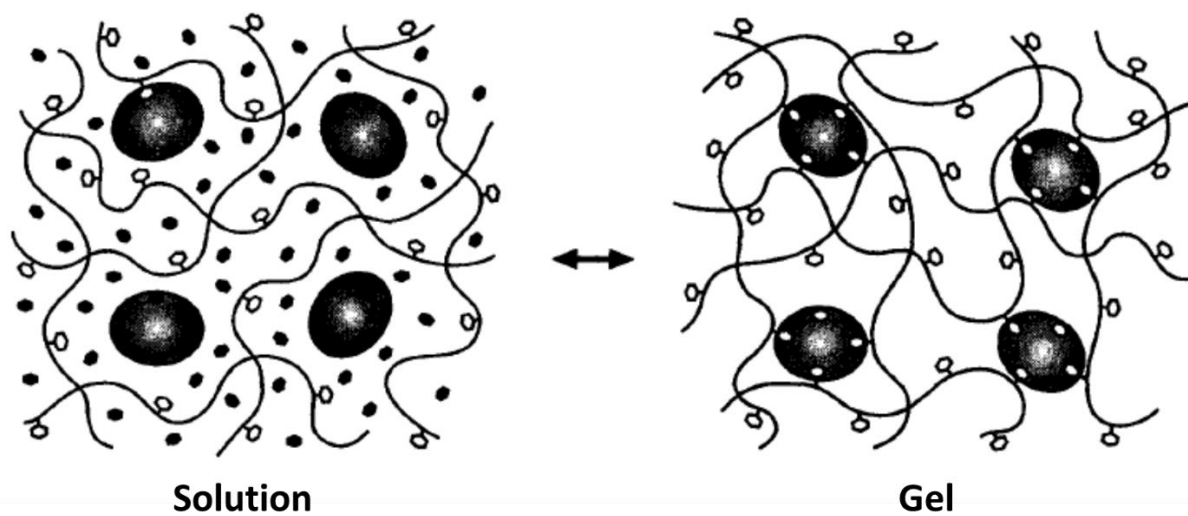


Figure 1.1: Representation of glucose responsive microgel. Large black ovals represent Con A, open circles are polymer attached glucose, and small dark circles represent free glucose. Reprinted from ref 16. Copyright 1998 John Wiley and Sons.

1.1.3 Microgel Fabrication Methods

1.1.3.1 Fabrication of microgels from monomers

Microgels of this type are traditionally synthesized by the polymerization of vinyl monomers via free radical polymerization in the presence of bi-functional monomers. The mechanism of this type of polymerization is well established. In brief, the vinyl monomer's π -bond is open by a radical initiation creating a propagating radical able to incorporate additional monomers until the polymerization comes to an end by the combination of two radicals or disproportionation. There are two main synthetic strategies to achieve the formation of microgels. One is by homogenous nucleation of precipitated polymer chains and the other is by inverse emulsion polymerization, as described below.

Homogenous nucleation fabrication of microgels begins with a homogenous solution in which the monomer and cross-linking agent are dissolved in solution. The subsequent polymer obtained from say so monomer is insoluble in that solution. As polymer chains begin forming, they precipitate out of solution. This newly formed precipitated polymer chains have a certain degree of cross-links. Therefore, they are now microgels. If the polymer was soluble, this would lead to a bulk hydrogel instead of microgels. pNIPAM microgels are commonly synthesized using this method in water at 70 °C because the monomer NIPAM is soluble at this temperature but the polymer pNIPAM precipitates (31). The cross-linking of the polymer chains with a bi-functional vinyl monomer prevents dissolution of the microgels upon cooling (32).

Inverse emulsion polymerization consists of dissolving monomer, cross-linking agent and initiator in an aqueous phase. This component is often refer to as the pregel. The pregel is then emulsified in an oil or organic phase and surfactants can be use as stabilizers to prevent coalescence of pregel droplets. The polymerization is initiated while in emulsion and the cross-

linking of the forming polymer leads to gelation within individual droplets and thus microgels are fabricated. This technique has been used to create poly(acrylic acid) (pAA) cross-linked with poly(ethylene glycol) (400) -di-methacrylate. The polymerization is carried out in an aqueous phase emulsified in paraffin oil and stabilized with the polymeric surfactants SpanTM 80 and TweenTM 80 (33).

1.1.3.2 Fabrication of microgels from polymers

This technique involves the use of already synthesized polymers which are dissolved in an aqueous phase also referred to as the pregel phase. The pregel phase polymer phase is accompanied by cross-linking agents. This technique is often used for the preparation of microgels based on biological polymers like chitosan, hyaluronic acid, dextran, alginate and cellulose (34). Mitra et al. prepared microgels by emulsifying an aqueous solution of chitosan with glutaraldehyde, a cross-linker, in n-hexane containing the surfactant sodium bis(ethyl hexyl) sulfosuccinate to stabilize the emulsion. A dextran-doxorubicin conjugate was present in the aqueous phase during microgel formation and thus it was entrapped within the matrix (35). It is also possible to modify polymers with moieties that add cross-linking functionality. For example, hyaluronic acid (HA) has been modified with the addition of thiol groups. The thiol functionalized HA is able to form disulfide bonds and form a cross-linked network. Lee et al. used thiol-functionalized HA (HA-SH) by dissolving HA-SH in PBS and emulsified the aqueous phase in hexanes stabilized with SpanTM and TweenTM (36). Pre-synthesized synthetic polymers can be used similarly for microgel fabrication. Four-arm PEG has been functionalized with norbornene via a condensation reaction. The four-arm PEG-norbornene was then crosslinked using dithiothreitol through a thiol-ene reaction. This process led to an emulsion, leading to microgel formation (37).

1.1.4 Microgels for Drug Delivery

Recent interest in microgels has driven a significant amount of research in the use of microgels as drug carriers for drug targeting and drug controlled release applications. The following defines the design criteria for microgel drug delivery

The design criteria for microgels for drug delivery applications depends on the drug to be delivered, the kinetics of release and the particular biological target. Both physical and chemical properties are important to consider to rationally design a microgel drug delivery system.

1.1.4.1 Microgel Size

Microgel size is designed with the therapeutic target in mind. If microgels are meant to for localized delivery and to reside within a specific tissue, sizes exceeding 10 μm are preferred to avoid clearance by phagocytic cells. Microgels for intracellular delivery into non-phagocytic cells have sizes of < 1 μm with < 200 nm being optimal (38,39). Intracellular delivery into phagocytic cells is optimal with microgel sizes between 1 and 3 μm (40,41). Size also dictates the pharmacokinetic profile of microgels in the blood stream and different tissues. Glomerular filtration promptly clears polymers below 40 kDa and nanoparticles < 10 nm (42,43). Microgels can be designed with sizes exceeding 10 nm to increase circulation time but microgel elasticity must be taken into consideration. Microgels are soft and deformable and can pass through pores 10 times smaller their size (44). Size can also contribute to degradation kinetics and transport through different tissues. Additionally, size plays a role in immunogenicity with same composition microgels inducing a different inflammatory response as a result of size alone (45).

1.1.4.2 Microgel Biodegradation

A key component of any drug delivery device is that it can be eliminated from the host once it delivers its payload. Degradation of materials through hydrolytic pathways or making use

of the body's own enzymatic reactions and metabolic pathways are common ways to achieve this desired elimination. Microgels should optimally be design as biodegradable materials to prevent accumulation in the body that can lead to harmful side effects. Degradable linkages are included into microgel's chemical to architecture to facilitate degradability into small enough molecules to allow for renal clearance. In addition, degradation contributes to release kinetics of any encapsulated drugs. The simplest way to add degradability to microgels is by the incorporation of biodegradable linkages containing labile bonds such as acetal, esters, thiols, and hydrozones (28,46–50). Biopolymers can also be incorporated to induce degradability. Polysaccharides are often used because they are biodegradable and nontoxic. Polysaccharide microgel degradation generally occurs through carbohydrate oxidation or enzymatic degradation and is typically slower than degradable cross-linkers (34,51,52). In addition to polysaccharides, other biopolymers can be used to form degradable microgels, including dextran, hyaluronic acid, and gelatin functionalized with methacrylates to yield macromers that can be polymerized into biodegradable microgels (53,54).

1.1.4.3 Microgel Morphology

Microgel morphology can influence targeting, pharmacokinetics and cell internalization. Morphology can be engineered at the molecular or at the nano/micro scale. At the molecular scale, coatings can be incorporated to add functionality and/or targeting. Kiser et al. coated microgels with lipids to control the environment at which the microgel swells and in turn triggers release of doxorubicin (55). Nayak et al. decorated the surface of thermoresponsive microgels with folic-acid to induce folate receptor mediated endocytosis into cancerous cells (56). Nano/micro scale morphology manipulations can be achieved by engineering the shape of the microgels. Sharma et al. demonstrated that shape alone influences particle phagocytosis (40).

Homogeneity over morphology and size are extremely important for clinical translation and to meet strict regulatory criteria. Microfluidics technology has been used for the creation of monodispersed microgels creating a homogenous population (50,57,58). Microfluidics have also been use to create microgels with multiple cores and even anisotropic microgels containing two faces of different components in one single microgel (59–61). Control over microgel morphology is a growing area of research and has potential for the development of microgels that will ultimately be clinically translated.

1.2 Delivery of Protein Therapeutics

1.2.1 Background of Protein Therapeutics

From a biological standpoint proteins perform diverse functions while remaining highly specific for their task. Their wide range of functions include structural support intra and extracellularly, catalysis of biochemical reactions, transport of molecules within the body, providing channels and receptors in cellular membranes and antibodies for fighting infections. Current estimates on the number of human genes encoding for proteins are at about 21,000 (62). This provides a vast library of proteins and functionalities that with a good understanding of disease mechanism can be used as therapeutics in their natural or perhaps modified forms. The first obstacle to the wide used of protein therapeutics was the high cost of isolation and absence of a manufacturing method. However, the introduction of recombinant DNA technology this limitation was largely overcome. The advent of modern biotechnology has seen a remarkable increase in the number of therapeutic proteins and more potential candidates are in the pipeline (63). Currently the FDA has approved more than 130 protein pharmaceutical products (64,65) with an estimated market annual growth rate of 7.08% projected until 2016 (66). Some advantages for the use of protein therapeutics over small molecule drugs are that: 1) proteins

serve complex and highly specific functions, 2) there is less potential for proteins to interfere with biological process, 3) and since many proteins used as therapeutics are derived and similar to native proteins they are well tolerated by the body (65).

While modern biotechnology has made the production of protein pharmaceuticals possible, there are substantial hurdles to be overcome. Protein function depends on a delicate three dimensional structure, which can be compromised by both proteolytic/chemical degradation and physical/shear forces. Because of these characteristics, combined with their high molecular weight, which makes transport through biological membranes difficult, oral administration is largely ineffective for systemic indications. To date, almost all therapeutic proteins are administered by the parenteral route and require frequent administration due to their short half-lives (64). The delivery of protein therapeutics at defined doses in a safe and minimally invasive manner remains a prominent challenge in the field. Therefore, there is an increasing need for well-defined controlled release protein delivery systems.

1.2.2 Strategies for Protein Therapeutic Delivery

1.2.2.1 Polymeric Microparticles

Perhaps one of the most widely investigated strategies for the delivery of proteins is the use of polymeric microparticles. They offer some advantages such as administration by injection and the possibility to control the rate of release. They can be formulated by both synthetic and natural polymers. Some examples of natural polymers include alginate microspheres for nerve growth factor slow release (67) and chitosan for vaccination purposes (68), albumin beads, dextran, gelatin and collagen. Among the types of synthetic polymers that have been studied are polyorthoesters, polyanhydrides, polyamides, polyesters, polycaprolactones, and polyphosphazenes(69). But in the realm of synthetic polymers for protein delivery

poly(lactic-*co*-glycolic acid) (PLGA) dominates the field with several marketed formulations (64). But there are still some notable disadvantages to PLGA systems such as polymer hydrophobicity, protein denaturation in the preparation step due to the use of organic solvents and high shear stresses, acidic microenvironment during degradation leading to protein damage, reactions between polymer and protein, and burst or incomplete release (70).

1.2.2.2 Protein Modifications

To increase the bioavailability of proteins administered via the parenteral route proteins can be chemically modified. There are three main forms of chemical modifications of proteins: amino acid substitution, acylation and PEGylation. Amino acid substitution is performed by mutating one or more amino acids to create a protein analogue. This protein analogue might have some advantageous characteristics such as increased bioavailability or rapid-acting (71). Acylation of proteins consists in the chemical attachment of fatty acids to the protein's surface to increase the protein's circulation time by increasing affinity towards albumin in the blood (72). PEGylation is the conjugation of poly(ethylene glycol) (PEG) polymers onto the surface of a protein. It increases the half-life of the protein by reducing metabolic degradation and shielding from uptake receptors. Additionally, it has a stealth effect in reducing immunogenicity as the PEG is able to shield antigenic and immunogenic epitopes (73). There are still concerns with the use of the protein modifications techniques highlighted above. Among them are the potential to reduce protein efficacy, increasing immunogenicity and chemistry compatibility leading to heterogeneous products that can be a challenge for drug approval (74).

1.2.2.3 Microgels for Protein Therapeutic Delivery

Polymeric hydrogel microparticles, referred to as microgels herein, have received recent attention for their potential use as controlled release protein delivery vehicles (75–77). Microgels

are micron-scale cross-linked three dimensional networks of hydrophilic polymers that swell in aqueous environments. The cross-linked networks can be formed by a variety of means including physical entanglement, ionic interactions, or covalent bonds (78). Biodegradable microgels can be synthesized by inclusion of degradable linkages in the polymer or the cross-linker. Microgels also can be designed to have unique characteristics such as the ability to undergo volume changes in response to external stimuli such as pH, temperature or ionic strength, which can be used to develop environmentally responsive drug delivery systems (18). Furthermore, the micron-scale size of microgels can allow for their injection by standard methods.

1.2.3 Summary of Proposed Research Project

Protein therapeutics were once a rare class of medicines partly due to a high cost of isolation and the absence of efficient industrial manufacturing methods. But since the introduction of recombinant insulin in 1982 (79), there has been a steady increase in the number of protein therapeutics. Currently, the FDA has approved more than 130 protein pharmaceutical products and even more are in the pipeline (64,65). While modern biotechnology has made the production of protein pharmaceuticals possible, there are substantial hurdles to be overcome. Protein function depends on a delicate three dimensional structure, which can be compromised by both proteolytic/chemical degradation and physical/shear forces. Because of these characteristics, combined with their high molecular weight, which makes transport through biological membranes difficult, oral administration is largely ineffective for systemic indications. To date, almost all therapeutic proteins are administered by the parenteral route and require frequent administration due to their short half-lives (64). The delivery of protein therapeutics at defined dosage in a safe and minimally invasive manner remains a prominent challenge in the field. Therefore, there is an increasing need for well-defined controlled release protein delivery

systems

Polymeric hydrogel microparticles, referred to as microgels herein, have received recent attention for their potential use as controlled release protein delivery vehicles (75–77). They can be synthesized from hydrophilic synthetic or natural polymers by cross-links formed by a variety of means including physical entanglement, ionic interactions or covalent bonds. Microgels can also absorb and retain large amounts of water, thus mimicking biological tissues. The following design criteria should be considered for the development of microgels for protein controlled release: 1) capture and release of proteins in a controlled fashion; 2) minimal damage to the protein's native structure or biological activity; 3) biodegradable once protein payload is delivered; 4) biocompatible degradation products that can be cleared from the body.

1.3 Phage Therapy and Phage Delivery

1.3.1 Background

There is an alarming worldwide surge in antibiotic resistant pathogens due to the increased over prescription of antibiotics (80). The Center for Disease Control and Prevention (CDC) recently report it that 1 in 7 surgical site infections in hospitals are caused by antibiotic resistant bacteria (81). It is evident that new sources of antimicrobial agents are needed to overcome the limitations of antibiotics. Worrisome “superbugs” have focused attention back on bacteriophage therapy (82–84). Phages have some advantages over antibiotics that make them attractive as an alternative or complementary therapy. Phages are pure natural agents not requiring any synthetic methods for fabrication and have never been shown to cause adverse side effects on humans. Additionally, phages are highly specific to a bacterial species therefore they can be used to target only the pathogenic bacteria while sparing and leaving intact the body’s microflora, compared to broad-spectrum antibiotics that kill all bacterial cells regardless whether or not they are pathogenic. Once a phage attacks a bacterial host, it replicates exponentially increasing its own concentration and ability to attack more pathogens (83,85). Following is a historical account of the discovery of phages and phage therapy, the current stage of phage therapy, and a summary of materials for phage delivery.

1.3.2 A Historical Account of Phage Therapy

There is an abundant and naturally occurring antimicrobial agent found in nature. This antimicrobial agent is found anywhere bacteria are found. That is an unnecessary long way to say that this antimicrobial agent is everywhere; in the ground, in the air, in rivers, in lakes, in seas, etc. They were discovered by Felix d’Herelle and presented in the Academie des Sciences in 1917 (86). D’Herelle’s discovery is a clear example of close observation to natural phenomena

exhibited in the lab. Bacteriophage was discovered through meticulous experimentation over a period of 10 years. D'Herelle stumble on this discovery without looking for it like many others in science.

D'Herelle was hired in 1907 by the Mexican government to study fermentation and developed a method for the production of schnapps from sisal, a species of Mexican agave. During his stay in Mexico, he attempted to stop a locust plague by isolating and culturing a dysentery causing bacillus from the guts of infected (diarrheal) locust. He was able to cause epidemics in locusts (87). His attempts to stop a locust plague using bacillus in Mexico and later in Argentina may have been the first attempted biological control of pests (88). During his crusade against the locust, he noticed clear patches in agar cultures of bacillus. Investigation of the spot scrapes under a microscope showed nothing and so d'Herelle assume that the clear patches were caused by something small enough to pass through a Chamberland filter (89), a filter use to remove bacteria from fluids. D'Herelle's studies in locust plague prevention lead him to be commission to stop locust epidemics in North Africa by using a bacterial epidemic against the locust. During his stay in North Africa he again observed the clear patches but still hadn't formulated an explanation for their source (90). During World War I, d'Herelle was asked to investigate an epidemic of dysentery in soldiers station near Paris. It was thought that d'Herelle's experience with locust dysentery will help understand the malady in humans. To this end, d'Herelle followed a patient afflicted with dysentery from hospital admission to recovery. D'Herelle examined the feces filtrate for the presence of the patch forming agent on culture and made a remarkable discovery. He noticed that the clear patches begin appearing on cultures at the time when the patient began making a recovery. Furthermore, he found out that adding the feces filtrate to a broth culture of bacillus cleared up the solution, a clear indication of bacterial

lysis. He recognized the potential for clinical translation and coined this bacterial lysing agent as “bacteriophage” (89). Today it is clearly established that bacteriophage is an abundant independent biological entity but in the time soon after d’Herelle’s discovery most scientists were skeptic of the findings. It was until definite proof was obtained using electron microscopy in 1942 that a scientific consensus was reached for the existence of bacteriophages (91).

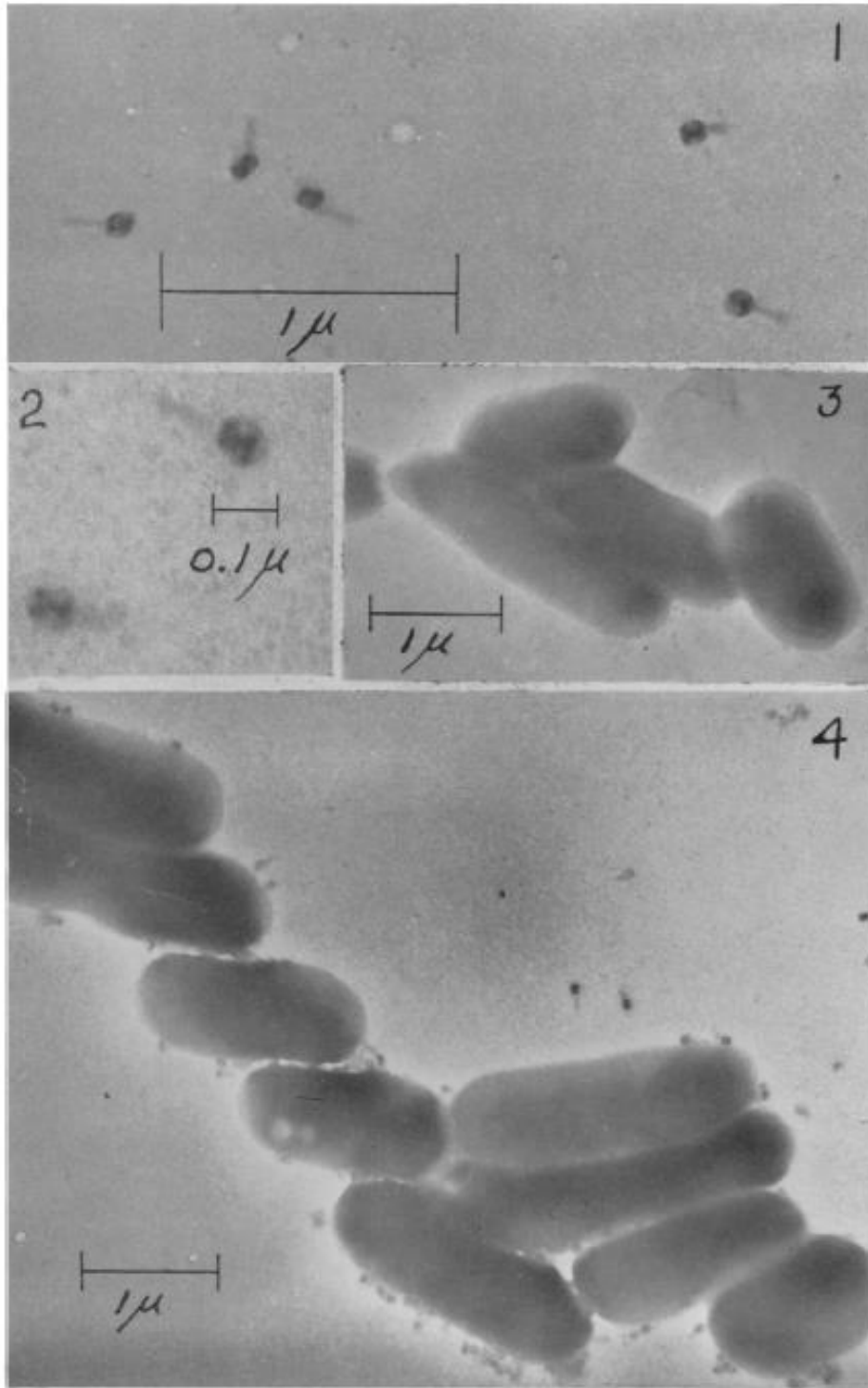


Figure 1.2: First electron microscopy images of phages. Reprinted from ref. (91).

A chicken typhoid epidemic in France gave d'Herelle the opportunity to study bacteriophage emergence in chickens. At the initial stage of the epidemic all infected chickens

died. Salmonella was present in their droppings but they were absent of any bacteriophage. This kept occurring until one hen made a recovery and consequentially the hen's excreta contained a powerful bacteriophage against the causative salmonella. All hens in proximity to this cured hen recovered and the epidemic ended. It was concluded that the epidemic begins with a single salmonella infected chicken that then infects others and ends with one chicken recovering thanks to increased number of bacteriophage, which then propagates to the other chickens (92). D'Herelle isolated the powerful bacteriophage cultures against salmonella and was able to cure the infected and stop the epidemic by introducing bacteriophage into the hens drinking water (90). Following promising clinical results in hens d'Herelle set out to prove that treatment of disease with bacteriophage, referred to as "phage therapy" from here on, was an effective way to cure patients and stop epidemics. D'Herelle traveled to India to study cholera disease. First he set up, along with Dr. M. N. Lahiri, to find phage effective against cholera in regions of Punjab where cholera is present naturally in populations. He then studied patients infected with cholera in two different populations in Calcutta and Lahore. Out of 33 control patients injected with saline solution 13 die. In comparison, 16 patients treated with one of d'Herelle's most potent phage preparation all 16 survived (93,94). This example are among others in which d'Herelle's phage therapy was successful at treating both veterinary and human disease (95). One must keep in mind that these early clinical studies lack the scientific rigor of today's clinical trials but nonetheless their significance cannot be understated. D'Herelle was later offered a position by his colleague Eliava and left Yale for Tbilisi in the former Soviet Republic of Georgia. There, among other colleagues and advocates of phage therapy, they established the leading world institute in phage therapy and reported major successes with phage therapy treatments.

There were early attempts to commercialize phage preparations for the treatment of

infection. D'Herelle was involved in commercializing cocktails that allegedly were clinically successful (96). Eli Lilly in the United States and the Oswaldo Cruz Institute in Brazil both produce commercially available phage; however, the clinical effectiveness was controversial (97). D'Herelle also arrived at this conclusion, claiming that other laboratories did not develop phage preparations with rigor and were only driven by capitalist profit motives (88). As a result of the poorly effective phage treatments in the west, the advent of antibiotics and the pressure for antimicrobials exerted by World War II, the use of phage therapy fell out of favor in the west. Phage therapy continued vigorously in the former Soviet Union, partly due to restricted access to antibiotics from the west. In fact, to date phage therapy continues to be used commonly in the Republic of Georgia (82).

1.3.3 Modern Phage Therapy

Phage therapy is widely used in the Republic of Georgia and as of 2010 phage preparations started to be exported to neighboring Azerbaijan. Two spin-off companies from the Eliava Institute of Bacteriophage have emerged. These are the “Eliava BioPreparations, Ltd.”, involved in the production of phages and “Eliava Diagnostics” which receives patients seeking phage treatment after an unsuccessful antibiotic regimen and the “Eliava Phage Therapy Center” which also treats foreign patients (98). A new product for the treatment of ulcers was developed called PhagoBioDerm, a combination of biodegradable polymer impregnated with lytic phages and antibiotics. PhagoBioDerm was used to treat ulcers in 107 patients who had not responded positively to conventional therapy. Of the unresponsive patients, 70% fully healed (99). Despite the long history of phage therapy in former Soviet countries, it is still relatively unknown to the general population of the west, in part due to regulatory hurdles. Phage cocktail preparations must meet higher standards of purity and stricter quality control practices to be used in humans.

A quality control phage cocktail was prepared for the treatment of burn wounds in the Burn Centre of the Queen Astrid Military Hospital in Brussels (100). This phage preparation was used in a small scale pilot clinical trial. The authors report no adverse effects were observed due to phage application but they also highlight the pitfalls of the study due to regulatory issues the study included flaws resulting in poor results in the bacterial load of biopsies between phage treated and conventional antibiotic treatment (101). Nonetheless, it is claimed that this small study helped start a conversation between healthcare givers and phage scientist. In fact, this study lead to the creation of the Phagoburn project, “a Phase I/II clinical study aiming at assessing the safety, effectiveness and pharmacodynamics of two therapeutic phage cocktails to treat either *E. coli* or *P. aeruginosa* burn wound infections.” The study began in July of 2015 (102). A preliminary study of nine patients with urinary tract infections treated with phage therapy showed a significant decrease in the presence of urine bacteria without any adverse side effects. This positive findings a multicenter clinical trial is expected to begin in 2016 (103,104). In the United States, a clinical trial evaluating safety concerns in 42 patients with chronic venous leg ulcers found no adverse effects following during 12 weeks of phage treatment (105). These are among other human trials that have been in a review by Vandenneuvel et al. (106).

1.3.4 Materials for Phage Delivery

Phage therapy can be administered via different routes: solutions and tablets for oral administration, dermal preparations, aerosols for lungs and intravenous formulations (83). Phage pharmacokinetics have proven challenging due to the self-replicating ability of the phage. The pharmacokinetics depend on initial and subsequent dosing, rate of phage clearance, phage and bacteria present at any time. Payne et al. demonstrated mathematically that inoculating too early or too late can lead to therapy failure (107). Therefore, enabling control over phage delivery by

using devices able to control the rate of release may prove useful at increasing the success of phage therapy. Few examples of phage controlled release devices are reported in the literature and of the few that have been reported they seem to be inefficient, they have released time frames in the order of minutes to a few hours, the release kinetics haven't been studied in detail and a clinical relevant model hasn't been used to evaluate if phage therapy can be improved with a delivery system. Chitosan-alginate microspheres were used by Ma et al. for phage controlled release. Phage was released over a period of 6 hours and the studies show that encapsulated phage can be protected from a denaturing acidic environment (108). The same research group showed that incorporating whey protein in alginate microspheres improves the survival of encapsulated phage (109). PLGA microspheres were used to encapsulate phage and release FITC labeled phage was measured over 6 hours. The lytic activity of encapsulated phage was poorly reported as no titers are given and only qualitative information about presence of plaques is reported (110). Korehei and Kadla used poly(ethylene oxide)/cellulose diacetate fibers to encapsulate T4 bacteriophage. Release of phage was studied only over 60 minutes (111). Vonasek et al. encapsulated phage in whey protein films and showed a total of 10^6 release over 5 hours (112). Phage was also encapsulated in poly(vinyl alcohol) nanofibers but the release kinetics were not studied (113). Lastly, Dini et al. encapsulated phage in a matrix blend of alginate/pepsin biopolymers. This study showed protection of encapsulated phage to low pH and to proteases in addition to release over 4 hours (114).

Extensive literature research yielded only the studies highlighted above expanding a time period between 2008 and 2014. The recent increasing interest in phage therapy suggests that formulating better preparations will play a key role in achieving clinical success.

1.4 References

1. Wichterle O, Lím D. Hydrophilic Gels for Biological Use. *Nature*. 1960;185(4706):117–8.
2. Blum G. Experimental observations of the use of absorbably and non-absorbable plastics in bone surgery. *Proc R Soc Med*. 1944;38(2):169–71.
3. Macret M, Hild G. Hydroxyalkyl methacrylates: hydrogel formation based on the radical copolymerization of 2-hydroxyethylmethacrylate and 2,3-dihydroxypropylmethacrylate. *Polymer*. 1982 May;23(5):748–53.
4. Garrett Q, Laycock B, Garrett RW. Hydrogel lens monomer constituents modulate protein sorption. *Investig Ophthalmol Vis Sci*. 2000;41(7):1687–95.
5. O’Driscoll, Kenneth F., Isen AA. Fabrication of Soft Plastic Contact Lens Blank. United States; 3700761, 1972.
6. Nicolson PC, Vogt J. Soft contact lens polymers: an evolution. *Biomaterials*. 2001 Dec;22(24):3273–83.
7. Caló E, Khutoryanskiy V V. Biomedical applications of hydrogels: A review of patents and commercial products. *Eur Polym J*. 2014;65:252–67.
8. Oxley H, Corkhill P, Fitton, Tighe B. Macroporous hydrogels for biomedical applications: methodology and morphology. *Biomaterials*. 1993 Nov;14(14):1064–72.

9. Ratner B, Hoffman A. Synthetic hydrogels for biomedical applications. *Med Relat Appl.* 1976.
10. Haldon RA, Leeb BE. Structure and Permeability of Porous Films of Poly (hydroxy ethyl methacrylate). *Br Polym J.* 1972;491–501.
11. Murphy SM, Skelly PJ, Tighe BJ. Synthetic Hydrogels. *J Mater Chem.* 1992;2(10):1007–13.
12. Peppas NA, Moynihan HJ, Lucht LM. The structure of highly crosslinked poly(2-hydroxyethyl methacrylate) hydrogels. *J Biomed Mater Res.* 1985;19:397–411.
13. Peppas NA, Gurny R, Doelker E, Buri P. Modelling of drug diffusion through swellable polymeric systems. *J of Memb Scie.* 1980;7:241–53.
14. Siepmann J, Peppas NA. Modeling of drug release from delivery systems based on hydroxypropyl methylcellulose (HPMC). *Adv Drug Deliv Rev.* 2001;48(2-3):139–57.
15. Hu J, Zhang G, Liu S. Enzyme-responsive polymeric assemblies, nanoparticles and hydrogels. *Chem Soc Rev.* 2012;41(18):5933.
16. Lee SJ, Park K. Synthesis and characterization of sol-gel phase-reversible hydrogels sensitive to glucose. *J Mol Recognit.* 1996;9(5-6):549–57.
17. Kim JJ, Park K. Modulated insulin delivery from glucose-sensitive hydrogel dosage forms. *J Control Release.* 2001 Nov;77(1-2):39–47.

18. Gupta P, Vermani K, Garg S. Hydrogels: from controlled release to pH-responsive drug delivery. *Drug Discov Today*. 2002 May 15;7(10):569–79.
19. Qiu Y, Park K. Environment-sensitive hydrogels for drug delivery. *Adv Drug Deliv Rev*. 2001 Dec;53(3):321–39.
20. Lee SC, Kwon IK, Park K. Hydrogels for delivery of bioactive agents: A historical perspective. *Adv Drug Deliv Rev*. 2013;65(1):17–20.
21. Cervidil Website. [cited 2016 Oct 5]. Available from: <http://www.cervidil.com/>
22. SUPPRELIN LA Website. [cited 2016 Oct 5]. Available from: <http://www.supprelinla.com/>
23. Baker W. Microgel, a new macromolecule. Relation to sol and gel as structural elements of synthetic rubber. *Rubber Chem Technol*. 1949;22(4):935–55.
24. Scott, R, Kuntzwillits R. Future applications of injectable biomaterials: the use of microgels as modular injectable scaffolds. In: Vernon B, editor. *Injectable Biomaterials: Science and Applications*. 1st ed. Woodhead Publishing; 2011.
25. DeCrosta, Mark T., Jain NB. Drug delivery systems including novel interpenetrating polymer networks and methods. United States; US 4575539A, 1985.
26. Sawai, Takashi, Shinsuke, Yamazaki, Ishigami Y. Rapid redispersion of pH-sensitive microgel flocculation with poly(lysine). *Macromolecules*. 1991;24(21):5801–5.

27. Snowden MJ. The use of poly(N-isopropylacrylamide) latices as novel release systems. *J Chem Soc, Chem Commun.* 1992;(11):803–4.
28. Murthy N, Xu M, Schuck S, Kunisawa J, Shastri N, Fréchet JMJ. A macromolecular delivery vehicle for protein-based vaccines: acid-degradable protein-loaded microgels. *Proc Natl Acad Sci USA.* 2003 Apr 29;100(9):4995–5000.
29. Zhang Y, Zhu W, Wang B, Ding J. A novel microgel and associated post-fabrication encapsulation technique of proteins. *J Control Release.* 2005 Jul 20;105(3):260–8.
30. Johansson C, Hansson P, Malmsten M. Mechanism of lysozyme uptake in poly(acrylic acid) microgels. *J Phys Chem B.* 2009 May 7;113(18):6183–93.
31. Heskins, Michael GJE. Solution properties of poly(N-isopropylacrylamide). *J Macromol Sci.* 1968;2(8):1441–55.
32. Pelton RH, Chibante P. Preparation of aqueous latices with N-isopropylacrylamide. *Colloids and Surfaces.* 1986 Oct;20(3):247–56.
33. Kriwet B, Walter E, Kissel T. Synthesis of bioadhesive poly(acrylic acid) nano- and microparticles using an inverse emulsion polymerization method for the entrapment of hydrophilic drug candidates. *J Control Release.* 1998 Dec;56(1-3):149–58.
34. Oh JK, Lee DI, Park JM. Biopolymer-based microgels/nanogels for drug delivery applications. *Prog Polym Sci.* 2009 Dec;34(12):1261–82.

35. Mitra S, Gaur U, Ghosh P., Maitra A. Tumour targeted delivery of encapsulated dextran–doxorubicin conjugate using chitosan nanoparticles as carrier. *J Control Release*. 2001 Jul;74(1-3):317–23.
36. Lee H, Mok H, Lee S, Oh Y-K, Park TG. Target-specific intracellular delivery of siRNA using degradable hyaluronic acid nanogels. *J Control Release*. 2007 Jun 4;119(2):245–52.
37. Fraser AK, Ki CS, Lin CC. PEG-based microgels formed by visible-light-mediated thiol-ene photo-click reactions. *Macromol Chem Phys*. 2014;215(6):507–15.
38. Rejman J, Oberle V, Zuhorn IS, Hoekstra D. Size-dependent internalization of particles via the pathways of clathrin- and caveolae-mediated endocytosis. *Biochem J*. 2004 Jan 1;377:159–69.
39. Prokov A. *Intracellular Delivery: Fundamentals and Applications*. Prokov A, editor. New York: Springer; 2011.
40. Sharma G, Valenta DT, Altman Y, Harvey S, Xie H, Mitragotri S, et al. Polymer particle shape independently influences binding and internalization by macrophages. *J Control Release*. 2010;147(3):408–12.
41. Champion JA, Walker A, Mitragotri S. Role of Particle Size in Phagocytosis of Polymeric Microspheres. *Pharm Res*. 2009;25(8):1815–21.
42. Fox ME, Szoka FC, Fréchet JMJ. Soluble polymer carriers for the treatment of cancer: the importance of molecular architecture. *Acc Chem Res*. 2009;42(8):1141–51.

43. Rippe C, Rippe A, Torffvit O, Rippe B. Size and charge selectivity of the glomerular filter in early experimental diabetes in rats. *Am J Physiol Renal Physiol*. 2007;293(5):F1533–8.
44. Hendrickson, Grant R., Lyon LA. Microgel Translocation Through Pores Under Confinement. 2010;49(12):2193–7.
45. Hoare T, Young S, Lawlor MW, Kohane DS. Thermoresponsive nanogels for prolonged duration local anesthesia. *Acta Biomater*. 2012;8(10):3596–605.
46. Murthy N, Thng YX, Schuck S, Xu MC, Frechet JMJ. A novel strategy for encapsulation and release of proteins: Hydrogels and microgels with acid-labile acetal cross-linkers. *J Am Chem Soc*. 2002;124(42):12398–9.
47. Metz N, Theato P. Synthesis and characterization of base labile poly(N-isopropylacrylamide) networks utilizing a reactive cross-linker. *Macromolecules*. 2009;42(1):37–9.
48. Ulbrich K, Šubr V, Seymour LW, Duncan R. Novel biodegradable hydrogels prepared using the divinyllic crosslinking agent N,O-dimethacryloylhydroxylamine. 1. Synthesis and characterisation of rates of gel degradation, and rate of release of model drugs, in vitro and in vivo. *J Control Release*. 1993;24(1-3):181–90.
49. Jung KO, Siegwart DJ, Lee H II, Sherwood G, Peteanu L, Hollinger JO, et al. Biodegradable nanogels prepared by atom transfer radical polymerization as potential drug delivery carriers: Synthesis, biodegradation, in vitro release, and bioconjugation. *J Am Chem Soc*. 2007;129(18):5939–45.

50. Kesselman LRB, Shinwary S, Selvaganapathy PR, Hoare T. Synthesis of monodisperse, covalently cross-linked, degradable “smart” microgels using microfluidics. *Small*. 2012;8(7):1092–8.
51. Bordenave N, Grelier S, Coma V. Advances on selective C-6 oxidation of chitosan by TEMPO. *Biomacromolecules*. 2008;9(9):2377–82.
52. Amsden BG, Sukarto A, Knight DK, Shapka SN. Methacrylated glycol chitosan as a photopolymerizable biomaterial. *Biomacromolecules*. 2007;8(12):3758–66.
53. Van Dijk-Wolthuis WNE, Franssen O, Talsma H, van Steenbergen MJ, Kettenes-van den Bosch JJ, Hennink WE. Synthesis, Characterization, and Polymerization of Glycidyl Methacrylate Derivatized Dextran. *Macromolecules*. American Chemical Society. 1995;28(18):6317–22.
54. Barbetta A, Massimi M, Di Rosario B, Nardecchia S, De Colli M, Devirgiliis LC, et al. Emulsion templated scaffolds that include gelatin and glycosaminoglycans. *Biomacromolecules*. 2008;9(10):2844–56.
55. Kiser PF, Wilson G, Needham D. Lipid-coated microgels for the triggered release of doxorubicin. *J Control Release*. 2000;68(1):9–22.
56. Nayak S, Lee H, Chmielewski J, Lyon LA. Folate-mediated cell targeting and cytotoxicity using thermoresponsive microgels. *J Am Chem Soc*. 2004;126(33):10258–9.

57. Kim JW, Utada AS, Fernández-Nieves A, Hu Z, Weitz DA. Fabrication of monodisperse gel shells and functional microgels in microfluidic devices. *Angew Chemie - Int Ed.* 2007;46(11):1819–22.
58. De Geest BG, Urbanski JP, Thorsen T, Demeester J, De Smedt SC. Synthesis of Monodisperse Biodegradable Microgels in Microfluidic Devices. *Langmuir. American Chemical Society*; 2005;21(23):10275–9.
59. Shah RK, Kim JW, Agresti JJ, Weitz DA., Chu L-Y. Fabrication of monodisperse thermosensitive microgels and gel capsules in microfluidic devices. *Soft Matter.* 2008;4(12):2303.
60. Seiffert S. Non-Spherical Soft Supraparticles from Microgel Building Blocks. *Macromol Rapid Commun.* 2012;33:1286–93.
61. Seiffert S, Weitz DA. Microfluidic fabrication of smart microgels from macromolecular precursors. *Polymer.* 2010;51(25):5883–9.
62. Pennisi E. ENCODE Project Writes Eulogy For Junk DNA. 2012;337:1159–61.
63. Carter PJ. Introduction to current and future protein therapeutics: a protein engineering perspective. *Exp Cell Res.* 2011;317(9):1261–9.
64. Vermonden T, Censi R, Hennink WE. Hydrogels for protein delivery. *Chem Rev.* 2012;112(5):2853–88.

65. Leader B, Baca QJ, Golan DE. Protein therapeutics: a summary and pharmacological classification. *Nat Rev Drug Discov.* 2008;7(1):21–39.
66. Research and Markets: Global Protein Therapeutics Market 2012-2016. *The Wall Street Journal.* 2008. Available from: <http://online.wsj.com/article/PR-CO-20130708-905749.html>
67. Maysinger D, Jalsenjak I, Cuello AC. Microencapsulated nerve growth factor: Effects on the forebrain neurons following devascularizing cortical lesions. *Neurosci Lett.* 1992;140:71–4.
68. Amidi M, Mastrobattista E, Jiskoot W, Hennink WE. Chitosan-based delivery systems for protein therapeutics and antigens. *Adv Drug Deliv Rev.* 2010;62(1):59–82.
69. Sinha VR, Trehan A. Biodegradable microspheres for protein delivery. *J Control Release.* 2003;90(3):261–80.
70. Van de Weert M, Hennink WE, Jiskoot W. Protein instability in poly(lactic-co-glycolic acid) microparticles. *Pharm Res.* 2000;17(10):1159–67.
71. Werle M, Bernkop-Schnürch a. Strategies to improve plasma half life time of peptide and protein drugs. *Amino Acids.* 2006;30(4):351–67.
72. Kurtzhals P, Havelund S, Jonassen IB, Kiehr B, Ribøl U, Markussen J. Albumin binding and time action of acylated insulins in various species. *J Pharm Sci.* 1996;85:304–8.

73. Bhadra D, Bhadra S, Jain P, Jain NK. Pegnology: a review of PEG-ylated systems. *Pharmazie*. 2002;57:5–29.
74. Frokjaer S, Otzen DE. Protein drug stability: a formulation challenge. *Nat Rev Drug Discov*. 2005;4(4):298–306.
75. Bysell H, Månsson R, Hansson P, Malmsten M. Microgels and microcapsules in peptide and protein drug delivery. *Adv Drug Deliv Rev*. 2011;63(13):1172–85.
76. Oh JK, Drumright R, Siegwart DJ, Matyjaszewski K. The development of microgels/nanogels for drug delivery applications. *Prog Polym Sci*. 2008;33(4):448–77.
77. Vinogradov S V. Colloidal microgels in drug delivery applications. *Curr Pharm Des*. 2007;12(36):4703–12.
78. Hennink WE, van Nostrum CF. Novel crosslinking methods to design hydrogels. *Adv Drug Deliv Rev*. 2012;64:223–36.
79. Goeddel D V, Kleid DG, Bolivar F, Heyneker HL, Yansura DG, Crea R, et al. Expression in *Escherichia coli* of chemically synthesized genes for human insulin. *Proc Natl Acad Sci USA*. 1979;76(1):106–10.
80. Laxminarayan R, Duse A, Wattal C, Zaidi AKM, Wertheim HFL, Sumpradit N, et al. Antibiotic resistance—the need for global solutions. *Lancet Infect Dis*. 2013;13(12):1057–98.

81. Superbugs threaten hospital patients. CDC Newsroom. 2016. Available from:
<http://www.cdc.gov/media/releases/2016/p0303-superbugs.html>
82. Reardon S. Phage therapy gets revitalized. Nature News. 2014.
83. Kutateladze M, Adamia R. Bacteriophages as potential new therapeutics to replace or supplement antibiotics. Trends Biotechnol. 2010;28(12):591–5.
84. Merril CR, Scholl D, Adhya SL. The prospect for bacteriophage therapy in Western medicine. Nat Rev Drug Discov. 2003;2(6):489–97.
85. Kutter E, De Vos D, Gvasalia G, Alavidze Z, Gogokhia L, Kuhl S, et al. Phage therapy in clinical practice: treatment of human infections. Curr Pharm Biotechnol. 2010;11(1):69–86.
86. D’Herelle F. Sur un microbe invisible antagoniste des bacilles dysenteriques. CR Acad Sci Paris. 1917;165:373–5.
87. Melville DuPorte E, Vanderleck J. Studies on *Coccobacillus Acridiorum* D’Herelle, and on Certain Intestinal Organisms of Locusts. Ann Entomol Soc Am. 1917;10(1):47–62.
88. Taylor MW. The Discovery of Bacteriophage and the d’Herelle Controversy. Viruses and man: a history of interactions. Springer; 2014.
89. Dublanchet A, Bourne S. The epic of phage therapy. Can J Infect Dis Med Microbiol. 2007;18(1):15–8.

90. D'Herelle F. *The Bacteriophage and its Behavior*. Baltimore, MD: Williams & Wilkins; 1926.
91. Luria SE, Anderson TF. The Identification and Characterization of Bacteriophages with the Electron Microscope. *Proc Natl Acad Sci U S A*. 1942;28(1):127–30.1.
92. D'Herelle F. Sur le role du microbe bacteriophage dans la typhose aviare. *Comptes rendus Acad Sci Paris*. 1919;169:932–4.
93. Summers WC. Cholera and plague in india: The bacteriophage inquiry of 1927-1936. *J Hist Med Allied Sci*. 1993;48(3):275–301.
94. d'Herelle F, Malone RH. A Preliminary Report of Work carried out by the Cholera Bacteriophage Enquiry. *Ind Med Gaz*. 1927;62(11):614–6.
95. Summers WC. Bacteriophage Therapy. *Annu Rev Microbiol*. 2001;(55):437–51.
96. Summers WC. Félix d'Herelle and the Origins of Molecular Biology. *J Hist Biol*. 2000;33(1).
97. Eaton MD, Bayne-Jones S. Bacteriophage therapy: review of the principles and results of the use of bacteriophage in the treatment of infections. *J Am Med Assoc*. 1934;103(23):1769–76.
98. Chanishvili N. Phage Therapy-History from Twort and d'Herelle Through Soviet Experience to Current Approaches. *Advances in Virus Research*. 2012;83:3-40.

99. Markoishvili K, Tsitlanadze G, Katsarava R, Glenn J, Sulakvelidze A. A novel sustained-release matrix based on biodegradable poly (ester amide)s and impregnated with bacteriophages and an antibiotic shows promise in management of infected venous stasis ulcers and other poorly healing wounds. *Int J Dermatol.* 2002;41(7):453–8.
100. Merabishvili M, Pirnay JP, Verbeken G, Chanishvili N, Tediashvili M, Lashkhi N, et al. Quality-controlled small-scale production of a well-defined bacteriophage cocktail for use in human clinical trials. *PLoS One.* 2009;4(3).
101. Rose T, Verbeken G, Vos D De, Merabishvili M, Vaneechoutte M, Lavigne R, et al. Experimental phage therapy of burn wound infection: difficult first steps. *Int J Burns Trauma.* 2014;4(2):66–73.
102. Phagoburn Clinical Trial. <http://www.phagoburn.eu/phagoburn-clinical-trial.html>
103. Uimajuridze A, Jvania G, Chanishvili N, Goderdzishvili M, Sybesma W, Managadze L, et al. Phage therapy for the treatment for urinary tract infection: Results of in-vitro screenings and in-vivo application using commercially available bacteriophage cocktails. *Eur Urol Suppl.* 2016;3(15):e265.
104. Sybesma W, Zbinden R, Chanishvili N, Kutateladze M, Chkhotua A, Ujmajuridze A, et al. Bacteriophages as Potential Treatment for Urinary Tract Infections. *Front Microbiol.* 2016;7.

105. Rhoads DD, Wolcott RD, Kuskowski MA, Wolcott BM, Ward LS, Sulakvelidze A. Bacteriophage therapy of venous leg ulcers in humans: results of a phase I safety trial. *J Wound Care*. 2009;18(6).
106. Vandenneuvel D, Lavigne R, Brüßow H. Bacteriophage Therapy: Advances in Formulation Strategies and Human Clinical Trials. *Annu Rev Virol*. 2015;2(1):599–618.
107. Payne, Robert J H and Jansen V. Understanding Bacteriophage Therapy as a Density-dependent Kinetic Process. *J Theor Biol*. 2001;208:37–48.
108. Yongsheng M, Pacan JC, Wang Q, Xu Y, Huang X, Korenevsky A, et al. Microencapsulation of bacteriophage felix O1 into chitosan-alginate microspheres for oral delivery. *Appl Environ Microbiol*. 2008;74(15):4799–805.
109. Tang Z, Huang X, Baxi S, Chambers JR, Sabour PM, Wang Q. Whey protein improves survival and release characteristics of bacteriophage Felix O1 encapsulated in alginate microspheres. *Food Res Int*. 2013;52(2):460–6.
110. Puapermpoonsiri U, Spencer J, van der Walle CF. A freeze-dried formulation of bacteriophage encapsulated in biodegradable microspheres. *Eur J Pharm Biopharm*. 2009;72(1):26–33.
111. Korehei R, Kadla JF. Encapsulation of T4 bacteriophage in electrospun poly(ethylene oxide)/cellulose diacetate fibers. *Carbohydr Polym*. 2014;100:150–7.
112. Vonasek E, Le P, Nitin N. Encapsulation of bacteriophages in whey protein films for extended storage and release. *Food Hydrocoll*. 2014;37:7–13.

113. Salalha W, Kuhn J, Dror Y, Zussman E. Encapsulation of bacteria and viruses in electrospun nanofibres. *Nanotechnology*. 2006;17(18):4675–81.

114. Dini C, Islan G a., de Urza PJ, Castro GR. Novel biopolymer matrices for microencapsulation of phages: Enhanced protection against acidity and protease activity. *Macromol Biosci*. 2012;12(9):1200–8.

2 Prolonged Release of Bioactive Model Proteins from Anionic Microgels Fabricated with a New Microemulsion Approach¹

2.1 Abstract

Purpose Therapeutic proteins have become an integral part of health care. However, their controlled delivery remains a challenge. Protein function depends on a delicate three dimensional structure, which can be damaged during the fabrication of controlled release systems. This study presents a microgel-based controlled release system capable of high loading efficiencies, prolonged release and retention of protein function.

Methods A new DMSO/Pluronic microemulsion served as a reaction template for the crosslinking of poly(acrylic acid) and oligo(ethylene glycol) to form microgels. Poly(acrylic acid) molecular weights and microgel crosslinking densities were altered to make a series of microgels. Microgel capacity to capture and retain proteins of different sizes and isoelectric points, to control their release rate (over ~30 days) and to maintain the biofunctionality of the released proteins were evaluated.

Results Microgels of different sizes and morphologies were synthesized. Loading efficiencies of 100% were achieved with lysozyme in all formulations. The loading efficiency of all other proteins was formulation dependent. Release of lysozyme was achieved for up to 30 days and the released lysozyme retained over 90% of its activity.

Conclusions High loading efficiencies and prolonged release of different proteins was achieved. Furthermore, lysozyme's functionality remained uncompromised after encapsulation and release. This work begins to lay the foundation for a broad platform for the delivery of therapeutic proteins.

¹Reprinted with permission from *Pharmaceutical Research*, 33(4). Rios JL, Lu G, Seo NE, Lambert T, Putnam D., Prolonged Release of Bioactive Model Proteins from Anionic Microgels Fabricated with a New Microemulsion Approach, 879-92, Copyright 2016 Springer.

2.2 Introduction

The advent of modern biotechnology has seen a remarkable increase in the number of therapeutic proteins, and many potential protein drug candidates are in the development pipeline (1). Currently the FDA has approved more than 130 protein-based pharmaceutical products (2,3) with an estimated market annual growth rate of 7.08% projected until 2016 (4). While modern biotechnology has made the production of protein pharmaceuticals possible, there are substantial hurdles to be overcome. Protein function depends on a delicate three dimensional structure, which can be compromised by both proteolytic/chemical degradation and physical/shear forces (5). Because of these characteristics, combined with their high molecular weight, which makes passive transport through biological membranes difficult, oral administration is largely ineffective for systemic indications. To date, almost all therapeutic proteins are administered by the parenteral route and often require frequent administration due to their short half-lives (2). The delivery of protein therapeutics at defined dosage in a safe and minimally invasive manner remains a prominent challenge in the field. Therefore, there is an increasing need for well-defined controlled release protein delivery systems.

Polymeric hydrogel microparticles, referred to as microgels herein, have received recent attention for their potential use as controlled release protein delivery vehicles (6–8). Microgels are micron-scale cross-linked three dimensional networks of hydrophilic polymers that swell in aqueous environments. The cross-linked networks can be formed by a variety of means including physical entanglement, ionic interactions, or covalent bonds (9). Biodegradable microgels can be synthesized by inclusion of degradable linkages in the polymer or the crosslinker. Microgels also can be designed to have unique characteristics such as the ability to undergo volume changes in response to external stimuli such as pH, temperature or ionic strength, which can be used to

develop environmentally responsive drug delivery systems (10). Furthermore, the micron-scale size of microgels can allow for their injection by standard methods.

Acrylic acid (AA) is one building block used in the synthesis of microgels and its polymerized form, poly(acrylic acid) (pAA), is generally biocompatible (11,12). Most studies that use AA for microgel synthesis report various forms of emulsion/suspension polymerization as the preferred formulation method. This method is effective but it has drawbacks. In particular, there is poor control over the overall molecular weight of the polymer backbone. Because the backbone of pAA is not biodegradable, its elimination from the body is largely restricted to glomerular filtration, but this route of elimination is restricted to lower molecular weights. Ideally, an injectable controlled release protein delivery system would be eliminable from the body to reduce accumulation over time.

In the present study, a new approach toward the synthesis and fabrication of microgels composed of pAA cross-linked with oligo(ethylene glycol) (OEG) is reported. The microgels are unique in two ways. First, the pAA backbone is first synthesized by RAFT polymerization to well-defined molecular weights with narrow polydispersity. Second, the microemulsion used to crosslink and fabricate the microgels is a newly developed system of DMSO microdroplets suspended by homogenization in Pluronic[®] L35 as the continuous phase to create well-defined and tunable microreaction templates. Specifically, a series of pAA-OEG cross-linked microgels was prepared by changing the cross-linking density and the molecular weight of the pAA. To our knowledge, this two-stage microgel synthesis and formulation approach has not been reported, and it provides a distinct opportunity to maintain control over the microgel architecture and molecular weight of the pAA, which was kept below its glomerular filtration limit of $M_w \sim 40,000$ (13). The ability of the microgels to retain proteins was assessed using proteins with

different molecular weights and different isoelectric points (pI) (Table 1) to help better understand the collective effects of microgel porosity and charge on protein absorption. The controlled release of proteins from the microgels was evaluated *in-vitro* and the protein activity (using lysozyme enzymatic activity as a model) was quantified to establish that protein activity was retained over the course of 30 day release.

Table 2.1. Properties of proteins loaded in microgels. Different physicochemical characteristics such as charge and molecular weight were investigated to explore the versatility of the microgels for controlled release.

Protein	Molecular Weight (kDa)	Isoelectric Point	Charge at pH=7.4
Lysozyme	14.3	11.35	+
Hemoglobin	64.5	6.8	~neutral
Myoglobin	17.7	7.2	~neutral
β -lactoglobulin	18.4	5.1	-
Bovine serum albumin	66.5	4.7	-

2.3 Materials and Methods

2.3.1 Materials

Acrylic acid, anhydrous methanol, 4-cyanopentanoic acid dithiobenzoate (CPA-DB), 4,4'-azobis(4-cyanopentanoic acid) (A-CPA), dimethyl sulfoxide, 4-methylmorpholine (NMM), tetraethylene glycol, Pluronic[®] L35, lysozyme, hemoglobin, myoglobin, β -lactoglobulin, bovine serum albumin and *M. lysodeikticus* were purchased from Sigma-Aldrich and used without further purification. 4-(4,6-Dimethoxy-1,3,5-triazin-2-yl)-4-methylmorpholinium chloride (DMTMM) was purchased from Tokyo Chemical Industry America. Phosphate buffered saline (PBS) was purchased from Cellgro. BCA Protein Assay Kit was purchased from Thermo Fisher Scientific.

2.3.2 Synthesis of poly(acrylic acid)

Acrylic acid was polymerized by reversible addition-fragmentation chain transfer (RAFT) polymerization. This technique allows for the synthesis of polymers with well controlled molecular weights and relatively narrow PDI. The polymerizations were carried out as previously reported by our group (14). The amounts of CPA-DB and A-CPA were adjusted to achieve different molecular weights. A representative polymerization to synthesize pAA with M_n of 15,500 and PDI of 1.3 was performed as follows: CPA-DB (184 mg, 0.659 mmol) and A-CPA (46 mg, 0.164 mmol) were combined in a Schlenk flask with a magnetic stir bar. Anhydrous methanol was purged with dry nitrogen for 10 minutes then added (36.6 mL) to the CPA-DB and A-CPA mixture in the Schlenk flask, followed by complete dissolution with stirring. AA (9.5 mL, 0.138 mol) was then added into the Schlenk flask, a condenser column fitted to the flask and the entire system was purge with dry nitrogen for an additional 15 minutes.

The reaction vessel was covered with aluminum foil to protect the reactants from light and the polymerization initiated by lowering the reaction flask into a 60 °C oil bath with continuous stirring. The reaction was stopped at 48 hours by placing the Schlenk flask in an ice bath and exposing the contents to air. The cooled solution was directly transferred into Spectra/Por regenerated cellulose dialysis tubing (3.5 kDa MWCO) and dialyzed against deionized water for one week. The product was recovered by lyophilization.

The M_w , M_n , and PDI of the resulting pAA were determined using a Waters gel permeation chromatography (GPC) system equipped with Ultrahydrogel columns in series, 1515 isocratic HPLC pump and 2414 refractive index detector with temperature controlled at 30 °C. The mobile phase used was phosphate buffer saline (pH=7.4) at a rate of 0.8 mlmin⁻¹ and calibrated with poly(acrylic acid), sodium salt standards. ¹H NMR was used to confirm the structure of the resulting pAA.

2.3.3 Preparation and Characterization of Microgels

The microgels were synthesized by cross-linking the carboxylate side chains of pAA with the alcohol end-groups of OEG via esterification. The esterification was facilitated with DMTMM, previously shown as an effective condensation reagent (15), see Figure 2.1 for a schematic of the reaction. In a typical reaction, pAA (120 mg) was dissolved in dimethyl sulfoxide (1.5 mL). Varying amounts of DMTMM and NMM were added to this solution depending on the molar ratios of the reaction, see Table 2. After complete dissolution, the OEG was added to this solution with stirring until homogeneity was achieved. The reaction solution was then added all at once to a 100 mL beaker containing Pluronic[®] L35 (40 g), which acts as the continuous phase, and the resulting microemulsion was stirred at 750 rpm using a Silverson L5M-A homogenizer with a 3/4" head for 4 hours at room temperature. The microgels were

isolated by centrifugation at 9500 rpm and the supernatant of Pluronic[®] L35 was decanted. The microgels were thoroughly washed by at least 5 cycles of re-suspension in deionized water, centrifugation and decantation. Lastly, the microgels were suspended in a small volume of deionized water and lyophilized to dryness. Size fractionation by differential centrifugation was also used to isolate ranges of microgel sizes. Specifically, microgels were suspended in deionized water and centrifuged at 1000 rpm for 2 minutes, at which point the supernatant and pellets were separated into different fractions of smaller and larger size microgels. The morphology and size of the microgels was observed using scanning electron microscopy (SEM) (Tescan MIRA3) and the incorporation of OEG was assessed by FTIR spectroscopy (Hyperion 2000, Bruker). To confirm that the microgels can degrade back into the original M_n of pAA used in the formulation, a forced degradation study was performed. Briefly, 10 mg of microgels were suspended in 1 N NaOH under stirring to create an initially turbid solution that became clear after 2 hours. This solution was then dialyzed against DI water using Spectra/Por regenerated cellulose dialysis tubing (3.5 kDa MWCO) overnight to remove residual NaOH, lyophilized and re-dissolved in buffer for GPC analysis (as above).

Table 2.2: Formulation parameters of synthesized microgels used in this study. The molecular weight of both polymers was kept under the glomerular filtration limit of ~40,000. The COOH:PEG molar ratio represents the ratio between the carboxylate side chains of the pAA to the OEG.

Microgel	Poly(acrylic acid) Mn (g/mol)	Oligo(ethylene glycol) Mn (g/mol)	Molar Ratio COOH:OEG	Molar Ratio COOH:DMTMM
M1	9,800	194	1:0.8	1:0.6
M2	9,800	194	1:0.4	1:0.6
M3	9,800	194	1:0.2	1:0.6
M4	9,800	194	1:0.8	1:0.2
M5	9,800	194	1:0.4	1:0.2
M6	9,800	194	1:0.2	1:0.2
M7	15,500	194	1:0.8	1:0.6
M8	15,500	194	1:0.4	1:0.6
M9	15,500	194	1:0.2	1:0.6
M10	15,500	194	1:0.8	1:0.2
M11	15,500	194	1:0.4	1:0.2
M12	15,500	194	1:0.2	1:0.2

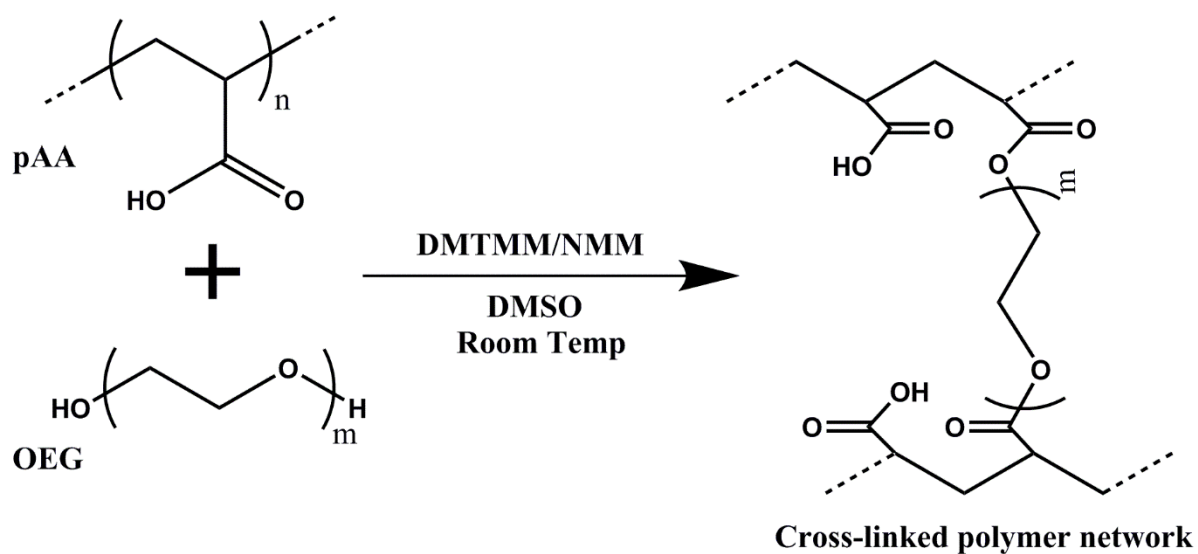


Figure 2.1. Schematic of cross-linking reaction to form microgels. The alcohol end-groups of OEG are condensed with the carboxylate side-chains of pAA facilitated by the addition of DMTMM.

2.3.4 Protein Loading

To quantify protein loading, dry microgels (5mg) were suspended in protein solution (2 mg/mL, 2 mL total) in PBS at 37 °C under gentle rotation (8 RPM) in polypropylene Eppendorf tubes. The microgels were allowed to incubate for 24 hours then recovered by centrifugation (5000 rpm, 5 min), followed by one wash with PBS in the same fashion. The supernatants were isolated and the protein-loaded microgels were flash frozen in liquid nitrogen and lyophilized to dryness. The supernatants were stored at 4 °C prior to quantitation of protein concentration. The supernatants were assayed using a Thermo Scientific Pierce bicinchoninic acid Protein Assay Kit (BCA assay) for protein concentration to calculate the amount of protein loaded. The protein loading efficiency (LE) was calculated using Eq. 1:

$$LE (\%) = \frac{P_L}{P_T} \times 100\%$$

where P_L is the amount of protein loaded in the microgels and P_T is total amount of protein.

The distribution of loaded lysozyme within the microgel network was investigated using confocal microscopy. Lysozyme was labeled with FITC by preparing 10 mL of a 2 mg/mL lysozyme solution in borate buffer at pH 8.5 and then adding 500 μ L of a 1 mg/mL solution of FITC in DMSO. The reaction was allowed to incubate overnight at 4°C under gentle stirring and protected from light. The FITC-labeled lysozyme was purified by dialysis against distilled water and lyophilized. Formulation M1 and M4 were loaded with FITC-labeled lysozyme as described above then imaged using a Zeiss LSM 710 confocal microscope.

2.3.5 Protein Release

Protein-loaded and lyophilized microgels were suspended in 1 mL of PBS in polypropylene Eppendorf tubes and incubated with rotation (8 RPM) at 37 °C. At specific time points, the microgels were separated from the buffer by centrifugation (5 min, 5000 rpm), whereupon the supernatant was collected in its entirety and replaced with 1 mL fresh PBS. The supernatant was then assayed using the BCA assay to quantify the protein concentration.

2.3.6 Lysozyme Activity Assay

The biological activity of released lysozyme was determined using the *M. lysodeikticus* assay (16). A 0.01% w/v suspension of *M. lysodeikticus* was made in potassium phosphate buffer (66 mM, pH 6.24) prepared from potassium phosphate monobasic and potassium phosphate dibasic crystals. A 15 μ L aliquot of appropriately diluted lysozyme solution was added into a 96 well-plate and mixed with 200 μ L of prepared *M. lysodeikticus* suspension. Immediately after, the plate was placed in a SpectraMAX Plus384 Microplate Reader (Molecular Devices Corp.) and the absorbance was monitored for 6 minutes (450 nm, 25 °C). Each sample was measured in triplicate. The lysozyme activity was determined from the slope of the linear portion in the plot of absorbance versus time. One Enzyme Unit (EU) was defined as the change in absorbance (450 nm) of 0.001 per minute at 25 °C. The activity was then compared to that of native lysozyme to quantify loss in activity relative to unencapsulated lysozyme.

2.4 Results and Discussion

pAA-OEG cross-linked microgels were synthesized using a new approach. Rather than mixing and reacting monomer mixtures in an uncontrolled fashion, microgels were synthesized by the crosslinking of well-defined pAA backbones within a DMSO/Pluronic microemulsion. Formulations with different characteristics were achieved by varying the M_n of pAA, the crosslinking density and the emulsion characteristics in which the crosslinking took place. In this study, we evaluated the microgel's ability to capture proteins of different sizes and pI's, control their release and to maintain the integrity and function of the released proteins. Lastly, to better understand how the microgels controlled the rate of protein release, ion-exchange was investigated by conducting the release experiments in buffers with variable ionic strength while holding the pH constant. The protein capture and release kinetics were formulation dependent, thereby allowing significantly different release kinetics for different potential clinical applications.

2.4.1 Synthesis and Characterization of Poly(acrylic acid)

pAA was synthesized by RAFT polymerization to enable control over M_n and polydispersity. Such control allows the synthesis and formulation of well-defined microgels to ensure that subsequent degradation products can be below the upper limit of glomerular filtration to prevent accumulation of the polymer and enhance the potential of clinical translation. For this report, pAA with two M_n 's were synthesized (M_n 9,800 and 15,500) with polydispersities of 1.2 and 1.3, respectively. These M_n 's are well below the upper limit of glomerular filtration for pAA (13), thereby allowing even soluble degradation products with a low degree of crosslinking to remain below the glomerular filtration limit. For the sake of brevity, these polymers are abbreviated as pAA(9) and pAA(15) throughout the manuscript. ^1H NMR confirmed the

structure of pAA with peaks at 1.3-2.0 ppm and 2.3-2.6 ppm corresponding to the backbone protons of the polymer (Figure 2.2) (14). A peak at around 3.7 corresponds to partial methylation of the carboxylate side-chains resulting from methanol as the polymerization solvent and peaks at 2.6 and 4.4 correspond to acrylic acid dimers that remain functional groups for crosslinking with OEG (17).

2.4.2 Characterization of pAA-OEG Microgels

The size and morphology of microgels are important to match the system characteristics with potential clinical applications. Furthermore, maintaining control over these parameters increases the versatility and functionality of the system. For example, for intracellular delivery into non-phagocytocic cells (e.g. endothelial, epithelial etc.), the upper particle diameter size limit is $<1 \mu\text{m}$ with optimal sizes $< 200 \text{ nm}$ (18,19). For delivery into phagocytic cells a size range between $1\text{-}3 \mu\text{m}$ is optimal (20,21) and lastly, if the particles are designed to remain localized at the site of administration, particle sizes exceeding $10 \mu\text{m}$ are desired to avoid clearance by phagocytic cells. SEM was used to visualize and determine the size and morphology of the microgels derived from various formulation conditions. Both the size and shape of the microgels depended greatly on the cross-linking density. The general pattern showed that as the cross-linking density decreased, the microgels became bigger and less spherical (Figure 2.3). Microgels of different size populations were isolated by differential centrifugation (Figure 2.4). The small fraction consists of microgels $< 5 \mu\text{m}$ in diameter and the large fraction contained microgels reaching up to $20 \mu\text{m}$ in diameter. As previously mentioned, the microgel sizes are important when considering potential therapeutic applications. The incorporation of OEG into the microgels was verified in two ways. First, when OEG was

omitted from the microgel synthesis protocol, no microgels were obtained. Second, FTIR was performed on pAA, OEG and microgels. It can be observed that FTIR spectra of the microgels is a combination of the pAA and OEG spectra (Figure 2.5). Another important aspect of the microgels is their ability to degrade into the original components, thus ensuring that degradation products are within the limits of glomerular filtration. Upon forced degradation in 1 N NaOH, the resulting product was analyzed by GPC (Figure 2.6). The chromatograms of the pAA used to synthesize the degraded microgels and the degradation product overlay well with each other, thereby supporting the premise that the microgels can degrade back into components used in their synthesis and are able to degrade to M_n below the glomerular filtration limit (2.7).

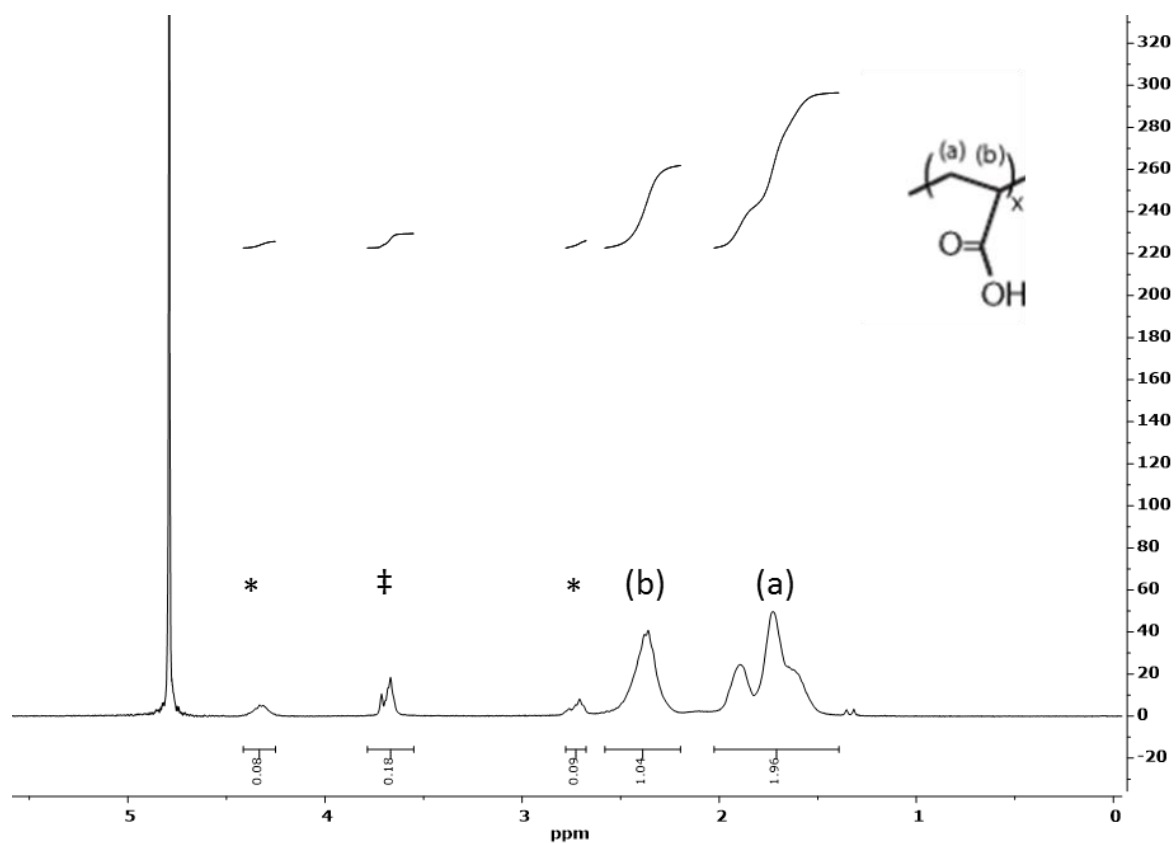


Figure 2.2. ^1H NMR of pAA synthesized by RAFT polymerization. Peaks (a) and (b) correspond to the backbone protons. Peak ‡ corresponds to partial methylation of the carboxylate side-chain which occurs during polymerization in methanol. Peak * corresponds to dimerization of the monomer, as has been previously reported in the literature (39).

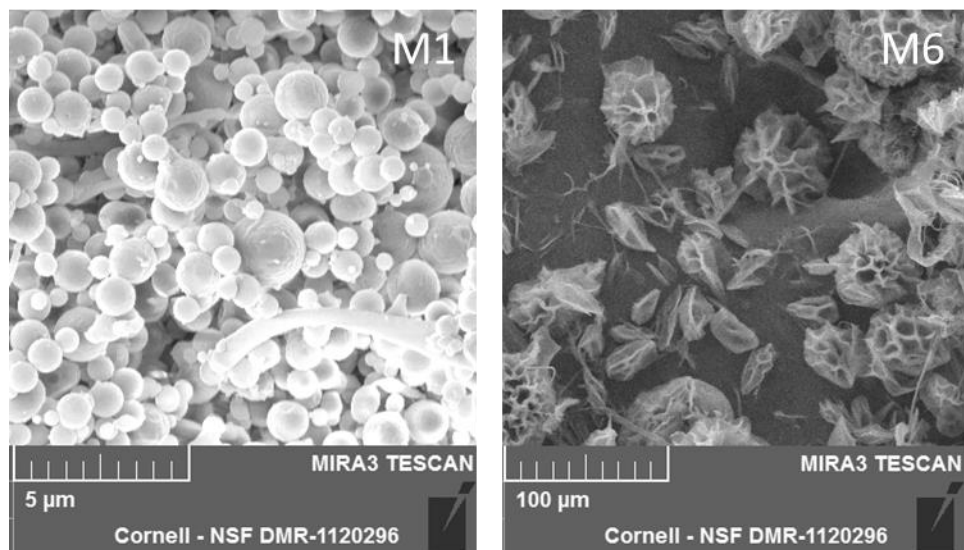


Figure 2.3. Representative scanning electron microscopy of representative microgels. Higher cross-linking density (M1) leads to smaller more spherical microgels compared to more loosely cross-linked formulations (M6) which leads to more porous microgels.

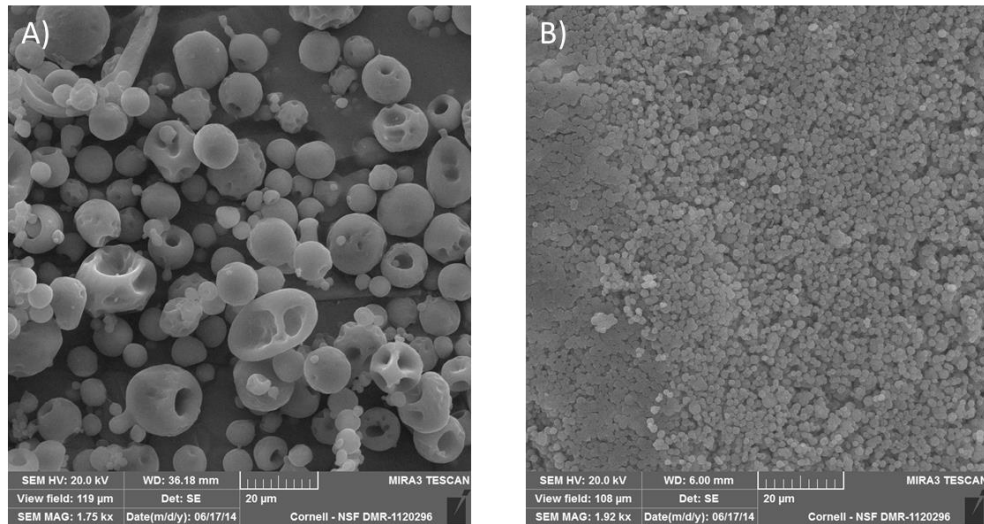


Figure 2.4. Differential centrifugation of microgels. A) shows the larger fraction that pellets at 1000 rpm and B) shows the microgels recovered from the supernatant. The larger fraction is more heterogeneous and contains particles of up to $\sim 20 \mu\text{m}$ while the smaller fraction contains particles less than $5 \mu\text{m}$.

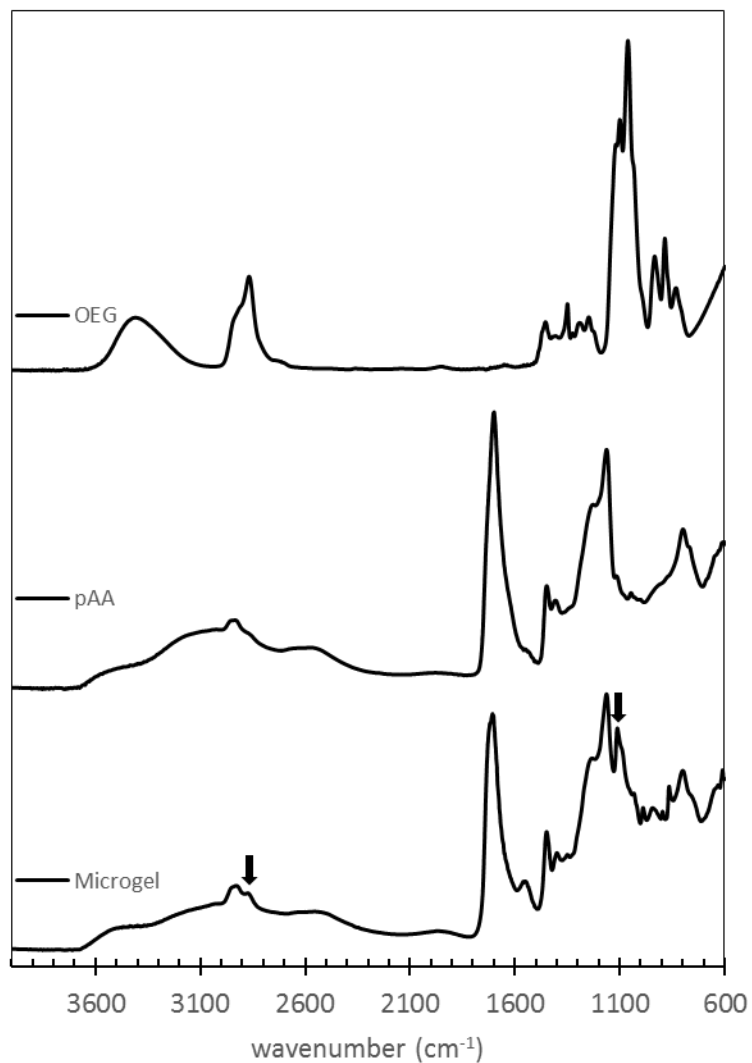


Figure 2.5. FT-IR spectroscopy of microgels, OEG and pAA. The FT-IR spectra of the microgels closely resembles that of pAA and distinct peaks from the OEG are shown with the black bold arrows.

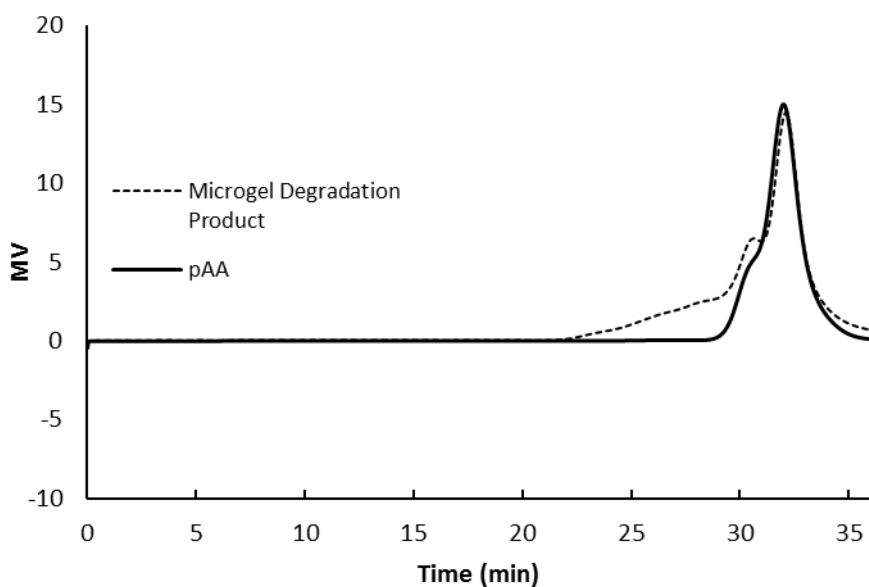


Figure 2.6. GPC chromatogram of pAA used in microgel synthesis (solid line) and product from forced microgel degradation (dashed line). The degradation product chromatogram overlays well with that of the pAA used to synthesize the microgels. The degradation chromatogram also exhibits a tail of higher molecular weight chains, most likely corresponding to lightly cross-linked pAA.

2.4.3 Protein Capture by Microgels

Unlike traditional microencapsulation methods, proteins were incorporated into microgels only after their synthesis, purification, lyophilization and characterization (i.e., post-loading). Using a post-loading approach prevents formulation complications, such as side reactions with the protein or protein denaturation from exposure to surfactants and high shear stresses, that can occur during microgel formation (22,23). However, one drawback to the post-loading method is the relatively low loading efficiencies, which can lead to the administration of large microgel quantities to achieve therapeutically relevant protein concentrations (23,24). The pAA-OEG microgels capture capability of proteins with varying molecular weights and pIs was assessed. Lysozyme was determined to have loading efficiencies approaching 100% (0.8 mg protein/mg microgel) (Figure 2.7a-d). This high degree of loading is attributed to lysozyme's relatively low molecular weight (14.3 kDa) and net positive charge at pH 7.4 (lysozyme pI = 11.35). The unreacted and free carboxyl groups of the pAA-OEG microgels ($pK_a \sim 4.35$) are negatively charged at pH 7.4, thereby facilitating polyionic interactions between the microgel backbone and the protein, leading to high loading efficiency. The maximum amount of lysozyme loaded was measured by incubating the M1 microgel (5 mg) with 2 mL of a 10 mg/mL lysozyme solution in PBS. It was determined that lysozyme loading was 63% w/w. This protein loading efficiency is significantly higher than other microgel/hydrogel systems that make use of the post-loading method. For example, the group of Ding et al. reported the loading of proteins into lactic acid-Pluronic[®] F127 microgels of 8.7% w/w for hemoglobin, 9.7% w/w for albumin and 7% w/w for lysozyme (23). Using principles of aqueous two-phase extraction McBride et al. reported increased loading efficiencies with the post-loading method into dextran gels achieving ovalbumin loading of 27% w/w and α -amylase of 6.7% w/w (24).

Myoglobin and hemoglobin also had relatively high loading efficiencies into the pAA-OEG microgels, approaching 100% for some formulations, following a trend in which the least cross-linked formulations led to higher loading efficiencies (Figure 2.7a-d). One advantage of hemoglobin and myoglobin loading is that it could be qualitatively assessed visually by observing the change in color of both the supernatant and the microgels (Figure 2.8). Albumin had lower overall loading efficiencies and did not load at all in some formulations, but was loaded into others with efficiencies exceeding 70%. The higher loading efficacy was unexpected because albumin is negatively charged at pH 7.4 and Coulombic repulsion was expected with the carboxyl groups of the microgel matrix. This phenomenon has been observed by other groups as well. Albumin adsorbs to pAA-coated microspheres even though both components are negatively charged (25,26). Furthermore, other proteins have been shown to complex with polyelectrolytes even under conditions in which both components are like-charged (27). A theoretical framework to explain this phenomenon in thermodynamic terms has been proposed (28–30). In brief, the thermodynamic argument to support the results is that while the net charge of albumin at pH 7.4 is negative, patches of positive charges remain on the protein surface that can interact with the negatively charged “patches” of pAA. The positive patch acts as a multivalent ion segment that can associate with the multiple negative charges on the pAA. The physical phenomenon of counterion release (or counterion release force) also contributes to the interaction by the favorable increase in entropy (31).

The distribution of loaded lysozyme within the microgels was also evaluated using microgels loaded with FITC-labeled lysozyme. The microgels were imaged under confocal microscopy and Z-stacks were taken to investigate the distribution of lysozyme within both high-crosslinked (M1) and low-crosslinked (M4) microgels. It was found that lysozyme is distributed

throughout the microgel and no apparent differences in the distribution are found between the formulations (Fig. 2.9)

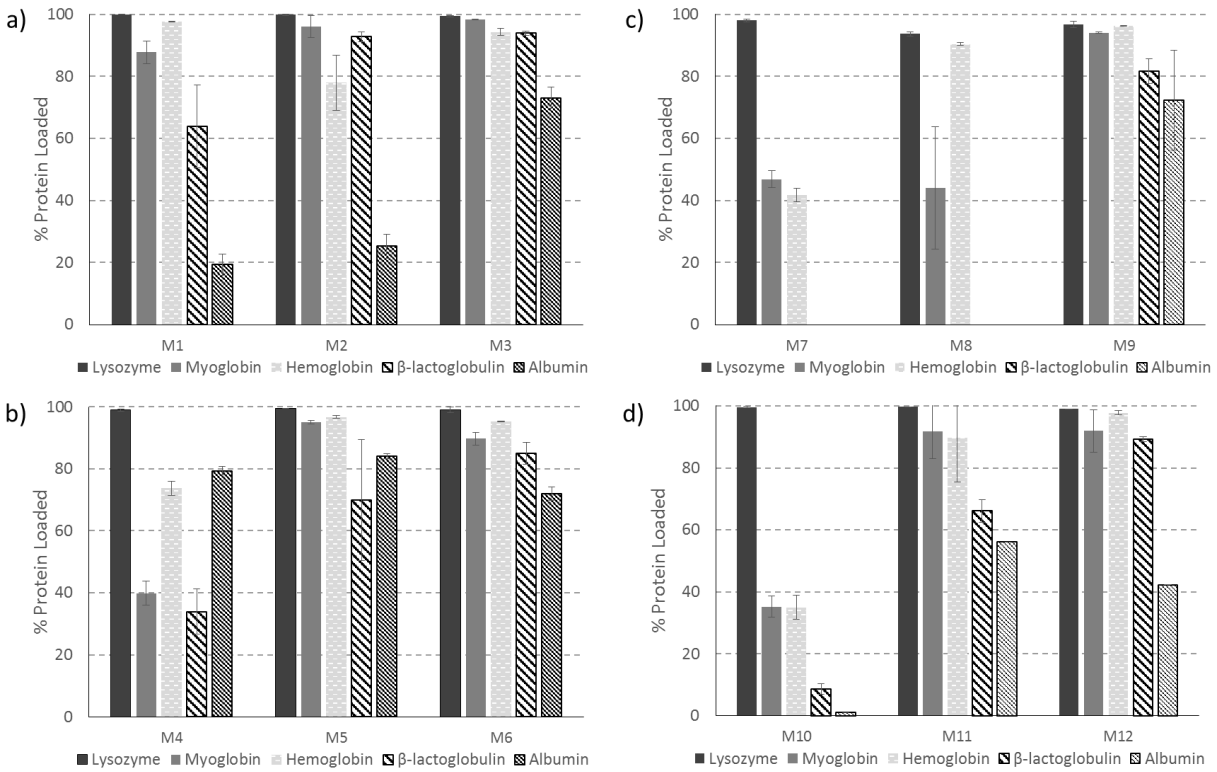


Figure 2.7. Protein loading efficiency into all microgel formulations, a) M1-M3, b) M4-M6, c) M7-M9, d) M10-M12. Lysozyme showed loading efficiencies greater than 90% for all formulations. There was a general trend of increasing loading efficiency with decreasing cross-linking density. All samples were conducted in triplicate.

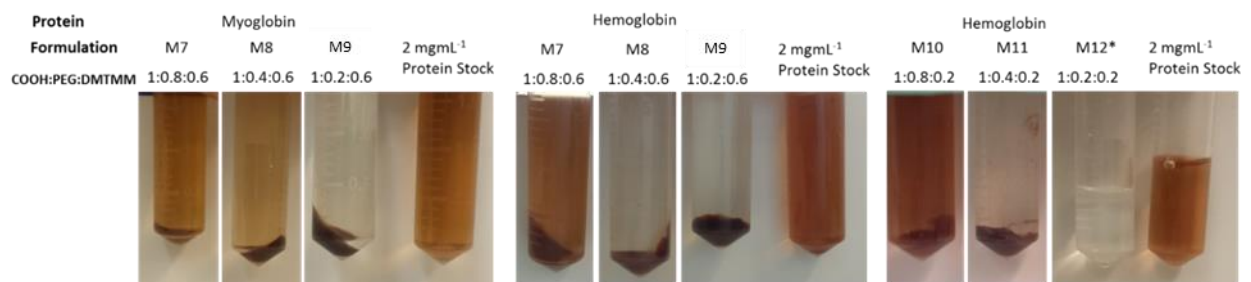


Figure 2.8: Images showing qualitative information on myoglobin and hemoglobin loading. Comparing the protein stock to the supernatant, one can infer successful loading from the color change. *M12 shows only the recovered supernatant, no pellet present.

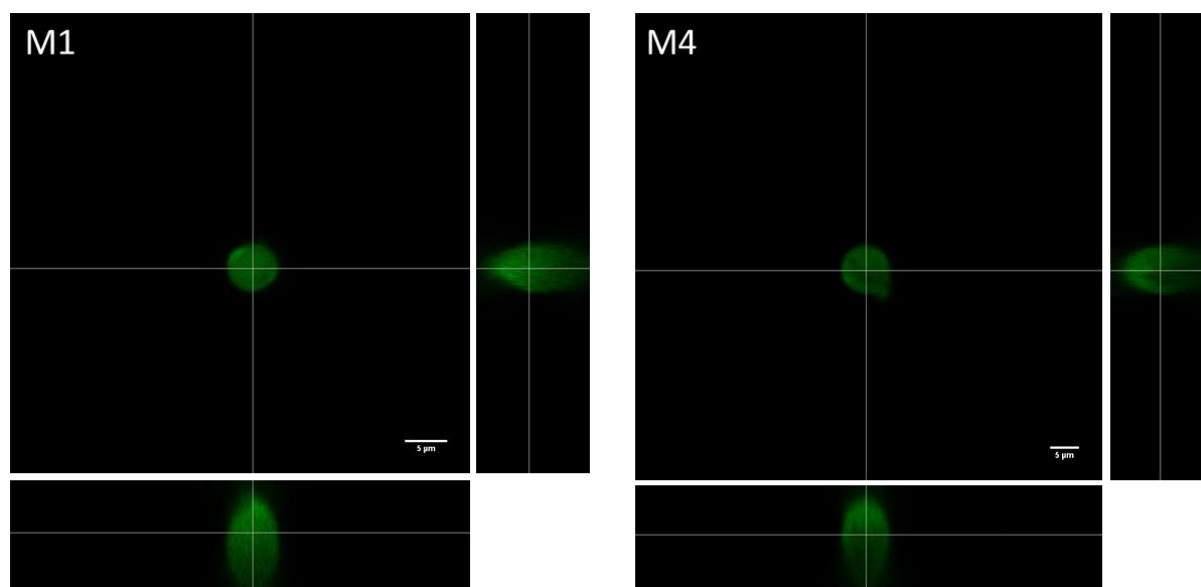


Figure 2.9 Confocal orthogonal images showing the distribution of lysozyme within formulation M1 (densely cross-linked, left figure) and M4 (lightly cross-linked, right figure). The circular image in the center of each figure is a Z-slice of the full microgel. The images to the right and bottom of each figure are the orthogonal images of the Z-slice. The continuous green dissemination throughout each image shows that lysozyme is distributed throughout the microgel in both formulations, thus ruling out loading distribution differences as the cause for differences in the release rate. Scale bar=5 µm.

2.4.4 In-vitro Protein Release and Activity

To evaluate how protein release kinetics related to microgel composition, in-vitro release studies were conducted for proteins loaded into the microgel formulations. The characteristics of each protein (e.g. molecular weight, pI) and of each microgel formulation (e.g. crosslinking density, anionic charge density) can influence protein release kinetics.

Lysozyme was released over periods of up to one month (Figure 2.10) with some formulations while retaining its enzymatic activity (Table 3). Lysozyme has been released from other hydrogel systems but rarely for such prolonged times. For example, over 65% of lysozyme was released within 30 hours from peptide nanofiber hydrogels (32) and full release of lysozyme was observed within 6 days from dextran hydrogels (33). Additionally, a study attempting to make use of opposite electrostatic interactions using anionic dextran hydrogels reported cumulative release of over 50% of cytochrome C (MW=12,384 kDa, pI=10.2) within 50 hours (22). In the pAA-OEG microgels, formulations M4-M6 released ~50% of lysozyme at 13 days and kept releasing lysozyme up to 30 days. Furthermore, lysozyme's release rate was slowest in the least cross-linked formulations, which is opposite of convention. Generally, compounds entrapped within hydrogel matrices release by diffusion more quickly in hydrogels with lower crosslinking densities (34). However, for these pAA-OEG microgels, low crosslinking density, due either to lower OEG content or lower DMTMM content during synthesis, leads to a higher free carboxyl content. Lysozyme retains a net positive charge at pH 7.4 and therefore has an electrostatic affinity towards the microgel matrix, and the magnitude of the electrostatic attraction increases with decreasing crosslinking density. We postulated that the mechanism of lysozyme release from the matrix was by ionic exchange with the salts present in the PBS release medium. To evaluate this proposed release mechanism, lysozyme release studies from

formulations M5 and M8 were conducted in 4X PBS to evaluate the effect of ionic strength on the rate of release (Figure 2.11). Lysozyme was fully released within two hours, strongly suggesting that a dominating mechanism of release is through ionic exchange. The M_n of the pAA used in the formulations also seem to influence the rate of release of the lysozyme. Formulations made with pAA(15) had a faster rate of release than formulations made with pAA(9). This trend might be attributed to a reduced total number of polymer chains within the microgel matrix thereby increasing the diffusivity of lysozyme within the matrix. In addition to prolonged release, the lysozyme released from the microgels retain its functionality as measured by its enzymatic activity relative to native lysozyme (Table 3). Lysozyme released from formulations M7 through M12 retained over 90% activity when compared to native lysozyme. From these results, it can be postulated that the post-loading incorporation of proteins and their retention within the microgels imparts minimal damage to the three dimensional structure of the protein.

Myoglobin release from the microgels was also investigated. The release mechanism for myoglobin appeared different from that of lysozyme highlighting the importance of considering the characteristics of the protein to be released. Myoglobin showed an initial burst release followed by slow release (Figure 2.12). It was also found that, in general, formulations with the least OEG content had a more pronounced burst release and a faster initial rate of release. The same trend was also seen with decreasing DMTMM content. The burst release amount varied from 30-50% of total protein for formulations with the higher DMTMM content. The burst release phase is followed by a period of very slow release. Even when 4X PBS was used, further release was not observed (data not shown). This is indicative of a strong and non-ionic interaction between the myoglobin and the pAA-PEG microgel. Furthermore, a studied by Cruise

et al. gives some insight into the mesh size of this network. They report that myoglobin was unable to diffuse through PEG-diacrylate hydrogels with a mesh size of less than 35 Å (35). Thus even the most cross-linked of the pAA-OEG microgels (e.g. formulations M1 & M7) have a mesh size bigger than 35 Å.

Hemoglobin released at a much slower rate than the other proteins from the microgels (Figure 2.13). The fact that hemoglobin had high loading efficiencies and slow release rates suggests that there is a strong interaction between the microgel matrix and hemoglobin. Switching the release medium to 4X PBS did not increase the rate of release suggesting that it is not an ionic interaction. To further investigate the nature of the hemoglobin affinity towards the microgel's matrix, the effect of free pAA and OEG in solution was investigated. The hemoglobin forms a cloudy solution when attempting to dissolve it in a 0.5 mg/mL solution of pAA in PBS, as opposed to a clear solution when dissolved in PBS or PBS with OEG. This is not surprising as pAA has been previously used for protein precipitation and it is known that hemoglobin can interact with pAA in solution (36–38). From this result it is postulated that the pAA component of the microgel matrix interacts with hemoglobin. β -lactoglobulin was fully released within the first 6 hours from all formulations (data not shown). It is an expected result because of β -lactoglobulin's negative charge and relatively low molecular weight.

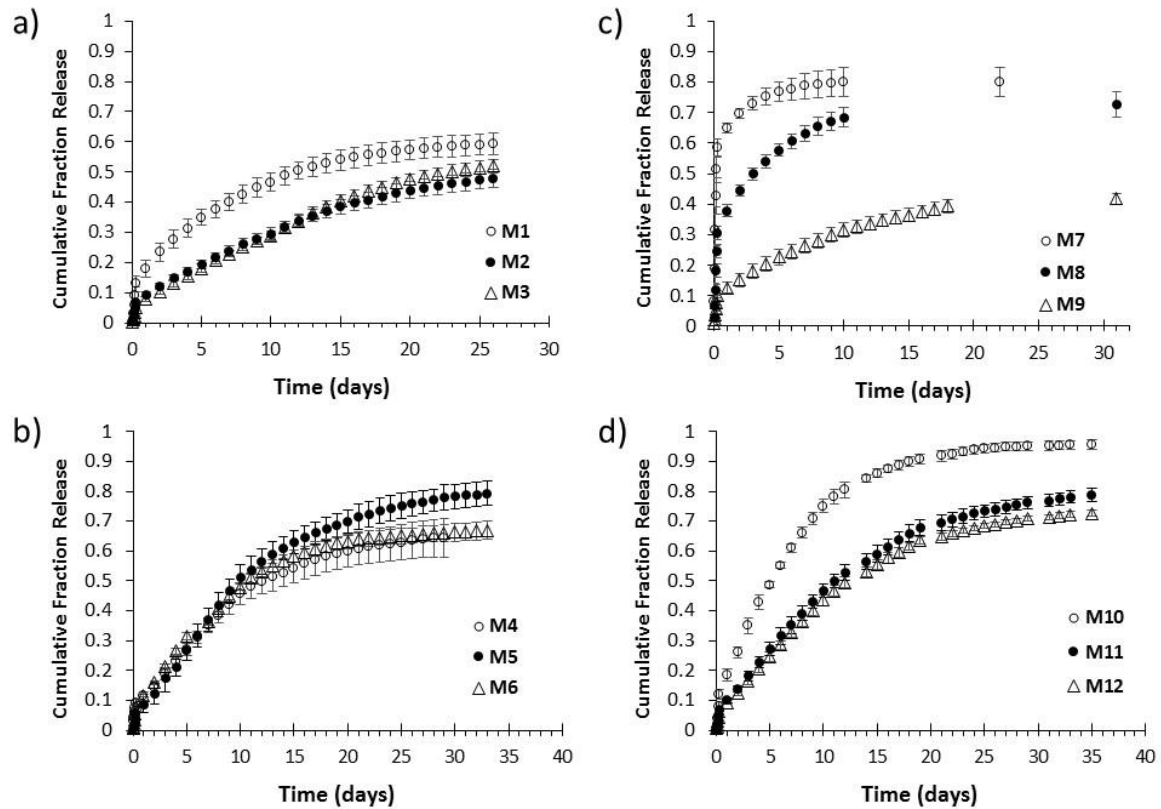


Figure 2.10: Lysozyme release kinetics from all formulations, a) M1-M3, b) M4-M6, c) M7-M9, d) M10-M12. There was a general trend in which the more densely cross-linked formulation, M1, M4, M7 and M10 showed the fastest release. The more densely cross-linked formulations have less free carboxylate side chains, thus are less negatively charged. Lysozyme is a positively charged protein at the experimental pH and its release can be modulated by the charge density of the microgel network.

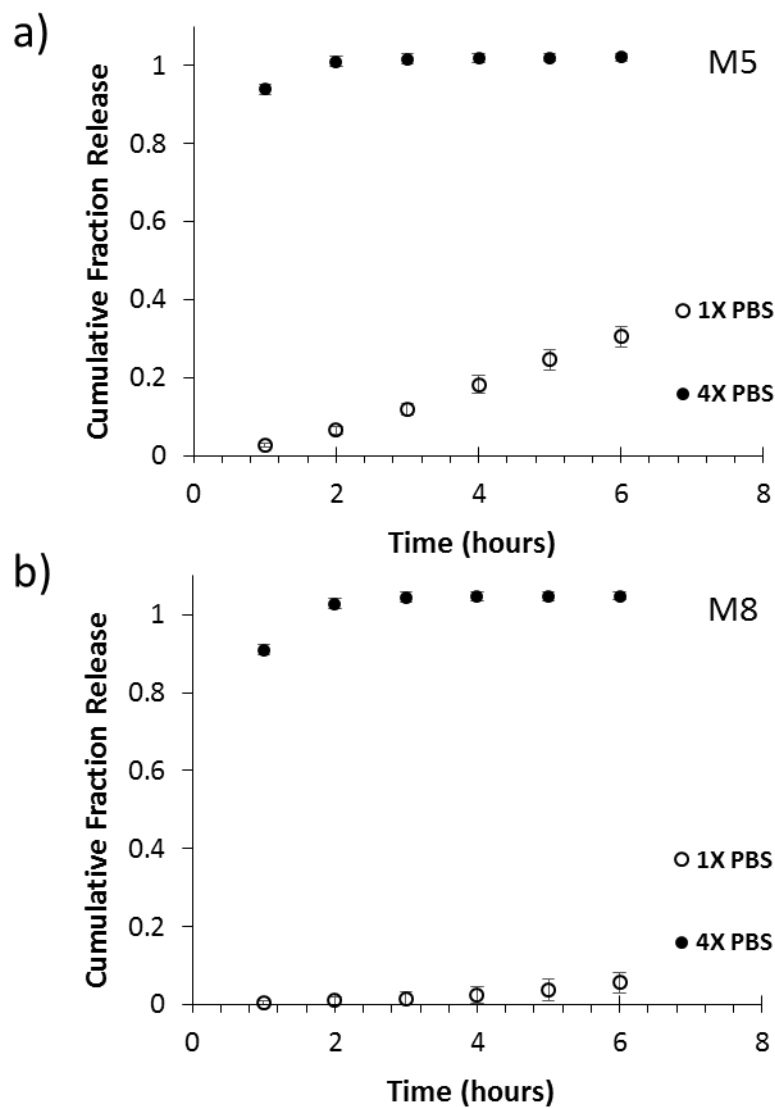


Figure 2.11: Comparison of lysozyme release in 1X and 4X PBS for microgel formulations M5 and M8. When released in higher ionic strength all lysozyme is released within 2 hours. This supports the premise that the main mechanism of lysozyme release is ionic exchange. The more ions present in solution, the quicker lysozyme can be displaced and released into solution.

Table 2.3: Percent of lysozyme activity remaining upon release from microgels relative to native lysozyme.

Formulation	Time (d)	% activity
M1	18	70 ± 19
M2	20	71 ± 8
M3	20	66 ± 5
M4	20	98 ± 6
M5	20	98 ± 20
M7	5	98 ± 14
M8	5	95 ± 12
M9	31	107 ± 7
M10	21	93 ± 3
M11	24	82 ± 35
M12	24	98 ± 4

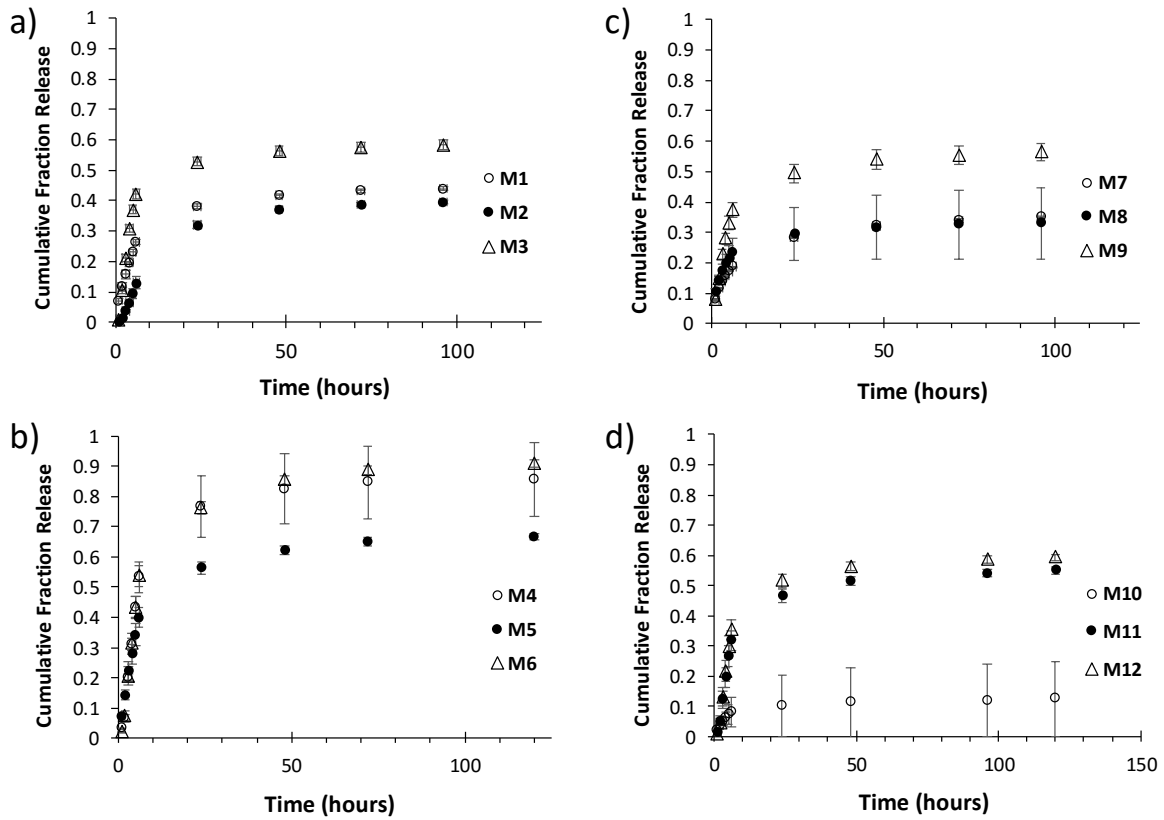


Figure 2.12: Myoglobin release from all formulations. Myoglobin showed a faster release rate than lysozyme and the least cross-linked formulation had the fastest initial rate of release as well as more complete total released protein.

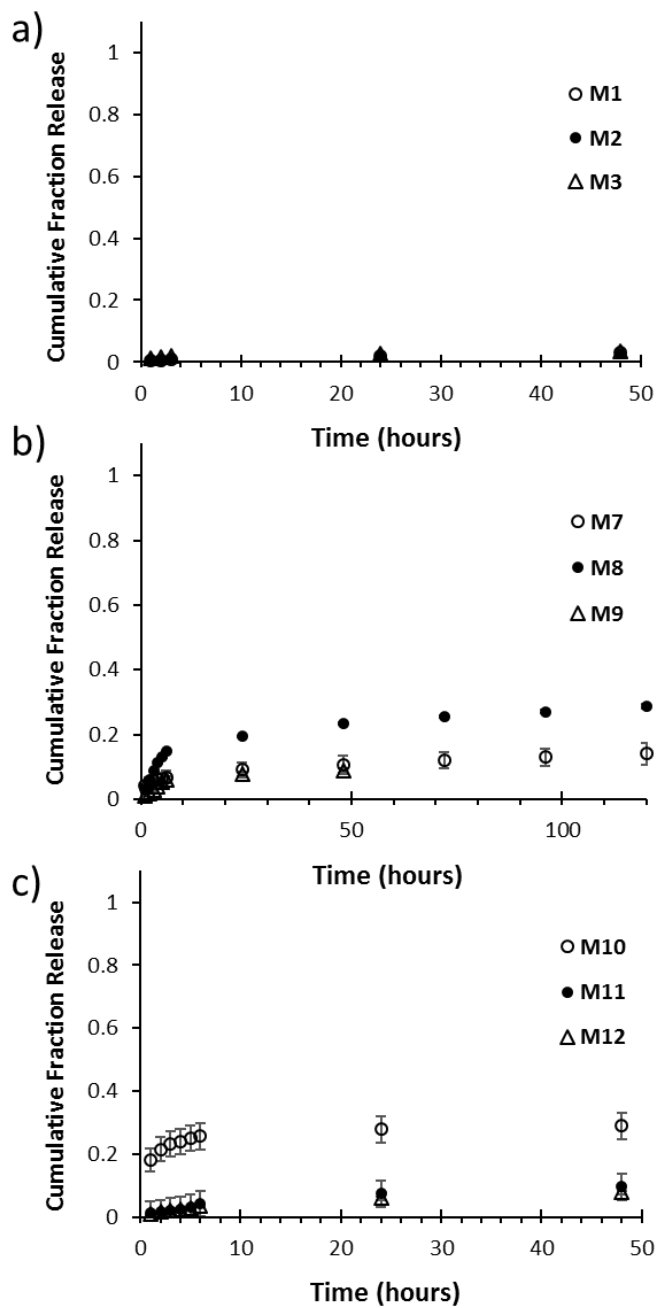


Figure 2.13: Hemoglobin release kinetics from microgels. Hemoglobin release was very slow compared to lysozyme and myoglobin.

2.5 Conclusion

A new method for the fabrication of microgels using pAA cross-linked with OEG was developed. Control over the size of the polymers ensures that the molecular weight of subsequently solubilized pAA resulting from microgel degradation will be below the glomerular filtration limit for elimination from the body. The pAA-OEG microgels captured proteins with high efficiency compared to other systems that use the post-loading method. It was also shown that the loading efficiency depends on the characteristics of both the protein and microgel formulation. *In-vitro* protein release kinetics were assessed and it was shown that the release of lysozyme is mechanistically governed by ionic exchange. Myoglobin's release appeared to be more diffusion dependent as the burst release and rate of the burst increased with decreasing cross-linking density. Hemoglobin had the slowest release and it was found that the pAA can interact strongly with hemoglobin in solution. Therefore, the release of hemoglobin might be more dependent on the degradability rate of the microgel matrix. The rate of release of the proteins can be modulated by changing the formulation parameters. The small negatively charged protein β -lactoglobulin released as a burst, as expected given its molecular characteristics. Also, as shown by the retention of lysozyme's enzymatic activity, the microgel network does not damage the incorporated proteins, which of the utmost importance when designing a therapeutic protein drug delivery system.

This work begins to lay the foundation for the creation of a broad platform for the delivery of therapeutic proteins. Depending on the characteristics of the protein of interest, the timeframe on which release is required and the therapeutic target, a formulation can be tailored made to satisfy pre-defined release requirements. It is anticipated that further fine-tuning of the

system and incorporation of functional modalities to the network can increase the range of potential applications.

Acknowledgements

We would like to gratefully acknowledge the Coleman Foundation and the NSF Graduate Research Fellowship for their support (J.L.R). This work made use of Cornell Center for Materials Research facilities funded through NSF MRSEC DMR-1120296 and the Cornell University NMR Chemistry facility.

2.6 References

1. Carter PJ. Introduction to current and future protein therapeutics: a protein engineering perspective. *Exp Cell Res.* 2011;317(9):1261–1269.
2. Vermonden T, Censi R, Hennink WE. Hydrogels for protein delivery. *Chem Rev.* 2012;112(5):2853–2888.
3. Leader B, Baca QJ, Golan DE. Protein therapeutics: a summary and pharmacological classification. *Nat Rev Drug Discov.* 2008;7(1):21–39.
4. Research and markets: Global protein therapeutics Market 2012-2016. *The Wall Street Journal.* 2008.
5. Manning MC, Chou DK, Murphy BM, Payne RW, Katayama DS. Stability of protein pharmaceuticals: An update. *Pharm Res.* 2010;27(4):544–575.
6. Bysell H, Månsson R, Hansson P, Malmsten M. Microgels and microcapsules in peptide and protein drug delivery. *Adv Drug Deliv Rev.* 2011;63(13):1172–1185.
7. Oh JK, Drumright R, Siegwart DJ, Matyjaszewski K. The development of microgels/nanogels for drug delivery applications. *Prog Polym Sci.* 2008;33(4):448–477.
8. Vinogradov S V. Colloidal microgels in drug delivery applications. *Curr Pharm Des.* 2007;12(36):4703–4712.
9. Hennink WE, van Nostrum CF. Novel crosslinking methods to design hydrogels. *Adv Drug Deliv Rev.* 2012;64:223–236.

10. Gupta P, Vermani K, Garg S. Hydrogels: from controlled release to pH-responsive drug delivery. *Drug Discov Today*. 2002;7(10):569–579.
11. Yim ES, Zhao B, Myung D, Kourtis LC, Frank CW, Carter D, et al. Biocompatibility of poly(ethylene glycol)/poly(acrylic acid) interpenetrating polymer network hydrogel particles in RAW 264.7 macrophage and MG-63 osteoblast cell lines. *J Biomed Mater Res A*. 2009;91(3):894–902.
12. De Giglio E, Cafagna D, Ricci M a., Sabbatini L, Cometa S, Ferretti C, et al. Biocompatibility of poly(acrylic acid) thin coatings electro-synthesized onto TiAlV-based implants. *J Bioact Compat Polym*. 2010;25(4):374–391.
13. Fox M, Szoka F, Frechet J. Soluble polymer carriers for the treatment of cancer: the importance of molecular architecture. *Acc Chem Res*. 2009;42(8):1141–1151.
14. Pelet J, Putnam D. An in-depth analysis of polymer-analogous conjugation using DMTMM. *Bioconjug Chem*. 2011;22(3):329–337.
15. Kunishima M, Morita J, Kawachi C, Iwasaki F, Terao K, Tani S. Esterification of carboxylic acids with alcohols by 4-(4 ,6-dimethoxy-1,3,5-triazin-2-yl)-4-methyl-morpholinium chloride (DMTMM). *Tetrahedron*. 1999;(8):1255–1256.
16. Weiser JR, Yueh A, Putnam D. Protein release from dihydroxyacetone-based poly(carbonate ester) matrices. *Acta Biomater*. 2013;9(9):8245–8253.

17. Pelet JM, Putnam D. Poly(acrylic acid) undergoes partial esterification during RAFT synthesis in methanol and interchain disulfide bridging upon NaOH treatment. *Macromol Chem Phys*. 2012;213:2536–2540.
18. Rejman J, Oberle V, Zuhorn IS, Hoekstra D. Size-dependent internalization of particles via the pathways of clathrin- and caveolae-mediated endocytosis. *Biochem J*. 2004;377:159–169.
19. Prokov A. Intracellular delivery: Fundamentals and applications. Prokop A, editor. New York: Springer; 2011.
20. Sharma G, Valenta DT, Altman Y, Harvey S, Xie H, Mitragotri S, et al. Polymer particle shape independently influences binding and internalization by macrophages. *J Control Release*. 2010;147(3):408–412.
21. Champion JA, Walker A, Mitragotri S. Role of particle size in phagocytosis of polymeric microspheres. *Pharm Res*. 2009;25(8):1815–1821.
22. Schillemans JP, Verheyen E, Barendregt A, Hennink WE, Van Nostrum CF. Anionic and cationic dextran hydrogels for post-loading and release of proteins. *J Control Release*. 2011;150(3):266–271.
23. Zhang Y, Zhu W, Wang B, Ding J. A novel microgel and associated post-fabrication encapsulation technique of proteins. *J Control Release*. 2005;105(3):260–268.
24. Gehrke SH, Uhden LH, McBride JF. Enhanced loading and activity retention of bioactive proteins in hydrogel delivery systems. *J Control Release*. 1998 Oct 30;55(1):21–33.

25. Wittemann A, Azzam T, Eisenberg A. Biocompatible polymer vesicles from biamphiphilic triblock copolymers and their interaction with bovine serum albumin. *Langmuir*. 2007;23(4):2224–2230.
26. Hollmann O, Czeslik C. Characterization of a planar poly(acrylic acid) brush as a materials coating for controlled protein immobilization. *Langmuir*. 2006;22(7):3300–3305.
27. Cooper CL, Dubin PL, Kayitmazer B, Turksen S. Polyelectrolyte–protein complexes. *Curr Opin Colloid Interface Sci*. 2005;10(1-2):52–78.
28. Czeslik C, Jackler G, Steitz R, von Grünberg H-H. Protein binding to like-charged polyelectrolyte brushes by counterion evaporation. *J Phys Chem B*. 2004;108(35):13395–13402.
29. Henzler K, Haupt B, Lauterbach K, Wittemann A, Borisov O, Ballauff M. Adsorption of beta-lactoglobulin on spherical polyelectrolyte brushes: direct proof of counterion release by isothermal titration calorimetry. *J Am Chem Soc*. 2010;132(9):3159–3163.
30. Wittemann A, Haupt B, Ballauff M. Adsorption of proteins on spherical polyelectrolyte brushes in aqueous solution. *Phys Chem Chem Phys*. 2003;5(8):1671–1677.
31. Meier-Koll AA, Fleck CC, Grünberg HH Von. The counterion-release interaction. *J Phys Condens Matter*. 2004;16(34):6041–6052.

32. Koutsopoulos S, Unsworth LD, Nagai Y, Zhang S. Controlled release of functional proteins through designer self-assembling peptide nanofiber hydrogel scaffold. *Proc Natl Acad Sci.* 2009;106(12):4623–4628.
33. Hennink WE, De Jong SJ, Bos GW, Veldhuis TFJ, van Nostrum CF. Biodegradable dextran hydrogels crosslinked by stereocomplex formation for the controlled release of pharmaceutical proteins. *Int J Pharm.* 2004;277(1-2):99–104.
34. Hoare TR, Kohane DS. Hydrogels in drug delivery: Progress and challenges. *Polymer.* 2008;49(8):1993–2007.
35. Cruise GM, Scharp DS, Hubbell JA. Characterization of permeability and network structure of interfacially photopolymerized poly (ethylene glycol) diacrylate hydrogels. *Biomaterials.* 1998;19:1287–94.
36. Thilakarathne VK, Briand VA, Kasi RM, Kumar C V. Tuning hemoglobin – poly(acrylic acid) interactions by controlled chemical modification with triethylenetetramine. *J Phys Chem B.* 2012;116(42):12783–12792.
37. Thilakarathne V, Briand V a, Zhou Y, Kasi RM, Kumar C V. Protein polymer conjugates: improving the stability of hemoglobin with poly(acrylic acid). *Langmuir.* 2011;27(12):7663–7671.
38. Sternberg M, Hershberger D. Separation of protein with polyacrylic acids. *Biochim Biophys Acta.* 1974;342(1):195–206.

39. Wampler FM. Formation of diacrylic acid during acrylic acid storage. Plant/Operations Prog. 1988;7(3):183–189.

3 Encapsulation and Prolonged Release of Bacteriophage from Anionic Microgels

3.1 Abstract

Purpose There is an alarming worldwide surge of antibiotic resistant pathogens due to antibiotic over-prescription. Phage therapy, an antibiotic therapy widely use in the Easter European nation of Georgia, is being considered again in western medicine to complement antibiotic treatment of resistant bacteria strains. This study presents a microgel-based phage controlled release system capable of encapsulating phage, prolonged release and retaining the phage lytic activity.

Methods A recently developed DMSO/Pluronic microemulsion was used to fabricate poly(acrylic acid) cross-linked with poly(ethylene glycol) microgels. P1 and EcoActive™ were encapsulated into microgels using the post-loading method. Controlled release of phage was evaluated over a period of 15 days and the lytic activity of released phage was evaluated.

Results Microgels successfully encapsulated phage and prolonged the release of phage over 20 days. The Korsmeyer-Peppas model was applied to the release profiles and it showed that the release is of the pseudo-Fickian type. Released phage also maintain lytic activity up to 15 days of release.

Conclusion The controlled release of phage is longer and the total amount of phage lytic activity released is greater than any phage delivery system reported on in the literature.

3.2 Introduction

The common historical narrative of antimicrobial agents begins with Alexander Fleming's discovery of penicillin, a finding he published in 1929 in the *British Journal of Experimental Pathology* (1). However, before penicillin, other ubiquitous and naturally occurring antimicrobial agents were discovered, known as bacteriophages and discovered by Felix d'Herelle in 1917 (2). Bacteriophages are viruses that infect bacteria, replicate within the host and lyse the bacterial cell. Soon after this discovery d'Herelle began studies on the use of bacteriophage for the treatment of infections, first in veterinary applications (3) and soon after in humans. Bacteriophage therapy, or "phage therapy" was used to effectively treat bubonic plague, cholera and wound infections (4–7). However, the discovery of antibiotics, which are relatively easy to manufacture in large scale and are effective towards a broad spectrum of pathogens, combined with the demand exerted by the second World War, cause a waning interest in bacteriophage therapy in the west. Behind the iron curtain of the Soviet Union the story was a little different. Phage therapy continued to be widely used due to restricted access to antibiotics from the west, and up to this date phage therapy is still being used in Russia, Georgia and Poland. In fact, the Elavia Institute, a leading institute in phage therapy, is located in Tbilisi, Georgia (8).

There is an alarming worldwide surge in antibiotic resistant pathogens due to the increased over prescription of antibiotics (9). The Center for Disease Control and Prevention (CDC) recently reported that 1 in 7 surgical site infections in hospitals are caused by antibiotic resistant bacteria (10). It is evident that new sources of antimicrobial agents are needed to overcome the current use of antibiotics. The worrisome concept of "superbugs" has focused attention back on bacteriophage therapy (8,11,12).

Phages have some advantages over antibiotics that makes them attractive as an alternative or complementary therapy. Phages are purely natural agents that do not require any synthetic methods for fabrication, and have never been shown to cause adverse side effects in humans. Additionally, phages are highly specific to a bacterial species; therefore, they can target only the pathogenic bacteria while sparing and leaving intact the body's microflora, compared to broad spectrum antibiotics that kill all susceptible bacterial cells regardless whether or not they are pathogenic. Once a phage attacks a bacterial host, it replicates exponentially, increasing its own concentration and ability to attack more pathogen (11,13). Recent examples of phage therapy include treatment of post-burn bacterial infections (14), chronic otitis (15) and other clinical studies conducted during the former Soviet Union era, which have been summarized by the Eliava Institute (16). A Phase I/Phase II clinical trial was launch by the European Union for the treatment of sepsis in burn victims (17).

In addition to medicinal applications, phages are being considered for food safety as well. Foods meant to be eaten fresh, such as produce and other ready-to-eat foods raise food safety concerns. The recent outbreak of food poisoning cases in Chipotle Mexican Grill restaurants highlights the risk presented by eating fresh produce (18), especially from high volume environments like restaurants. Phages eradicate and limit the growth of susceptible bacteria. Some current products on the market (EcoshieldTM and FinalyseTM) are intended to be used on meat products and effectively target *E. coli* O157:H7 (19). Phages have been shown to also reduce the amount of unwanted bacteria on fresh produce, deli meats and milk products (20–22). Current research trends, with already established products on the market, are indicative that phage technology will play a more important role in food safety, and potentially in human health.

Current phage preparations for human treatment can be delivered via different routes,

including solutions and tablets for oral administrations, dermal preparations, aerosols and intravenous formulations (11). Regardless of the method of administration, it is well documented that bacteriophage concentration is highest at the site of infection (23–25). In addition, the pharmacokinetics of phages are highly temporal and dose dependent because of phage's ability to self-replicate. Payne et al. showed mathematically that inoculating too early or too late can lead to therapy failure (26). As such, devices able to control the rate of release of phage maybe useful in increasing the success of therapy. At present, there are few examples of novel delivery systems for phage therapy. Delivery systems presented in the current literature have phage released time frames in the order of minutes to a few hours. Additionally, release kinetics haven't been studied in detail and a clinically relevant model hasn't been used to evaluate whether phage therapy can be improved with a delivery system.

Herein, we present the development of a controlled release system for phage using polymeric microgels. Previously, similar microgels made by our group were shown to control the release of model proteins (27). The microgels are unique in two ways. First, a poly(acrylic acid) (pAA) backbone is synthesized by RAFT polymerization to a well-define molecular weight with narrow polydispersity. Second, the microemulsion used to crosslink and fabricate the microgels is a newly developed system of dimethyl sulfoxide (DMSO) microdroplets suspended by homogenization in Pluronic[®] L35 as the continuous phase to create well-defined and tunable microreaction templates. The pAA is then cross-linked with poly(ethylene glycol) (PEG) via a condensation reaction within the microreaction template leading to microgel formation. A series of pAA-PEG cross-linked microgels was prepared by changing the cross-linking density. The controlled release of phages was evaluated *in-vitro* and the phages' lytic activity was quantified using a plaque assay.

3.3 Materials and Methods

3.3.1 Materials

Acrylic acid, pol(ethylene glycol) M_n -1500, anhydrous methanol, 4-cyanopentanoic acid dithiobenzoate (CPA-DB), 4,4'-azobis(4-cyanopentanoic acid) (A-CPA), dimethyl sulfoxide, 4-methylmorpholine (NMM), tetraethylene glycol, Pluronic[®] L35. 4-(4,6-Dimethoxy-1,3,5-triazin-2-yl)-4-methylmorpholinium chloride (DMTMM) was purchased from Tokyo Chemical Industry America. Phosphate buffered saline (PBS) was purchased from Cellgro. BCA Protein Assay Kit was purchased from Thermo Fisher Scientific. LB Miller and LB Agar Miller were purchased from VWR.

3.3.2 Synthesis of Poly(acrylic acid)

Acrylic acid was polymerized by reversible addition-fragmentation chain transfer (RAFT) polymerization. This technique allows for the synthesis of polymers with well controlled molecular weights and relatively narrow PDI. The polymerizations were carried out as previously reported by our group (28). The amounts of CPA-DB and A-CPA were adjusted to achieve different molecular weights. A representative polymerization to synthesize pAA with M_n of 15,500 and PDI of 1.3 was performed as follows: CPA-DB (184 mg, 0.659 mmol) and A-CPA (46 mg, 0.164 mmol) were combined in a Schlenk flask with a magnetic stir bar. Anhydrous methanol was purged with dry nitrogen for 10 minutes then added (36.6 mL) to the CPA-DB and A-CPA mixture in the Schlenk flask, followed by complete dissolution with stirring. AA (9.5 mL, 0.138 mol) was then added into the Schlenk flask, a condenser column fitted to the flask and the entire system was purge with dry nitrogen for an additional 15 minutes. The reaction vessel was covered with aluminum foil to protect the reactants from light and the polymerization initiated by lowering the reaction flask into a 60 °C oil bath with continuous

stirring. The reaction was stopped at 48 hours by placing the Schlenk flask in an ice bath and exposing the contents to air. The cooled solution was directly transferred into Spectra/Por regenerated cellulose dialysis tubing (3.5 kDa MWCO) and dialyzed against deionized water for one week. The product was recovered by lyophilization.

The M_w , M_n , and PDI of the resulting pAA were determined using a Waters gel permeation chromatography (GPC) system equipped with Ultrahydrogel columns in series, 1515 isocratic HPLC pump and 2414 refractive index detector with temperature controlled at 30 °C. The mobile phase used was phosphate buffer saline (pH=7.4) at a rate of 0.8 mlmin⁻¹ and calibrated with poly(acrylic acid), sodium salt standards. ¹H NMR was used to confirm the structure of the resulting pAA.

3.3.3 Preparation and Characterization of Microgels

The microgels were synthesized by cross-linking the carboxylate side chains of pAA with the alcohol end-groups of PEG via esterification. The esterification was facilitated with DMTMM, previously shown as an effective condensation reagent (29), see Figure 3.1 for a schematic of the reaction. In a typical reaction, pAA (120 mg) was dissolved in dimethyl sulfoxide (1.5 mL). Varying amounts of DMTMM and NMM were added to this solution depending on the molar ratios of the reaction, see Table 2. After complete dissolution, the PEG was added to this solution with stirring until homogeneity was achieved. The reaction solution was then added all at once to a 100 mL beaker containing Pluronic[®] L35 (40 g), which acts as the continuous phase, and the resulting microemulsion was stirred at 750 rpm using a Silverson L5M-A homogenizer with a 3/4” head for 4 hours at room temperature. The microgels were isolated by centrifugation at 9500 rpm and the supernatant of Pluronic[®] L35 was decanted. The microgels were thoroughly washed by at least 5 cycles of re-suspension in deionized water,

centrifugation and decantation. Lastly, the microgels were suspended in a small volume of deionized water and lyophilized to dryness. Different formulations were prepared by varying the molar ratios of the carboxylate side chains of pAA to PEG and to DMTMM. Formulations are named by these ratios in the following manner COOH:PEG:DMTMM. For example, 1:0.6:0.6 means 0.6 moles of PEG and of DMTMM for every mole of carboxylate side-chain. The morphology and size of the microgels was observed using scanning electron microscopy (SEM) (Tescan MIRA3) and the incorporation of PEG was assessed by FTIR spectroscopy (Hyperion 2000, Bruker).

3.3.4 Bacteriophage Propagation, Encapsulation and Release

Phage P1 was propagated on late-log-phase cultures of *E. coli* K12 in 250 mL Erlenmeyer flasks with lysogeny broth (LB) containing 5 mM CaCl₂, 10 mM MgSO₄ and 0.2% glucose. P1 phage was allowed to incubate with its host for 4 hours at 37 °C under shaking. The lysate was then centrifuged at 5000 rpm to pellet cell debris. The lysate was recovered; chloroform was added at 1:100 and stored at 4 °C. Phage labeled as EcoActive (EA) Phage provided by Intralytix, Inc. was propagated in *E. coli* NC101, kindly provided by the laboratory of Dr. Kenneth W. Simpson at Cornell University, using the same method described above.

Phage lysate was concentrated using Amicon[®] Ultra-15 centrifugal filters with a 100 kDa NMWL. Phage was then re-suspended in PBS and 1 mL of re-suspended Phage (2.15 X 10⁹ pfu/mL) was added to 5 mg of dry microgels and incubated for 16 hours at 4 °C under gentle rotation (8 rpm) in polypropylene Eppendorf tubes. Microgels were then recovered by centrifugation (5000 rpm, 5 min), supernatants were isolated and immediately tittered with a plaque assay for lytic activity and stored at 4 °C for subsequent protein quantification. Phage-loaded microgels were then re-suspended with 1 mL of PBS and incubated at 37 °C under

rotation (8 rpm). At specific time points, the microgels were separated from the buffer by centrifugation (5 min, 5000 rpm), the supernatant was collected and replaced with 1 mL of fresh PBS. Supernatants were then tittered with plaque assay and assayed for protein content using the BCA assay to quantify the protein concentration.

3.3.5 Plaque Assay

Serial dilutions of bacteriophage, from concentrate, from microgel-loading supernatants and from microgel-released supernatants, were prepared and 50 μ L aliquots were mixed with equal volumes of overnight bacterial culture, *E. coli* K12 for phage P1, *E. coli* NC101 for phage EA, and allowed to incubate for 30 minutes. The inoculant was then mixed into 1 mL of soft LB agar and poured over an agar plate and incubated overnight at 37 °C. Following incubation, the number of plaques were counted and the dilutions were used to calculate the number of plaque forming units per mL (PFU/mL).

3.4 Results and Discussion

pAA-PEG microgels were synthesized using a new approach previously reported by our group (27). A series of formulations with varying cross-linking densities was synthesized by changing the reaction parameters. The microgel's ability to encapsulate phage and control the rate of release of phage while maintaining phage lytic activity was evaluated and quantified.

3.4.1 Synthesis and Characterization of Poly(acrylic acid)

RAFT polymerization of acrylic acid was performed as previously described to achieve pAA with predictable M_n and low polydispersity. Such control is desired for the synthesis of well-defined microgels which subsequent degradation results in compounds below the glomerular filtration limit (30) and prevent accumulation. In this study, pAA with an M_n of 9,800 and polydispersity of 1.2, as obtained by GPC, was synthesized. This M_n is well below the

glomerular filtration limit, thus preventing accumulation and promoting future clinical translation. pAA structure was confirmed using ^1H NMR with peaks at 1.3-2.0 ppm and 2.3-2.6 ppm corresponding to the backbone protons of the polymer (Fig. 3.1). Partial methylation of the carboxylate side-chains and acrylic acid dimers peaks are shown at 3.7 ppm, 2.6 ppm, and 4.4 ppm respectively (31,32).

3.4.2 Characterization of pAA-PEG Microgels

Microgels were synthesized by cross-linking the carboxylate side-chains with the alcohol end groups of the PEG (Fig. 3.2). The size and morphology of microgels are relevant when thinking about potential applications. Scanning electron microscopy was used to visualize and determine the size and morphology of microgels derived from various formulations. It was observed that microgels' morphology was greatly influenced by different formulation parameters. For instance, formulations 1:0.4:0.6, 1:0.6:0.2 and 1:0.4:0.2 seem to form amorphous mesh-like structures. Formulations 1:0.6:0.6 and 1:0.4:0.6 form spherical microgels less than 10 μm in diameter. Formulations 1:0.2:0.2 formed spherical microgels of $\sim 20 \mu\text{m}$ in diameter (Fig. 3.3). All of these formulations were colloidal while in suspension. The incorporation of PEG in the microgels was confirmed in two ways. First, a control reaction in which PEG was omitted led to no microgel formation. Second, FTIR was performed on pAA, PEG and microgels. The spectrum of microgels is a combination of the pAA and PEG spectra. In Figure 3.4a, the microgel spectrum of formulation 1:0.6:0.2 clearly shows PEG absorbance peaks at $\sim 3000 \text{ cm}^{-1}$ and at and below 1100 cm^{-1} . This same spectrum shows a distinct pAA absorbance peak at $\sim 1700 \text{ cm}^{-1}$. Additionally, variations in the amount of PEG can be seen from the spectrum of the three formulations. As the amount of PEG in the formulation decreased so did the intensity of the absorbance peaks (Figure 3.4b).

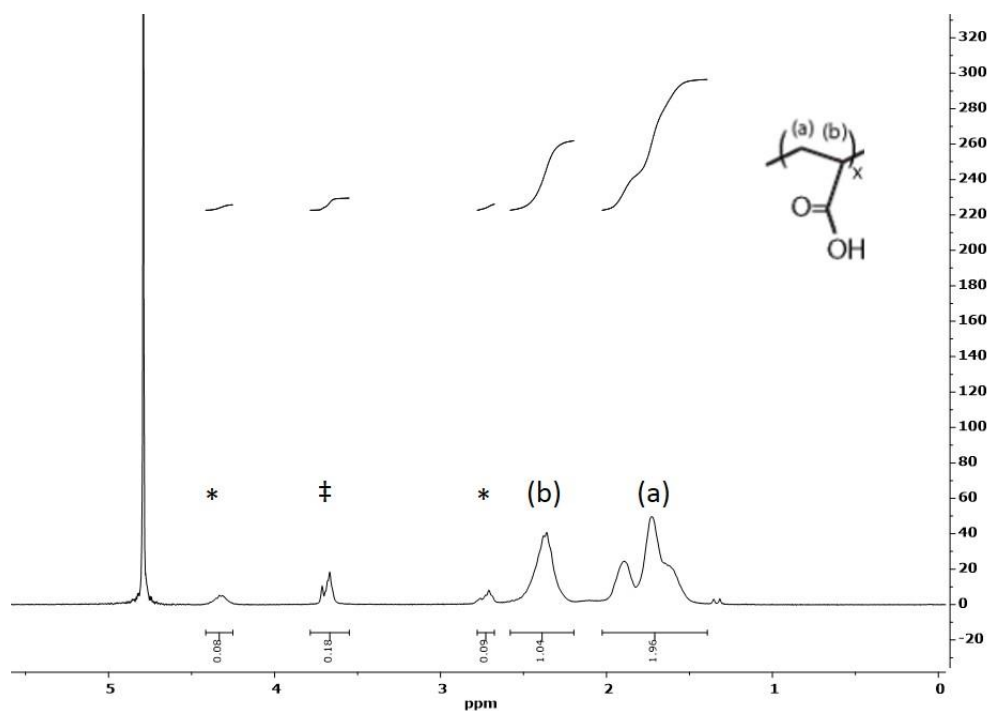


Figure 3.1 ^1H NMR of pAA synthesized by RAFT polymerization. Peaks (a) and (b) correspond to the backbone protons. Peak ‡ corresponds to partial methylation of the carboxylate side-chain which occurs during polymerization in methanol. Peak * corresponds to dimerization of the monomer.

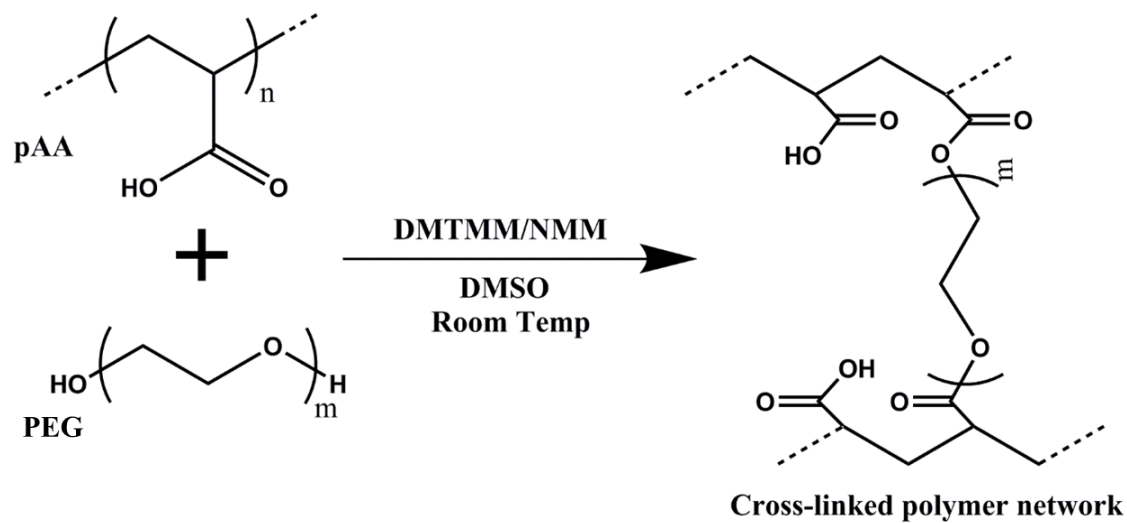


Figure 3.2. Schematic of cross-linking reaction for microgel fabrication. The hydroxyl groups of PEG are condensed with the carboxylate side-chains of pAA. The reaction is facilitated by the addition of DMTMM and NMM provides an organic base to deprotonate the carboxylate side-chains.

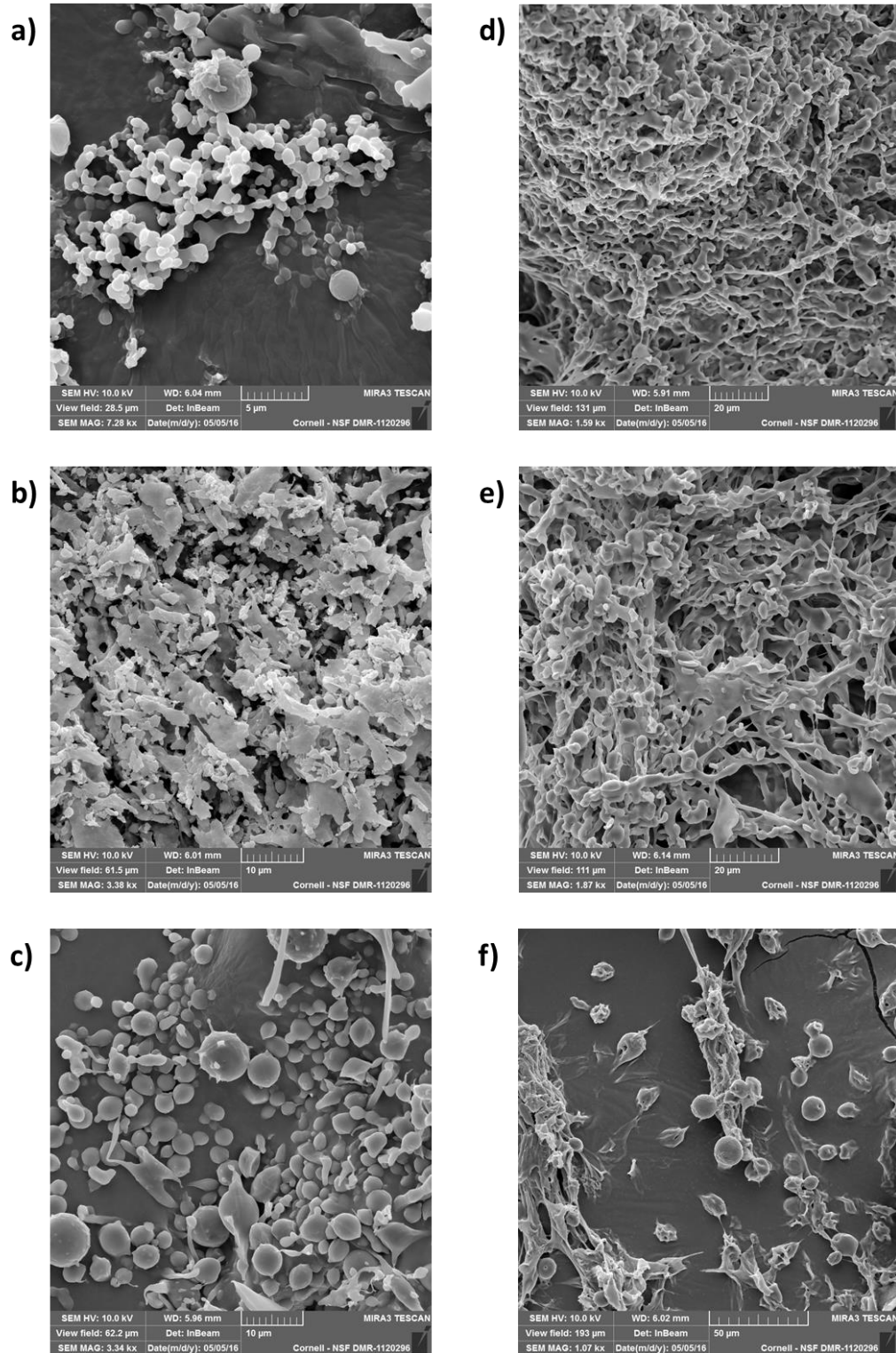


Figure 3.3. Representative SEM images of microgel. a) 1:0.6:0.6, b) 1:0.4:0.6, c) 1:0.2:0.6, d) 1:0.6:0.2, e) 1:0.4:0.2, f) 1:0.2:0.2. The morphology and size of microgels are altered by the formulation parameters.

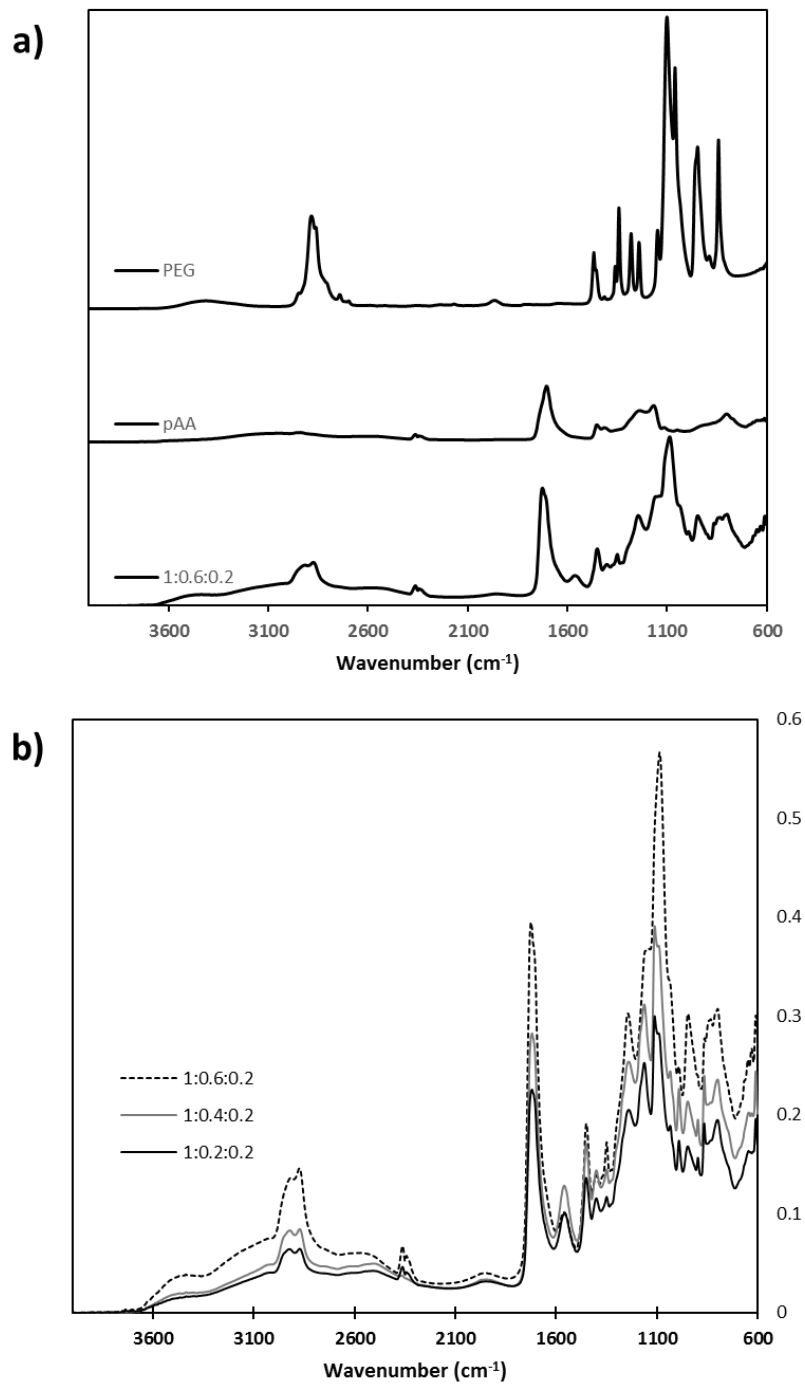


Figure 3.4. FTIR analysis of microgels. a) FTIR spectra of pAA, PEG and microgels. The microgels spectrum is a combination of the spectra of pAA and PEG. b) FTIR spectra of three microgel formulations. The intensity of the PEG peaks decreased as the amount of PEG in the formulation decreased.

3.4.3 In-Vitro Phage Encapsulation, Release and Lytic Activity

Phage P1 and EA phage were encapsulated in the microgels using the post-loading method rather than during microgel fabrication. The post-loading method helps prevent damage to the phage during fabrication due to exposure to surfactants, possible side reactions with DMTMM and high sheer stress during microgel synthesis (27,33,34). Dried microgels were incubated with a phage solution at 4 °C overnight and the phage-loaded microgels were recovered via centrifugation. The supernatants were analyzed using a BCA assay for protein content which subsequently gives a measure of phage content. The loading efficiency was calculated using the following equation:

$$LE = \frac{(V_i C_i - V_r C_f)}{V_i C_i}$$

where LE is the loading efficiency, V_i is the initial volume (1 mL), C_i is the initial concentration, V_r is the recovered volume and C_f is the final concentration. The loading efficiency of EA phage was over 0.6 in all formulations. This loading efficiency is relatively high when compared to similar studies that make use of the post-loading method (34,35). The loading efficiency of P1 phage was lower (~0.4) (Fig. 3.5).

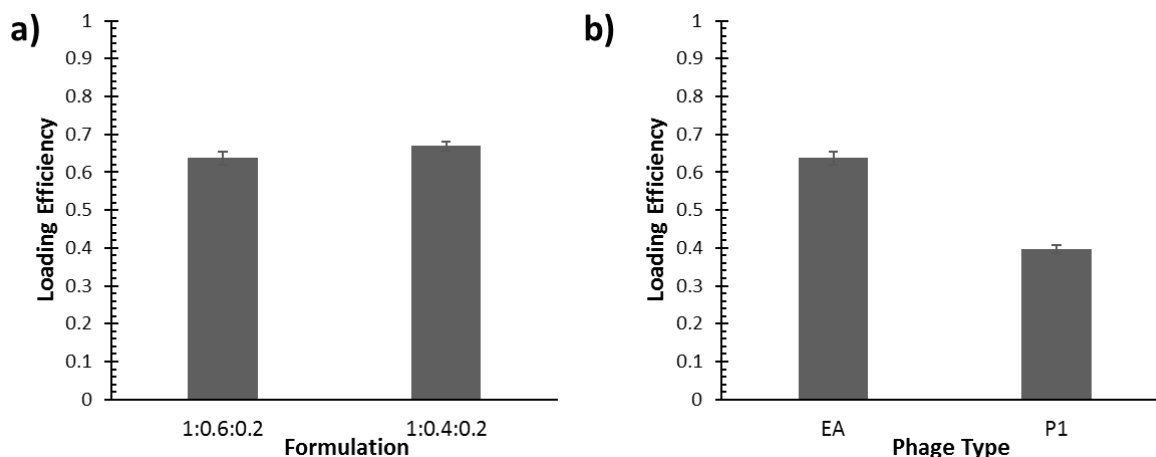


Figure 3.5. Loading efficiency of EA and P1 phage. a) Loading efficiency of EA phage in two different formulations. b) Loading efficiency of EA and P1 phage in formulation 1:0.6:0.2. EA had higher loading efficiency.

EA phage and P1 phage were released from the microgels to evaluate how microgel composition and phage type can influence the release kinetics. Phage release showed an initial burst release followed by a slow prolonged release for a period of up to 20 days (Fig. 3.6). This release time-frame is significantly longer than any previous phage delivery systems reported in the literature (36–41). Vonasek et al. studied the encapsulation and release of phage T4 from whey protein films but release was only measured up to 5 hours (39). Ma et al. encapsulated phage Felix O1 in chitosan-alginate microspheres and measured phage release only up to 6 hours (36). PLGA microspheres fabricated in a double emulsion were used by Puapermpoonsiri et al. to encapsulate phage and release was limited to a maximum of 350 minutes. Phage T4 in electrospun poly(ethylene glycol)/cellulose diacetate fibers was release within 1 hour (38). This extended release presents a significant improvement over all previous studies aiming at encapsulating and controlling the release rate of phage.

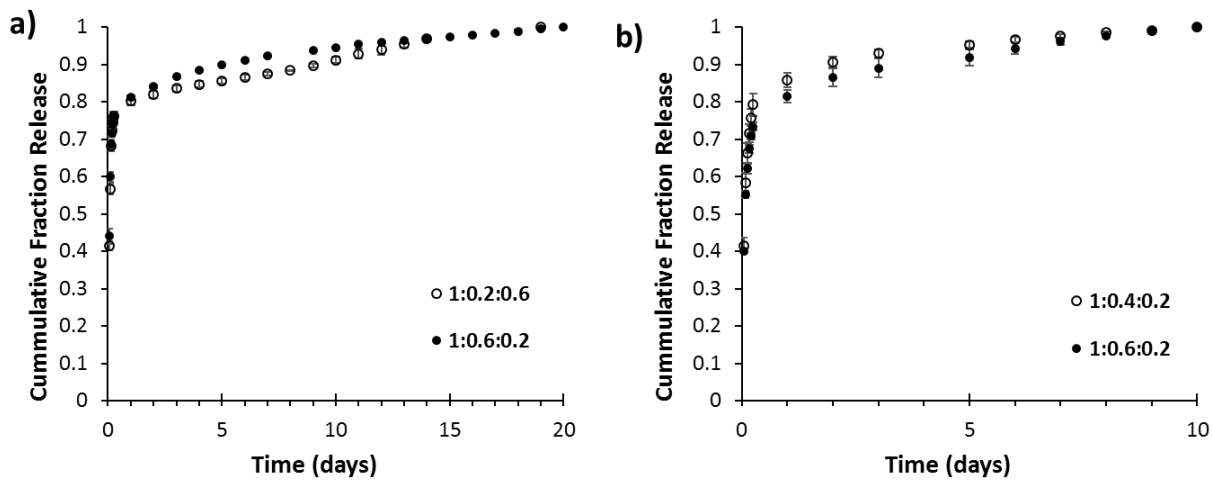


Figure 3.6. Release of phage P1 (a) and EA (b) from different formulations. All formulations show a quick release of 0.4 fraction release within 1 hour and nearly 0.8 fraction release at 6 hours. The release of phage slows down subsequently and continues at a slower rate for up to 20 days.

A basic understanding of the mechanism by which phage is release from the microgels can inferred on using the Korsmeyer-Peppas model (42). In short, release of phage from the microgels will depend in polymer/phage interactions, degree of microgel swelling, and diffusion of phage in microgel (43). The Korsmeyer-Peppas model is a semi-empirical model that describes the rate of release from a swelling controlled system in terms of a power law (42) using equation 2:

$$\frac{M_t}{M_\infty} = kt^n$$

This equation expresses the fraction of release phage M_t/M_∞ at time t , k is a kinetic constant and n characterizes the release mechanism. The value of n is indicative of the type of release, whether it is Fickian diffusion, a combination of diffusion and matrix swelling, or pseudo-Fickian in which other more complex interactions are at play (44). Equation 2 was applied to the release profiles and a least-squares regression was used to obtain values for k and n . The model overlaid well on all release curves (Fig. 3.7) and the calculated R^2 values show a high degree of correlation (Table 1).

The kinetic parameter n helps identify the type of release. An n value of 0.5 indicates Fickian diffusion, $0.5 < n < 1.0$ indicates anomalous (non-Fickian) diffusion, values of 1 or greater is defined as Case II or Super Case II transport and for $n < 0.45$ is pseudo-Fickian diffusion. Table 1 shows how all n values are well below 0.45 suggesting that the type of release is complex depending on phage diffusion and matrix-phage interactions within the network contribute to the release profile (45).

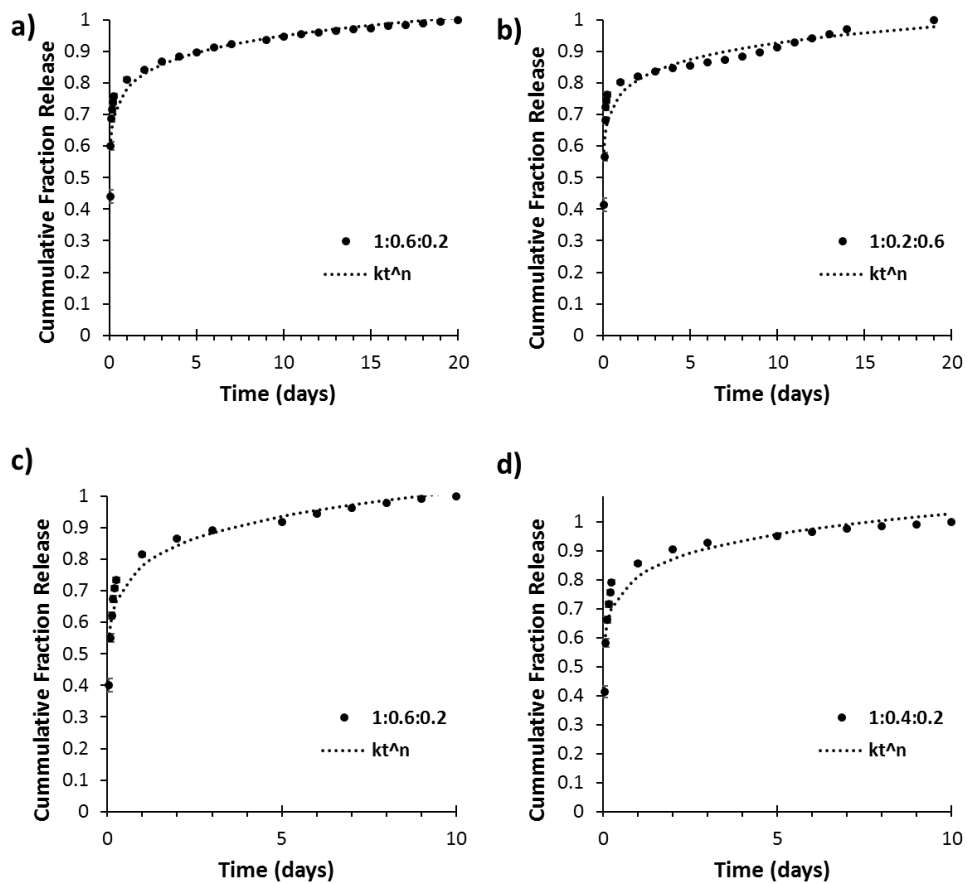


Figure 3.7. Trend lines of the Korsmeyer-Peppas model overlaid on the fraction release data of phage P1 (a,b) and EA (c,d) from different formulations.

Table 4. Kinetic parameters obtained by fitting the Korsmeyer-Peppas model fraction cumulative release of phage.

Formulation	Phage	Korsmeyer-Peppas Model		
		k ($days^{-n}$)	n	R^2
1:0.6:0.2	P1	0.76	0.08	0.86
1:0.2:0.6	P1	0.78	0.08	0.92
1:0.6:0.2	EA	0.78	0.11	0.93
1:0.4:0.2	EA	0.81	0.10	0.88

Retained lytic activity in the released phage is an essential pre-requisite for the success of a phage controlled release system. Plaque assays to enumerate the amount of active phage particles were performed against the common k1 *E. coli* for P1 phage and NC101 *E. coli* for EA phage. NC101 is an adhesive-invasive *E. coli* (AIEC) strain that has been associated with Crohn's disease and other chronic colitis (46,47). The use of EA against NC101 was chosen because NC101 can provide a potential therapeutic target for the treatment of colitis in future studies. EA phage release was measured over 15 days (Fig. 3.8) from two different microgel formulations. Formulation 1:0.4:0.2 released a greater amount of total PFU. This formulation has less PEG and, therefore, it forms a looser network which is able to incorporate a total higher amount of phage. Figure 3.5 shows a slight increase in loading efficiency for formulation 1:0.4:0.2 when compared to 1:0.6:0.2. Overall for both formulations, release of active phage, as measured by lytic activity, was observed through day 15, with the phage release at day 15 having a lytic activity of over 10^6 PFU/mL. The total cumulative EA phage PFU released formulations 1:0.6:0.2 and 1:0.4:0.2 were 4.1×10^8 and 5.4×10^8 respectively. Not only is the period of controlled release longer than any phage delivery system reported in the literature, but the total amount of PFU release is greater per weight of release matrix (e.g. microgels). Chitosan-alginate microspheres loaded with phage Felix O1 released a total of $\sim 5 \times 10^6$ PFU over 6 hours from 200

mg of microspheres (36), poly(ethylene oxide)/cellulose diacetate fibers release $\sim 10^{10}$ PFU from 1 g of fibers (38). T4 phage encapsulated in whey protein films and released from 1.5 cm diameter disks amounted to a total release of 5×10^6 PFU (39). In comparison, the pAA-PEG microgels released at levels of 10^8 using only 5 mg of microgels. A quick comparative analysis of the amount of PFU released per weight of matrix yields (PFU/mg of matrix) 2.5×10^4 PFU/mg for chitosan-alginate microspheres, 10^7 PFU/mg for poly(ethylene oxide)/cellulose diacetate fibers and 1.08×10^8 PFU/mg for pAA-PEG microgels.

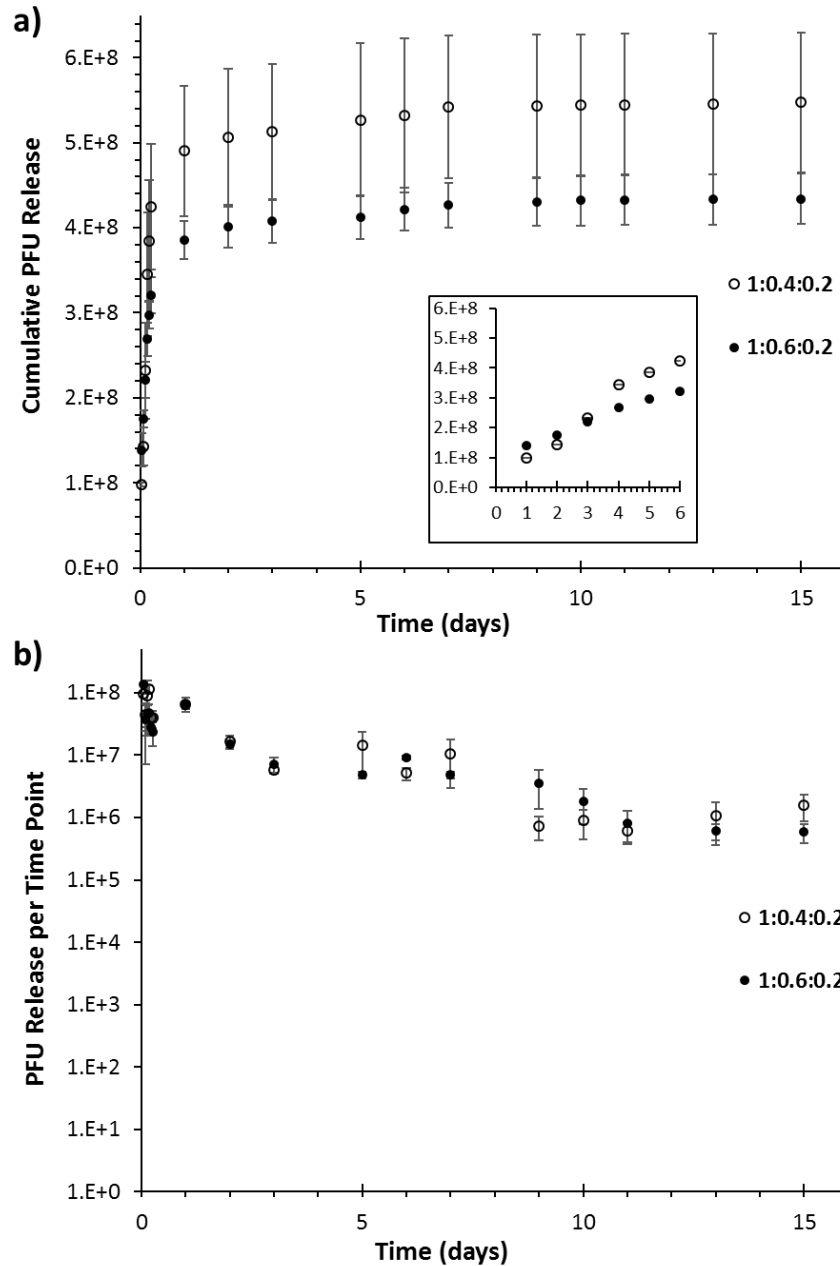


Figure 3.8. Lytic activity of released EA phage. a) Cumulative PFU release over a 15 days. Inlet image shows cumulative PFU release in the first 6 hours. b) PFU measured at each time point. The supernatant at day 15 still contained a lytic activity above 1×10^6 PFU/mL. This prolonged release is significantly greater than any other study currently presented in the literature.

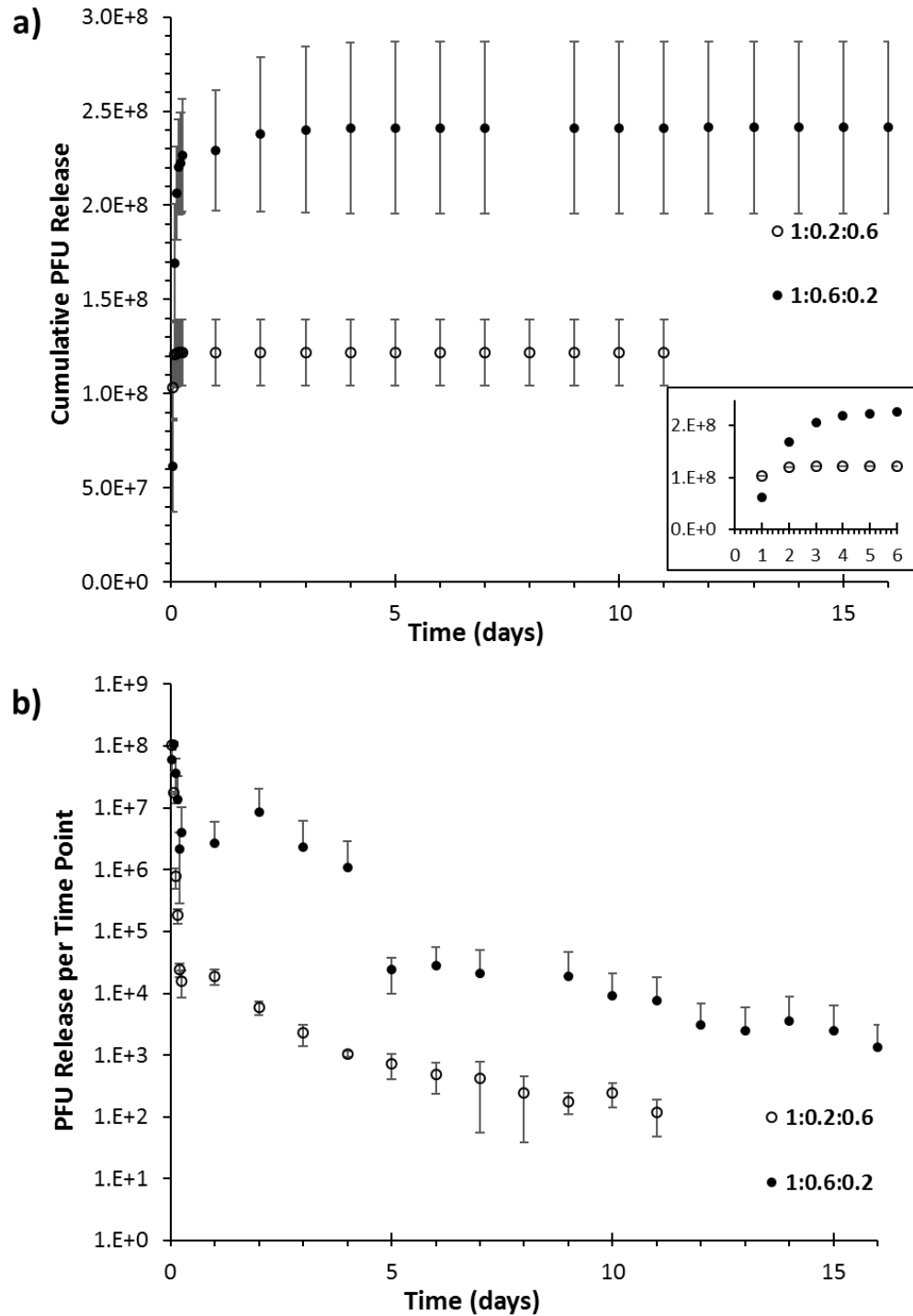


Figure 3.9. Lytic activity of released P1 phage. a) Cumulative PFU release of P1 phage. Inlet image shows cumulative PFU release in the first 6 hours. b) PFU measured at each time point. Formulation 1:0.6:0.2 showed activity of over 10^6 for the first 4 days and dropped by two orders of magnitude on day 5. Formulation 1:0.2:0.6 showed a steady drop in the first six hours and seems inadequate for this application.

3.5 Conclusion

Previously, we reported on the use of pAA-OEG microgels for the prolonged release of proteins (27). In this study, the microgels were modified by increasing the cross-linker size with the aim of encapsulating and retaining phage, prolonging the rate of release and maintaining the lytic activity of released phage. These new pAA-PEG microgels were able to effectively encapsulate phage with loading efficiencies of ~ 0.6 for EA phage and 0.4 for P1 phage. Considering phage was encapsulated using the post-loading method the obtained loading efficiencies are high relative to those found in the literature and comparative to those we previously found using model proteins. Release kinetic studies showed that phage was released over 20 days and by implementing the Korsmeyer-Peppas model it was determined, as expected, that the release is pseudo-Fickian, confirming that phage diffusion and matrix-phage interactions contribute to release. Overall, this phage controlled release system presents a significant improvement to systems currently in the literature.

3.6 References

1. Fleming A. On the antibacterial action of cultures of a penicillium, with special reference to their use in the isolation of *B. influenzae*. 1929. *Br J Exp Pathol.* 1929;226–36.
2. D’Herelle F. Sur un microbe invisible antagoniste des bacilles dysenteriques. *CR Acad Sci Paris.* 1917;165:373–5.
3. D’Herelle F. *The Bacteriophage and its Behavior.* Baltimore, MD: Williams & Wilkins; 1926.
4. D’Herelle, F., Reginald, MH, Mahendra L. *Studies on Asiatic Cholera.* *Indian Med Res Mem.* 1930;14.
5. Summers WC. Cholera and plague in india: The bacteriophage inquiry of 1927-1936. *J Hist Med Allied Sci.* 1993;48(3):275–301.
6. Summers WC. Bacteriophage Therapy. *Annu Rev Microbiol.* 2001;(55):437–51.
7. D’Herelle F. Essai de traitement de la peste bubonique par le bacteriophage. *Presse Med.* 1925;(33):1393–4.
8. Reardon S. Phage therapy gets revitalized. *Nature News.* 2014.
9. Laxminarayan R, Duse A, Wattal C, Zaidi AKM, Wertheim HFL, Sumpradit N, et al. Antibiotic resistance-the need for global solutions. *Lancet Infect Dis.* 2013;13(12):1057–98.

10. Superbugs threaten hospital patients. CDC Newsroom. 2016.
11. Kutateladze M, Adamia R. Bacteriophages as potential new therapeutics to replace or supplement antibiotics. *Trends Biotechnol.* 2010;28(12):591–5.
12. Merrill CR, Scholl D, Adhya SL. The prospect for bacteriophage therapy in Western medicine. *Nat Rev Drug Discov.* 2003;2(6):489–97.
13. Kutter E, De Vos D, Gvasalia G, Alavidze Z, Gogokhia L, Kuhl S, et al. Phage therapy in clinical practice: treatment of human infections. *Curr Pharm Biotechnol.* 2010;11(1):69–86.
14. Ahmad SI. Treatment of post-burns bacterial infections by bacteriophages, specifically ubiquitous *Pseudomonas* spp. notoriously resistant to antibiotics. *Med Hypotheses.* 2002;58(4):327–31.
15. Wright A, Hawkins CH, Anggard EE, Harper D. A controlled clinical trial of a therapeutic bacteriophage preparation in chronic otitis due to antibiotic resistant *Pseudomonas aeruginosa*: a preliminary report of efficacy. *Clin Otolaryngol.* 2009;34:349–57.
16. Chanishvili N. A literature review of the practical application of bacteriophage research. 2012.
17. Phagoburn Clinical Trial. Available from: <http://www.phagoburn.eu/phagoburn-clinical-trial.html>

18. Multistate Outbreaks of Shiga toxin-producing *Escherichia Coli* O26 Infections Linked to Chipotle Mexican Grill Restaurants. Centers for Disease Control and Prevention. 2016.
19. Sillankorva SM, Oliveira H, Azeredo J. Bacteriophages and their role in food safety. *Int J Microbiol.* 2012;2012.
20. Guenther S, Herzig O, Fieseler L, Klumpp J, Loessner MJ. Biocontrol of *Salmonella* Typhimurium in RTE foods with the virulent bacteriophage FO1-E2. *Int J Food Microbiol.* 2012;154(1-2):66–72.
21. Abuladze T, Li M, Menetrez MY, Dean T, Senecal A, Sulakvelidze A. Bacteriophages reduce experimental contamination of hard surfaces, tomato, spinach, broccoli, and ground beef by *Escherichia coli* O157:H7. *Appl Environ Microbiol.* 2008;74(20):6230–8.
22. Modi, R., Hirvi, Y., Hill, A., Griffiths MW. Effect of phage on survival of *Salmonella* enteritidis during manufacture and storage of cheddar cheese made from raw and pasteurized milk. *J Food Prot.* 2001;64(7):927–33.
23. Smith HW, Huggins MB. Successful treatment of experimental *Escherichia coli* infections in mice using phage: its general superiority over antibiotics. *J Gen Microbiol* [Internet]. 1982;128(2):307–18.
24. Dubos RJ, Hookey Straus J, Pierce C. The multiplication of bacteriophage in vivo and its protective effect against an experimental infection with *Shigella dysenteriae*. *J Exp Med.* 1943;78(3):161–8.

25. Kucharewicz-Krukowska A, Slopek S. Immunogenic effect of bacteriophage in patients subjected to phage therapy. *Arch Immunol Ther Exp.* 1987;35(5):553–61.
26. Payne, Robert J H and Jansen V. Understanding Bacteriophage Therapy as a Density-dependent Kinetic Process. *J Theor Biol.* 2001;208:37–48.
27. Rios JL, Lu G, Seo NE, Lambert T, Putnam D. Prolonged Release of Bioactive Model Proteins from Anionic Microgels Fabricated with a New Microemulsion Approach. *Pharm Res.* 2015;33(4):879-892.
28. Pelet J, Putnam D. An in-depth analysis of polymer-analogous conjugation using DMTMM. *Bioconjug Chem.* 2011;22(3):329–37.
29. Kunishima M, Morita J, Kawachi C, Iwasaki F, Terao K, Tani S. Esterification of Carboxylic Acids with Alcohols by 4-(4 ,6-Dimethoxy-1,3,5-triazin-2-yl)-4-methyl-morpholinium Chloride (DMTMM). *Tetrahedron.* 1999;(8):1255–6.
30. Fox M, Szoka F, Frechet J. Soluble polymer carriers for the treatment of cancer: the importance of molecular architecture. *Acc Chem Res.* 2009;42(8):1141–51.
31. Pelet JM, Putnam D. Poly(acrylic acid) undergoes partial esterification during RAFT synthesis in methanol and interchain disulfide bridging upon NaOH treatment. *Macromol Chem Phys.* 2012;213:2536–40.
32. Wampler FM. Formation of diacrylic acid during acrylic acid storage. *Plant/Operations Prog.* 1988;7(3):183–9.

33. Schillemans JP, Verheyen E, Barendregt A, Hennink WE, Van Nostrum CF. Anionic and cationic dextran hydrogels for post-loading and release of proteins. *J Control Release*. 2011;150(3):266–71.
34. Zhang Y, Zhu W, Wang B, Ding J. A novel microgel and associated post-fabrication encapsulation technique of proteins. *J Control Release*. 2005;105(3):260–8.
35. Gehrke SH, Uhden LH, McBride JF. Enhanced loading and activity retention of bioactive proteins in hydrogel delivery systems. *J Control Release*. 1998;55(1):21–33.
36. Yongsheng M, Pacan JC, Wang Q, Xu Y, Huang X, Korenevsky A, et al. Microencapsulation of bacteriophage *phi*1 into chitosan-alginate microspheres for oral delivery. *Appl Environ Microbiol*. 2008;74(15):4799–805.
37. Puapermpoonsiri U, Spencer J, van der Walle CF. A freeze-dried formulation of bacteriophage encapsulated in biodegradable microspheres. *Eur J Pharm Biopharm*. 2009;72(1):26–33.
38. Korehei R, Kadla JF. Encapsulation of T4 bacteriophage in electrospun poly(ethylene oxide)/cellulose diacetate fibers. *Carbohydr Polym*. 2014;100:150–7.
39. Vonasek E, Le P, Nitin N. Encapsulation of bacteriophages in whey protein films for extended storage and release. *Food Hydrocoll*. 2014;37:7–13.
40. Salalha W, Kuhn J, Dror Y, Zussman E. Encapsulation of bacteria and viruses in electrospun nanofibres. *Nanotechnology*. 2006;17(18):4675–81.

41. Tang Z, Huang X, Baxi S, Chambers JR, Sabour PM, Wang Q. Whey protein improves survival and release characteristics of bacteriophage Felix O1 encapsulated in alginate microspheres. *Food Res Int.* 2013;52(2):460–6.
42. Korsmeyer RW, Gury R, Doelker E, Buri P, Peppas NA. Mechanisms of solute release from porous hydrophilic polymers. 1983;15:25–35.
43. Reis A V, Guilherme MR, Rubira AF, Muniz EC. Mathematical model for the prediction of the overall profile of in vitro solute release from polymer networks. *J Colloid Interface Sci.* 2007;310(1):128–35.
44. Weiser JR, Yueh A, Putnam D. Protein release from dihydroxyacetone-based poly(carbonate ester) matrices. *Acta Biomater.* 2013;9(9):8245–53.
45. Natu M V., Gil MH, de Sousa HC. Supercritical solvent impregnation of poly(ϵ -caprolactone)/poly(oxyethylene-b-oxypropylene-b-oxyethylene) and poly(ϵ -caprolactone)/poly(ethylene-vinyl acetate) blends for controlled release applications. *J Supercrit Fluids.* 2008;47(1):93–102.
46. Ellermann M, Huh EY, Liu B, Carroll IM, Tamayo R, Sartor RB. Adherent-invasive *Escherichia coli* production of cellulose influences iron-induced bacterial aggregation, phagocytosis, and induction of colitis. *Infect Immun.* 2015;83(10):4068–80.
47. Yang Y, Jobin C. Microbial imbalance and intestinal pathologies: connections and contributions. *Dis Model Mech.* 2014;7(10):1131–42.

4 Conclusions and Recommendations for Future Work

4.1 Conclusions

Hydrogels for biomedical use were proposed over half a century ago by Otto Wichterle and Drahoslav Lim. They proposed that a polymer suitable for biological use should meet the following criteria: “1. a structure permitting the desired water content, 2. inertness to normal biological processes, 3. permeability to metabolites”. The first soft contact lenses were developed by adhering to the above mentioned criteria out of poly(hydroxyalkyl methacrylate) hydrogels (1). Since then hydrogels have been used in a myriad of applications and most relevant to this thesis is the area of controlled release of pharmaceuticals (2). Micron size hydrogels, referred to as microgels, have also been used extensively for drug delivery applications (3–5). The research presented in this thesis highlights the development of poly(acrylic acid)/poly(ethylene glycol) (pAA/PEG) microgels fabricated with a new microemulsion approach. pAA/PEG microgels were tested as controlled release devices for proteins and bacteriophages. pAA/PEG microgels captured proteins with high efficiency. The protein release was studied and shown that lysozyme (high isoelectric point) was released over a period of 30 days while retaining biological activity. Also shown were that the loading efficiency and release kinetics depend on the formulation parameters and protein physico-chemical characteristics (6). The success of pAA/PEG microgels at both protein encapsulation and release motivated work to study the capture and release of higher order constructs. We identified bacteriophages as a promising candidate for this study because of the rising interest in phage therapy (7,8). Phages (size in nanometers) are significantly larger than the previous studied proteins (size in angstroms) and the pAA/PEG microgels were modified by increasing the PEG cross-linker size

to allow permeation of the bacteriophage into the microgel interior. Phage was encapsulated successfully and released over 20 days while still retaining lytic ability. These results showed higher encapsulation, longer release, and higher total release per weight of microgel matrix than any other controlled release material for phage published in the literature.

pAA/PEG microgels have promise as controlled release devices for macromolecules and higher order constructs. Further research with these microgels could lead to a clinically translatable controlled release device. The following steps are proposed for future work to improve on this microgel system. a) to increase the degradability of microgels, b) use of microfluidic fabrication methods for the synthesis of more homogenous and well-defined microgel formulations, c) in vivo studies to assess the toxicity and therapy efficacy.

4.2 Future Work

4.2.1 Engineer Better Biodegradability into pAA/PEG Microgels

pAA/PEG microgels reported in this thesis did not show significant degradation into pAA and PEG under physiological conditions (pH 7, 37 °C). This poses a potential problem for microgel clinical translation for internal use, but may not be an issue for dermal use, such as in the treatment of burns. Two synthetic routes are proposed to enhance the degradability potential of the microgels. The first includes the use of a biodegradable backbone and the second pertains to increasing the degradability of the cross-linking bonds.

4.2.1.1 Enhanced biodegradability of microgel polymer backbone using biodegradable pAA analogs

Zhang et al. reported on the synthesis of a new biodegradable poly(glyceric acid carbonate) (PGAC), a pAA analog (Fig. 1) (9). This new polymer showed degradability within two weeks and bulk hydrogels prepared from this material degraded within 2 hours. A 2-hour degradation for the microgels would be unsuitable for sustained prolonged release. Therefore, I

propose the use of pAA/PGAC blends cross-linked with PEG using the microemulsion approach presented in this thesis. Table I shows a series of microgels that can be synthesized to identify those with suitable degradation kinetics.

4.2.1.2 Enhanced biodegradability of cross-linking bonds

Cross-linking bonds can be engineered to promote biodegradability. Currently, the pAA/PEG microgels were engineered using ester bonds for their susceptibility to hydrolysis. However, the degradation kinetics seem to be too slow and this must be overcome to achieve clinical success for internal use. Inspired by the work of Weiser et al., introduction of carbonate groups near the ester bond similar to those of in the poly(carbonate esters) synthesized by Weiser et al. and reviewed by Ricapito et al. (10,11) may enhance the kinetics of degradation. A sample synthetic scheme is shown in Figure 2, but significant experimental work will be needed to create the proposed cross-links with enhanced biodegradability.

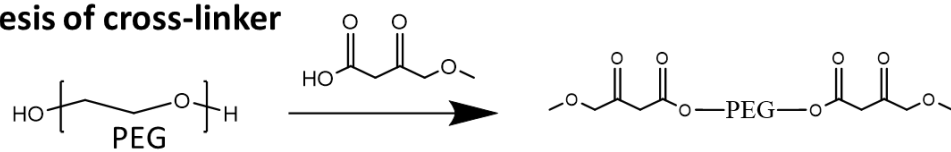


Figure 4.1 Chemical structure of non-degradable pAA (left) and biodegradable PGAC (right). Reprinted with permission from reference 9. Copyright 2015 American Chemical Society.

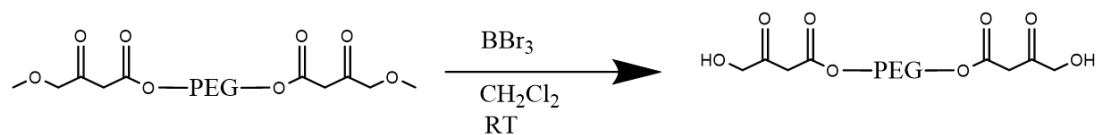
Table 4.1 Proposed formulation blend of PGAC/pAA for synthesis of biodegradable microgels.

Formulation	PGAC %	pAA %	% cross-linking
1	100	0	25
2	75	25	25
3	50	50	25
4	25	75	25
5	0	100	25
6	100	0	45
7	75	25	45
8	50	50	45
9	25	75	45
10	0	100	45

Synthesis of cross-linker



Hydroxyl deprotection



pAA cross-link formation

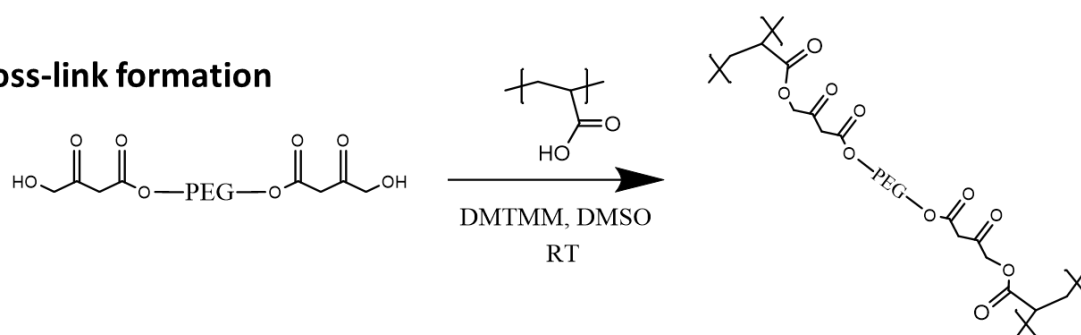


Figure 4.2. Sample synthetic scheme for the fabrication of microgels with cross-links with enhanced biodegradability.

4.2.2 Microfluidic Fabrication of Microgels

The polydispersity and heterogeneity in the current microgel formulations may present a hurdle to clinical translation. Microfluidic devices have been used for the fabrication of monodisperse, homogenous microgels (12–15). Microfluidic fabrication techniques could be useful for the synthesis of pAA/PEG microgels using the new microemulsion discussed earlier in this thesis of DMSO droplets in a Pluronic continuous phase.

4.2.3 In Vivo-Studies to Assess Toxicity and Therapeutic Efficacy

Success of any biomedical device must meet the criteria of minimal side effects and toxicity in the body. Once degradability and fabrication issues are resolved, as described in the future work proposed above, in-vivo studies must be used to evaluate toxicity. International standards for local toxicity are established in the ISO 10993-6:2007 and this standard protocol should be followed when assessing the toxicity of the pAA/PEG microgels. Lastly, showing therapeutic efficacy in a disease model is paramount to show the full potential of pAA/PEG microgels. I believe that the greatest need in protein sustained release is for ophthalmic treatments. Both glaucoma and wet aged-related macular degeneration (wAMD) are significant causes of vision impairment worldwide (16,17). Glaucoma is treated with intraocular pressure (IOP) lowering drugs but poor patient compliance and lack of neuroprotection of the optic nerve results in ineffective treatment and vision loss (18). Therefore, a system able to deliver nerve neuroprotection and IOP reduction is needed. I believe that a combination therapy in conjunction with pAA/PEG microgels sustained delivery will provide sufficient therapy to prevent vision loss. wAMD standard of care is monthly or bimonthly intravitreal injections of anti-angiogenic monoclonal antibodies against vascular endothelial growth factor (VEGF) and platelet derived growth factor (PDGF). Benefit can be derived by reducing the frequency of administration to

once every 6 months, for example. I propose the encapsulation of anti-angiogenic proteins and subsequent intravitreal delivery of degradable pAA/PEG microgels as salient future work. Lastly, the possibility of phage therapy using this microgels could be evaluated in a wound animal model similar to current clinical trials in the European Union (8).

4.3 References

1. Wichterle O, Lím D. Hydrophilic Gels for Biological Use. *Nature*. 1960;185(4706):117–8.
2. Caló E, Khutoryanskiy V V. Biomedical applications of hydrogels: A review of patents and commercial products. *Eur Polym J*. 2014;65:252–67.
3. Bysell H, Hansson P, Schmidtchen A, Malmsten M. Effect of hydrophobicity on the interaction between antimicrobial peptides and poly(acrylic acid) microgels. *J Phys Chem B*. 2010;114(3):1307–13.
4. Bysell H, Månsson R, Hansson P, Malmsten M. Microgels and microcapsules in peptide and protein drug delivery. *Adv Drug Deliv Rev*. 2011;63(13):1172–85.
5. Oh JK, Drumright R, Siegwart DJ, Matyjaszewski K. The development of microgels/nanogels for drug delivery applications. *Prog Polym Sci*. 2008;33(4):448–77.
6. Rios JL, Lu G, Seo NE, Lambert T, Putnam D. Prolonged Release of Bioactive Model Proteins from Anionic Microgels Fabricated with a New Microemulsion Approach. *Pharm Res*. 2015; 33(4):879-892.
7. Vandenheuveel D, Lavigne R, Brüßow H. Bacteriophage Therapy: Advances in Formulation Strategies and Human Clinical Trials. *Annu Rev Virol* [Internet]. 2015;2(1):599–618.
8. Phagoburn Clinical Trial [Internet]. [cited 2016 Jul 4]. Available from: <http://www.phagoburn.eu/phagoburn-clinical-trial.html>

9. Zhang H, Lin X, Chin S, Grinstaff MW. Synthesis and Characterization of Poly(glyceric Acid Carbonate): A Degradable Analogue of Poly(acrylic Acid). *J Am Chem Soc.* 2015;137(39):12660–6.
10. Weiser JR, Yueh A, Putnam D. Protein release from dihydroxyacetone-based poly(carbonate ester) matrices. *Acta Biomater.* 2013;9(9):8245–53.
11. Ricapito NG, Ghobril C, Zhang H, Grinstaff MW, Putnam D. Synthetic Biomaterials from Metabolically Derived Synthons. *Chem Rev.* 2016;116(4):2664-2704.
12. Kesselman LRB, Shinwary S, Selvaganapathy PR, Hoare T. Synthesis of monodisperse, covalently cross-linked, degradable “smart” microgels using microfluidics. *Small.* 2012;8(7):1092–8.
13. Kim JW, Utada AS, Fernández-Nieves A, Hu Z, Weitz D a. Fabrication of monodisperse gel shells and functional microgels in microfluidic devices. *Angew Chemie - Int Ed.* 2007;46(11):1819–22.
14. De Geest BG, Urbanski JP, Thorsen T, Demeester J, De Smedt SC. Synthesis of Monodisperse Biodegradable Microgels in Microfluidic Devices. *Langmuir. American Chemical Society;* 2005;21(23):10275–9.
15. Shah RK, Kim J-W, Agresti JJ, Weitz D a., Chu L-Y. Fabrication of monodisperse thermosensitive microgels and gel capsules in microfluidic devices. *Soft Matter.* 2008;4(12):2303.

16. Johnson T V, Bull ND, Martin KR. Neurotrophic factor delivery as a protective treatment for glaucoma. *Exp Eye Res.* 2011;93(2):196–203.
17. Gaudana R, Ananthula HK, Parenky A, Mitra AK. Ocular drug delivery. *AAPS J* [Internet]. 2010 Sep [cited 2013 Jun 4];12(3):348–60.
18. Ghate D, Edelhauser HF. Barriers to glaucoma drug delivery. *J Glaucoma.* 2008;17:147–56.

A. Delivery of Bacteriophage Loaded-Microgels for the Treatment of Intracellular Pathogens

A.1 Abstract

Purpose Phage therapy offers a complementary therapy to antibiotics for the treatment of multi drug resistant bacteria. However, treatment of intracellular pathogens remains a challenge due to the phage inability to enter the cell and reach its bacterial host. Phage loaded microgels were fabricated to serve as carrier to deliver phage intracellularly to treat adherent-invasive *e. coli* in J774 A.1 macrophages.

Methods Microgels were prepared by cross-linking poly(acrylic acid) and polyethylene glycol. Phage was encapsulated in the microgels. Confocal microscopy was used to evaluate if the microgels can be internalized by the macrophages. An invasion assay was established to assess treatment of adherent-invasive *e. coli* infected macrophages with phage loaded microgels.

Results Microgels were readily phagocytosed by J774 A.1 macrophages. However, treatment with phage loaded microgels did not reduced the amount of internal bacteria.

Conclusions Phage loaded microgels are not suitable for this particular application and it is hypothesized that they may interfere with the macrophage pathways for bacterial killing.

A.1 Introduction

An alarming global rise in antibiotic resistant bacteria is pressuring scientist to find alternative antimicrobial agents for the treatment of drug resistant and multi drug resistant pathogenic bacteria (1). The use of bacteriophages to treat infection, known as phage therapy, is being revisited in western science (2). This resurgence in interest is reflected in the literature and has been reviewed extensively (3–6). There are even clinical trials underway for the treatment of wound burns (7). Phages also have desirable properties that make them attractive anti-microbial agents. They are natural agents that have never been shown to have adverse side effects, they self-replicate and are highly specific allowing for targeting of only pathogenic bacteria and sparing the body's natural microflora (8). However, phage therapy is restricted to extracellular pathogens due the inability of phages to enter mammalian cells. This greatly limits the range of infections that can be treated by phage therapy.

Polymeric drug carriers offer a potential strategy to enable phage treatment of intracellular infections. In this thesis, I demonstrated the use of polymeric microgels for the controlled release of proteins (Chapter 2) and bacteriophages (Chapter 3). Therefore, it was hypothesized that these microgels could be use as phage-carriers to target adherent-invasive *e. col* (AIEC) which had taken residence intracellularly in J774 A.1 macrophage cells.

In this study, the uptake of microgels by J774 A.1 macrophages was studied using confocal microscopy and an invasion assay was established to assess the effect of phage therapy treatment of AIEC infected J774 A.1 macrophages.

A.2 Materials and Methods

A.2.1 Materials

Acrylic acid, anhydrous methanol, 4-cyanopentanoic acid dithiobenzoate (CPA-DB), 4,4'-azobis(4-cyanopentanoic acid) (A-CPA), dimethyl sulfoxide, 4-methylmorpholine (NMM), tetraethylene glycol and Pluronic[®] L35 were purchased from Sigma. 4-(4,6-Dimethoxy-1,3,5-triazin-2-yl)-4-methylmorpholinium chloride (DMTMM) was purchased from Tokyo Chemical Industry America. Dulbecco's modified eagle medium, fetal bovine serum and gentamicin reagent solution (50 mg/mL) were purchased from Gibco. LB Miller and LB Agar Miller were purchased from VWR. Phosphate buffered saline (PBS) was purchased from Cellgro. NC101 and 528-2 *e. coli* strained was obtained from the Simpson Lab in Cornell University. J774 A.1 macrophages were donated by the Simpson Lab and originally purchased from ATCC. EcoActive[™] phage was donated by Intralytix, Inc.

A.2.2 Synthesis of poly(acrylic acid)

Acrylic acid (AA) was polymerized as described in section 2.3.2 of this thesis and Rios *et al.* (9). Briefly, AA was polymerized using reversible addition-fragmentation chain transfer (RAFT) polymerization to allow control over molecular weight and polydispersity. CPA-DB and A-CPA were dissolved in anhydrous methanol in a Schlenk flask with a magnetic stir bar. Upon complete dissolution AA was added, a condenser column was fitted to the flask and the entire system was purge with dry nitrogen for 15 minutes. Reaction vessel was protected from light and polymerization was initiated by heating to 60 °C in an oil bath with continuous stirring. The reaction was stopped at 48 h by cooling with reaction vessel in an ice bath and exposing the contents to air. Product was purify by dialysing against DI water with a Spectra/Por

regenerated cellulose membrane (3.5 kDa MWCO). Product was then recovered by lyophilization.

The M_w , M_n , and PDI of the resulting pAA were determined using a Waters gel permeation chromatography (GPC) system equipped with Ultrahydrogel columns in series, 1515 isocratic HPLC pump and 2414 refractive index detector with temperature controlled at 30 °C. The mobile phase used was phosphate buffer saline (pH=7.4) at a rate of 0.8 mlmin⁻¹ and calibrated with poly(acrylic acid), sodium salt standards. ¹H NMR was used to confirm the structure of the resulting pAA.

A.2.3 Preparation of Microgels

The microgels were synthesized by cross-linking the carboxylate side chains of pAA with the alcohol end-groups of OEG via esterification. The synthesis was carried out as described in section 2.3.3. Briefly, the carboxylate side-chains (COOH) of pAA were cross-linked with the alcohol end-groups of PEG ($M_n = 1,500$ Da). The molar ratios of COOH to PEG and the condensing agent DMTMM were varied to change cross-linking density. Reaction was carried out in DMSO and emulsified in Pluronic[®] L35 with a Silver L5M-A homogenizer at 750 rpm for 4 hours. Upon completion of reaction, microgels were isolated by centrifugation at 9500 rpm and the supernatant was decanted. Microgels were purified by several cycles of re-suspension in deionized water, centrifugation and decantation. Dry microgels were obtained by flash freezing purified microgels in a small volume of deionized water and lyophilization.

A.2.4 Bacteriophage Propagation and Encapsulation

EcoActive[™] (EA[™]) phage was propagated on late-log-phase cultures of *E. coli* NC101, an adhesive-invasive strain, in 250 mL Erlenmeyer flasks with lysogeny broth (LB) containing 5

mM CaCl₂, 10 mM MgSO₄ and 0.2% glucose. EATM phage was allowed to incubate with its host for 4 hours at 37 °C under shaking. The lysate was then centrifuged at 5000 rpm to pellet cell debris. The lysate was recovered, chloroform was added at 1:100 v/v and stored at 4 °C.

EATM phage lysate was concentrated using Amicon[®] Ultra-15 centrifugal filters with a 100 kDa NMWL and then re-suspended in PBS. The concentrated phage was subjected to a plaque assay to quantify the phage's lytic activity. A 1 mL aliquot of re-suspended Phage (~ 2.15 X 10⁹ pfu/mL) was added to 5 mg of dry microgels and incubated for 16 hours at 4 °C under gentle rotation (8 rpm) in polypropylene Eppendorf tubes. Microgels were then recovered by centrifugation (5000 rpm, 5 min), supernatants were isolated and immediately tittered with a plaque assay for lytic activity and stored at 4 °C for subsequent protein quantification.

A.2.5 Macrophage cell culture

J774 A.1 monocyte/macrophage mouse cell line was purchased from ATCC. They were cultured in DMEM with 4.5 g/L D-Glucose, L-Glutamine and supplemented with 10% heat inactivated fetal bovine serum. Cells were maintained in 75 cm² flasks at 37 °C and 5% CO₂. Cells were passaged by dislodging the cells from the flask surface by scraping and preparing subcultures at 1:6.

A.2.6 Confocal Microscopy of Microgel Phagocytosis by Macrophages

Synthesized microgels were fluorescently labeled by conjugating fluorescein-5-thiosemicarbazide via condensation chemistry facilitated with DMTMM. J774 A.1 cells were seeded onto 35 mm tissue culture dishes at concentrations of 1 × 10⁵ and 1 × 10⁶ cells/mL and allow to incubate for 24 hours. At 24 hours, culture medium was replaced and fluorescently label microgels were added at 3 different concentrations. J774 A.1 cells and fluorescent microgels at three different concentrations (100, 250 and 500 µg/mL) were allow to incubate for 4 hours.

Upon 4 hours, media was removed and cells were washed 3 × with PBS 3 to remove free floating microgels. Cells were fixed in 10% formalin and permeabilized with 0.1% Triton X-100. Cells were incubated in 1% Phalloidin Alexa Fluor 568 to stain actin filaments and DAPI was used to stain the nuclei. Cell dishes were carefully cut, mounted on slides with vectashield and sealed. J774 A.1 cells were then imaged under confocal microscopy (Zeiss LSM710 confocal microscope).

A.2.7 Invasion Assay and Bacteriophage Treatment

J774 A.1 cells were seeded in 24 well-plates at 2×10^5 cells/mL and allow to incubate for 24 h (37 °C, CO₂, humidified). Cell were then washed 3× with PBS and 0.5 mL of fresh DMEM (supplemented with 10% FBS) was added. Cells were then infected with NC101 or 528-2 at a multiplicity of infection (MOI) of 10 bacteria per cell. Following a 60 min incubation (37 °C, CO₂, humidified), infected macrophages were washed 3× with PBS and 1 mL of DMEM (10% FBS) containing 200 µg of gentamicin/mL was added to kill extracellular bacteria. Cells were allowed to incubate for 1 hour (37 °C, CO₂, humidified), then washed 3× with PBS and media containing 15 µg of gentamicin/mL was added to prevent grow of extracellular bacteria. Control group was allowed to incubate in media containing 200 µg of gentamicin/mL. Treatment was administered in 3 distinct fashions. a) Phage loaded microgels suspended in PBS were added to infected cells and allowed to incubate with cells for the duration of the experiment, b) phage loaded microgels suspended in PBS were added to infected cells and allowed to incubate for 1 or 4 hours then non-internalized microgels were remove by washing 3× with PBS and media containing 15 µg of gentamicin/mL was added, c) concentrated phage lysate was added to infected cells. Upon desired time-points, cells were washed 3× with PBS and lyse with 1 mL of 0.1% Triton X-100 in PBS. A cell lysate serial dilution was prepared and plated onto LB agar

plates to determine the colony forming units (surviving bacteria). Each experimental condition was performed in triplicate.

A.3 Results and Discussion

Microgels were successfully synthesized in the same manner as described in sections 2.3.2 and 2.3.3 of this thesis but were slightly modified to accommodate for the larger size of bacteriophage by increasing the size of the PEG cross-linker. The microgels were successfully internalized by J774 A.1 macrophage cells and were capable of encapsulating and releasing phage as demonstrated in Chapter 3. Following these findings, treatment of intracellular pathogens seen a viable application for this technology.

Confocal microscopy images show that J774 A.1 macrophages readily phagocytized microgels as shown in Figure A.1. Upon exposing macrophages to the microgels for 4 hours, the microgels were phagocytosed by virtually all cells. Confocal images seem to indicate that more microgels per cell were phagocytosed at higher concentration of microgels and at lower cell seeding density. Z plane cross sections obtained with confocal microscopy are also shown to demonstrate that the microgels are within the cell membrane (Figure A.2). This finding provided the motivation for attempting to intracellularly deliver bacteriophage to treat intracellular pathogens.

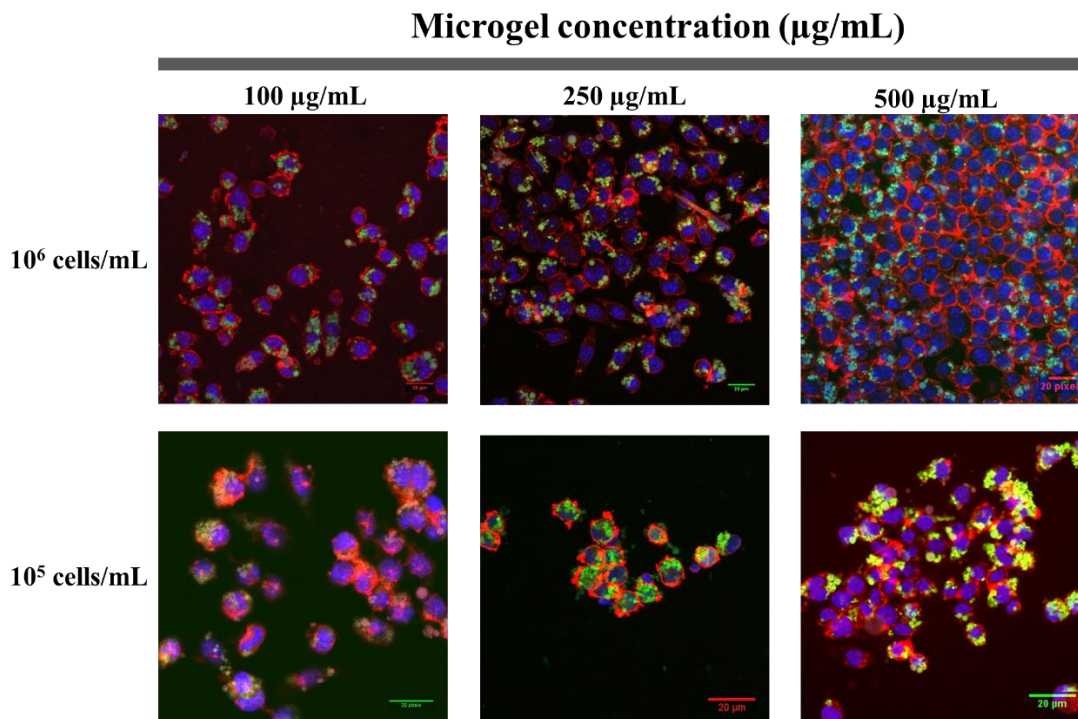


Figure A.1: Phagocytosis of microgels by J774 A.1 macrophage cells after 4-hour exposure. Microgels are labeled with fluorescein (green), actin was stained with phalloidin-Alexa Fluor 568 (red) and the nuclei is stained with DAPI (blue). Microgels were readily phagocytosed by J774 A.1 macrophages.

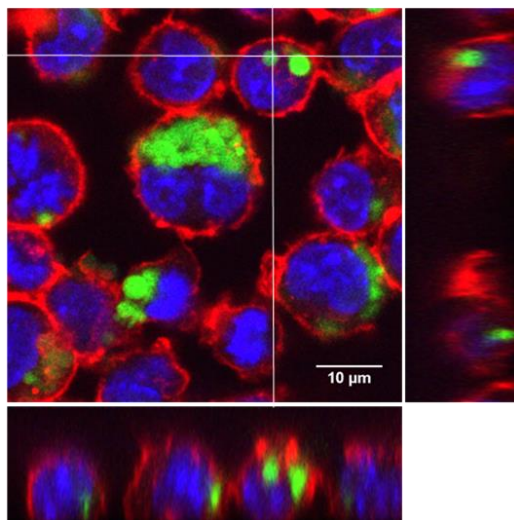


Figure A.2: Confocal z-section images were taken and cross-sections of the y-z plane (right) and x-z plane (bottom) are shown demonstrating that microgels are internalized within the cell membrane and not just adhering to the macrophages.

In order to assess the microgels' ability to deliver bacteriophage intracellularly for the treatment of intracellular pathogens two adherent-invasive *e. col* (AIEC) were obtained from the Simpson Lab at Cornell University (NC101 and 528-2). Both of these strains were shown to be susceptible to lysis by EATM phage by using plaque assays as described in section 3.3.5. Macrophages were infected with both strains of AIEC and were treated with two distinct formulations of phage loaded microgels for 1 or 4 hours. Infected macrophages were allowed to incubate for 24 hours, then they were lysed to quantify the amount of intracellular bacteria. Phage loaded microgel treatment did not help combat the intracellular infection (Figure A.3). In fact, if macrophages are exposed to the microgels for 4 hours, it had a detrimental effect allowing 528-2 to better proliferate within the cell. Treatment with phage alone showed a slight decrease in the amount of intracellular 528-2 *e. col* but still several orders of magnitude higher than the gentamicin control. Macrophages infected with NC101 *e. col* showed similar results. Treatment with phage loaded microgels did not help reduce the amount of intracellular bacteria and if exposed to microgels for 4 hours the amount of intracellular bacteria increased. Macrophages clear bacteria by engulfing it into a phagosome which then matures into a phagolysosome. The phagolysosome contains antimicrobial peptides, proteases and lysozyme (10). In addition, macrophages make use of toxic reactive oxygen species (ROS) to clear bacteria. Macrophages synthesize the ROS nitric oxide by making use of arginine and oxygen (11). The exact mechanism by which AIEC strains are able to proliferate is not exactly understood but it is the case that they proliferate at a higher rate than the macrophage's killing rate. It is hypothesized that the anionic microgels are scavenging the arginine and other nitrogen species necessary for the macrophage to synthesize nitric oxide and in doing so negatively affecting the macrophages ability to kill the intracellular AIEC thus increasing the amount of intracellular bacteria.

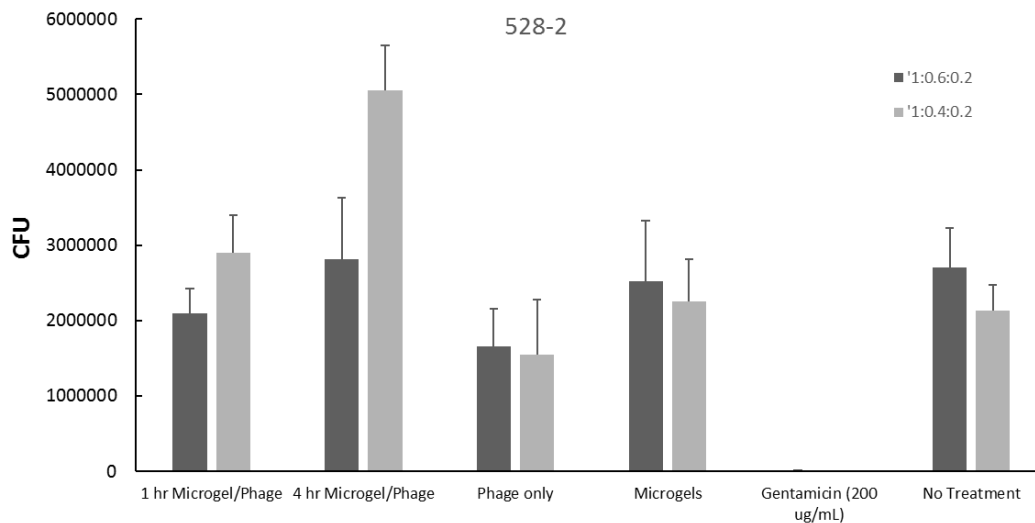


Figure A.3: Phage loaded microgel treatment of 528-2 *e. coli* infected macrophages. Macrophages were treated with two distinct microgel formulations. Phage loaded microgels had no effect in the amount of intracellular bacteria, calculated in colony forming units (CFU) and upon 4 hr exposure even increased it. Treatment with free phage showed a slight decreased CFU. Exposure to microgels loaded with phage or blank microgels for 1 hour had no effect. Legend refers to molar ratios of the microgel formulation (COOH:PEG:DMTMM).

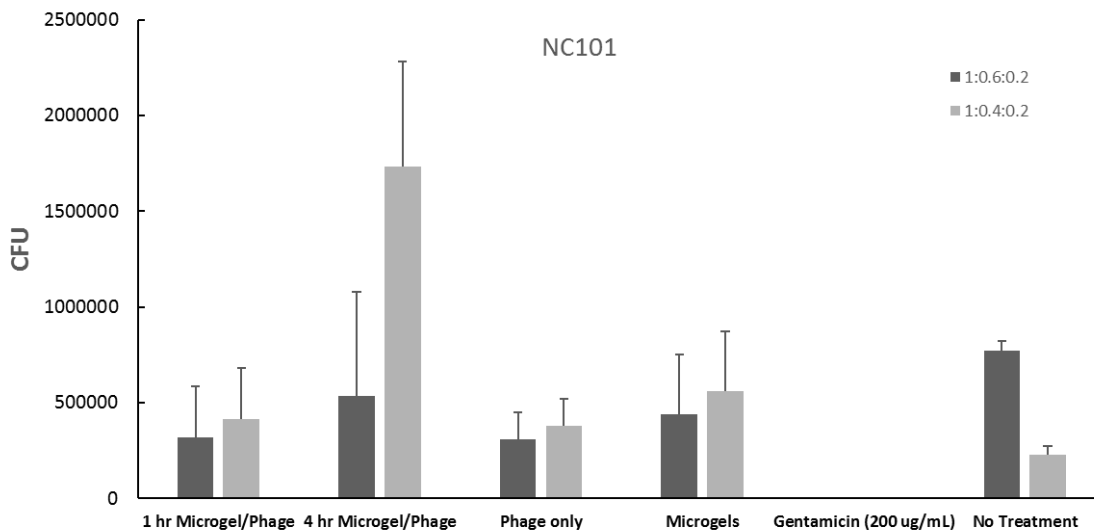


Figure A.4: Phage loaded microgel treatment of NC101 *e. coli* infected macrophages. Macrophages were treated with two distinct microgel formulations. Phage loaded microgels had no effect in the amount of intracellular bacteria, calculated in colony forming units (CFU) and upon 4 hr exposure even increased it. Treatment with free phage showed a slight decreased CFU. Exposure to microgels loaded with phage or blank microgels for 1 hour had no effect. Legend refers to molar ratios of the microgel formulation (COOH:PEG:DMTMM).

A.4 Conclusion

Microgels are readily phagocytosed by J774 A.1 macrophages as demonstrated by confocal microscopy experiments. The potential of phage loaded microgels to treat intracellular pathogens was evaluated by treating AIEC infected macrophages. Unfortunately, this study did not yield a positive outcome and showed that phage loaded microgels do not help combat intracellular infections and that in fact it has a detrimental effect. It is hypothesized that the anionic nature of the microgels affects the mechanistic pathways by which macrophages kill bacteria and thus allowing for faster/further proliferation of both AIEC strains tested.

A.5 References

1. Laxminarayan R, Duse A, Wattal C, Zaidi AKM, Wertheim HFL, Sumpradit N, et al. Antibiotic resistance-the need for global solutions. *Lancet Infect Dis.* 2013;13(12):1057–98.
2. Reardon S. Phage therapy gets revitalized. *Nature News.* 2014.
3. Matsuzaki S, Rashel M, Uchiyama J, Sakurai S, Ujihara T, Kuroda M, et al. Bacteriophage therapy: A revitalized therapy against bacterial infectious diseases. *J Infect Chemother.* 2005;11(5):211–9.
4. Abedon ST, Kuhl SJ, Blasdel BG, Kutter EM. Phage treatment of human infections. *Bacteriophage.* 2011;1(2):66–85.
5. Vandenhoevel D, Lavigne R, Brüssow H. Bacteriophage Therapy: Advances in Formulation Strategies and Human Clinical Trials. *Annu Rev Virol.* 2015;2(1):599–618.
6. Gandham P. Bacteriophages: their use in the treatment of infections in the future. *Int J Curr Microbiol Appl Sci.* 2015;4(2):867–79.
7. Phagoburn Clinical Trial [Internet]. [cited 2016 Jul 4]. Available from: <http://www.phagoburn.eu/phagoburn-clinical-trial.html>
8. Kutter E, De Vos D, Gvasalia G, Alavidze Z, Gogokhia L, Kuhl S, et al. Phage therapy in clinical practice: treatment of human infections. *Curr Pharm Biotechnol.* 2010;11(1):69–86.

9. Rios JL, Lu G, Seo NE, Lambert T, Putnam D. Prolonged Release of Bioactive Model Proteins from Anionic Microgels Fabricated with a New Microemulsion Approach. *Pharm Res.* 2015;33(4):879-892.
10. Garin J, Diez R, Kieffer S, Dermine J, Duclos S, Gagnon E, et al. The Phagosome Proteome : Insight into Phagosome Functions. 2001;152(1):165–80.
11. Nathan CF, Hibbs JB. Role of nitric oxide synthesis in macrophage antimicrobial activity. *Curr Opin Immunol.* 1991;3(1):65–70.